

https://dspace.org/

Gauge gravity dualities from group representation theory

Gandote, Sonagnon Eunice Edwige

2022
https://hdl.handle.net/10539/37127

Downloaded from a DSpace repository. https://dspace.org/

Gauge Gravity Dualities from Group Representation Theory

Sonagnon Eunice Edwige Gandote
(1727931@students.wits.ac.za)
Faculty of Science, School of Physics
University of the Witwatersrand, South Africa

Supervised by Professor Robert de Mello Koch

A thesis submitted to the University of the Witwatersrand in fulfilment of the requirements for the degree of Doctor of Philosophy.

Johannesburg, 2022.



Declaration

I, Eunice Gandote, declare that the work presented in this thesis is my own unless otherwise stated. This work has not been submitted before for examination in any other university.



October 4, 2022

Abstract

This thesis considers two distinct problems. First we discuss scrambling and equilibration in $\mathcal{N} = 4$ super Yang-Mills theory using operators that have a very large dimension, of order N^2. A basis for these operators, is provided by the so-called Gauss graph operators. The operators are labelled by a pair of Young diagrams and a graph. We characterize the typical graph and the dynamics associated to it. We show that the resulting dynamics is that of a fast scrambler. Our system equilibrates in a time scale given by $t \sim \frac{p}{\lambda}$ where p is an order N number equal to the number of nodes in the graph and λ is the 't Hooft coupling. Finally we use bilocal holography to explore the duality between the free $O(N)$ vector model and higher spin gravity. We demonstrate a mapping between the CFT and the higher spin gravity that is determined by the symmetry of the problem. We then turn to a study of the geometry of this mapping. Using a specific code subspace, we demonstrate that bilocal holography reproduces the entanglement wedge reconstruction. We also make contact with ideas that have been influential in the holographic computation of entanglement entropy.

Acknowledgements

I would like to thank my supervisor, Professor Robert de Mello Koch, for his invaluable supervision, contribution and continuous support. His immense knowlege has encouraged and inspired me to succeed in Physics. I am deeply greatful to have you as my supervisor.

I am greatful to Herve Ewinsou and my parents for their support. Thanks to Warren Carlson for the useful discussions.

I would like to thank NRF for supporting this research and the university of the Witwatersrand for making it achievable.

Contents

1 Introduction **1**
- 1.1 AdS/CFT correspondence . . . 2
  - 1.1.1 Anti-de Sitter Spacetime . . . 2
  - 1.1.2 CFT . . . 4
  - 1.1.3 Relation between parameters . . . 6
- 1.2 AdS/CFT dictionary . . . 6
  - 1.2.1 Matching symmetries . . . 7
  - 1.2.2 Mapping between bulk fields and boundary operators . . . 7
- 1.3 Black holes as fast scrambler . . . 8
- 1.4 Holography as quantum error correction code . . . 9
- 1.5 Non-Perturbative String Theory from AdS/CFT . . . 10

2 Scrambling in Yang-Mills **14**
- 2.1 Introduction . . . 14
- 2.2 Dynamics on Gauss graphs . . . 17
- 2.3 Properties of Gauss Graphs . . . 19
  - 2.3.1 Generating interaction graphs . . . 19
  - 2.3.2 Characterizing interaction graphs . . . 24
- 2.4 Scrambling on typical graphs . . . 27
  - 2.4.1 Lieb-Robinson bound for typical graph dynamics . . . 27
  - 2.4.2 Entanglement Generation . . . 29
- 2.5 Equilibration during intervals . . . 31
- 2.6 Discussion . . . 36

3 Quantum Error Correction and Holographic Information from Bilocal Holography **38**
- 3.1 Introduction . . . 38
- 3.2 Bilocal Bulk Reconstruction . . . 41
- 3.3 Subregion duality . . . 47
- 3.4 Code Subspace and Quantum Error Correction . . . 49
  - 3.4.1 Quantum Error Correction . . . 50
  - 3.4.2 Entanglement Entropy and Bit Threads . . . 51
  - 3.4.3 Entanglement Wedge Reconstruction . . . 53
- 3.5 Non-localities from large N . . . 53
- 3.6 Conclusions . . . 56

4 Conclusion **58**

A Gauss Graph Hamiltonian from Yang-Mills **59**

B Coordinate Transformation **62**
- B.1 Motivational Example . . . 62
- B.2 Conformal Transformations . . . 63

C Other approaches **66**

List of Figures

1 The interaction graph shown can be decomposed into two paths, each of length 3 as shown on the left, or into two paths, one of length 2 and one of length 4 as shown on the right. 20

2 The above plots show histograms of the maximum vertex degree D_V, for Gauss graphs with 5 vertices and $E = 6, 8, 10, 12, 14$ and 16 edges. 25

3 The above plots show the average vertex degree for graphs with $p = 4$ vertices versus the number of edges E. For $E = 16$ the average vertex degree is 2.55. This indicates that most vertices that have been averaged over must assume the maximum value of $p - 1 = 3$. 26

4 The above plot shows the Von Neumann entropy versus v^2t, for $p = 100$. . . 31

5 The bilocal describing a pair of excitations localized at (x_1, p_1^+) and (x_2, p_2^+) correspond to a bulk excitation localized at (X, Z) as shown. This figure lives on a constant $x^+ = X^+$ slice. The angle θ is related to p_1^+ and p_2^+ according to (3.3.2). 48

6 It is possible to choose distinct bilocals from the subregion $\mathcal{R}$ that correspond to different semicircles passing through point P. This allows us to obtain the value of the bulk field $\Phi(X^+, X^-, X, Z, \theta)$ at P for a number of distinct θ. . . 50

7 The fields at point P can be reconstructed using bilocals taken from region A or region B. It is however not possible to reconstruct the bulk fields at point P using bilocals from the intersection $A \cap B$. 51

8 It is not possible to reconstruct the bulk operator at P if we restrict to either subregion A or B. The reconstruction is however possible if bilocals from $A \cup B$ are used. 51

9 Constraints that arise when $N = 2$. 55

10 Two of the diagrams participating in the constraint that arises for general N. 56

Preface

- Chapter 2 is based on the work entitled "Scrambling in Yang-Mills", published in the Journal of High Energy Physics (JHEP), 2001(2021)058. ArXiv number: 2008.12409. For this paper I contributed the ideas for and carried out the numerical analysis that determines what a typical random graph is, and I conceptualized the approach towards demonstrating thermalization and carried out the detailed numerical analysis. In addition, I wrote the first draft of sections 3, 4 and 5 of the paper and proof read and polished the entire paper.

- Chapter 3 is based on the work entitled "Quantum Error Correction and Holography Information from Bilocal Holography" published in the Journal of High Energy Physics (JHEP), 11(2021)192. ArXiv number: 2106.00349. I carried out the detailed analysis leading to the proof that the representation of the conformal group in the higher spin gravity matches the representation provided by the bilocal field. In addition, I wrote the first draft of sections 3, 5 and Appendix A of the paper and proof read and polished the entire paper.

1 Introduction

The study of the large N expansion was proposed by 't Hooft to investigate a gauge theory for strong interactions with colour gauge group $SU(N)$[1]. He showed that while keeping the 't Hooft coupling $\lambda = g_{YM}^2 N$ fixed with N large, the major contribution to each order in λ comes from planar diagrams. The large N expansion was later also used to investigate non-perturbative string theory. Madalcena proposed in [2] a relationship between Quantum Field Theory (QFT) and string theory. QFT is analyzed perturbatively in the weak coupling limit using Feynman diagrams. Observables can be expanded as a power series when the coupling of the theory is small. Despite the fact that we often get accurate results when the coupling of the theory is very small, it is important to mention that most observables can't be expanded as a power series in the coupling and there are non-perturbative contributions. In QFT, one origin of the non-perturbative contributions is provided by instantons[3]. The non-perturbative string theory is not yet understood in complete detail. Physicists have recently discovered that we can gain access to the non-perturbative contributions from the perturbative contributions using resurgence [4]. In this thesis, we are interested in the structure of the $\frac{1}{N}$ expansion of heavy operators. We take up this question in chapter 2 where we study operators with a bare dimension of order N^2. This is the first step towards understanding the structure of the $\frac{1}{N}$ expansion of correlators implied by resurgence.

Giant gravitons are non-perturbative objects that are dual to operators built using order N fields. Conformal field theory correlators of giant gravitons are by now well understood, as reviewed in section 1.5. Another non-perturbative object that we consider in this thesis corresponds to new spacetime geometries containing black holes. These non-perturbative objects are dual to operators built using order N^2 fields. Operators with a large bare dimension of order N^2 have a large R-charge and are dual to heavy states in the gravitational theory. Correlation functions of these classes of operators are computed in the large N but non-planar limit. These operators of $\mathcal{N} = 4$ super Yang-Mills theory are given by Schur polynomials. A Schur polynomial that has a Young diagram of a single column of J boxes corresponds to a point like graviton. When J is order $\sqrt{N}$, we have a string and operators comprised of $J = O(N)$ fields are duals to giant graviton branes. By varying J, we then move from one particular physical description to another, like point graviton to string and string to giant graviton.

In chapter 2, we focus on operators having a large bare dimension of order N^2. The AdS/CFT correspondence maps the conformal dimensions of operators in $\mathcal{N} = 4$ super Yang-Mills theory to energies in the gravitational theory. The dilatation operator of field theory thus defines a Hamiltonian acting on a graph. We find after simplification that this class of operators are linear combinations of the Gauss graph operators. We use this Hamiltonian to study scrambling and equilibration of $\mathcal{N} = 4$ super Yang-Mills theory.

Although there is a lot of evidence for the duality between gauge theory and gravity, it is still very poorly understood. A simpler example of the correspondence is the duality between the $O(N)$ vector model and higher spin gravity in anti-de Sitter space. This example

is simple because the $O(N)$ vector model is so simple. It is a free field theory and we know the complete space of gauge invariant local operators. In chapter 3 we will study the bilocal holography of the vector model and show that the geometry of the map between the CFT and the dual gravity realizes many of the general features expected in holography. In particular, we will make contact with entanglement wedge reconstruction and with holographic computations of entropy.

Now that we have described what is in the thesis, we will give a very brief review of some general background.

1.1 AdS/CFT correspondence

Many attempts to quantize gravity have failed. A promising recent development is the AdS/CFT correspondence which proposes a framework to investigate the theory of quantum gravity. This correspondence is a conjectured duality between quantum gravity theory in Anti-de Sitter space (AdS) in $d+1$ dimensions and a Conformal Field Theory (CFT) in d dimensions. For example, the first example of AdS/CFT claims an equivalence between type IIB string theory on $\mathrm{AdS}_5 \times S^5$ and $\mathcal{N}=4$ super Yang-Mills theory[2]. The duality implies a one-to-one mapping between the full dynamics of both theories. Due to the fact that the two theories are defined on spaces with different dimensions, the AdS/CFT correspondence is the realization of the holographic principle: the CFT lives in the d dimensional boundary of AdS_{d+1}. The original idea of holography [5] is motivated by the study of black holes. It states that quantum gravity in a region R can also be described using a non-gravitational theory on the boundary of R. An important feature of gauge/gravity duality is that it relates a strongly coupled gauge theory to a weakly coupled string theory and the conjecture is then a strong/weak coupling duality. To better understand the duality, we will review the geometry of AdS spaces and CFT.

1.1.1 Anti-de Sitter Spacetime

Anti-de Sitter spaces are the maximally symmetric spacetimes with constant negative scalar curvature. By maximally symmetric spacetimes we mean the maximal number of independent spacetime symmetries. In a $d+1$ dimensional flat spacetime, we have $\frac{1}{2}(d+1)(d+2)$ spacetime symmetries[6], which correspond to $d+1$ translations, $\frac{1}{2}d(d-1)$ rotations and d boosts. The isometry group of $d+1$-dimensional AdS space also has $\frac{1}{2}(d+1)(d+2)$ generators. Due to the translation and rotation symmetries, the curvature of a maximally symmetric space is the same everywhere in the space, that is, it is constant. To distinguish different spaces, we should know the sign of the Ricci scalar R. The maximally symmetric space with positive curvature $R>0$ corresponds to de Sitter Space (dS), the maximally symmetric space with $R<0$ corresponds to Anti-de Sitter Space (AdS) and the space with $R=0$ corresponds to Minkowski space. A $d+1$-dimensional Anti-de Sitter space can be represented using the hyperboloid of radius a[7]

$$(X^0)^2 - \sum_{i=1}^{d}(X^i)^2 + (X^{d+1})^2 = a^2 \tag{1.1.1}$$

By embedding it in $\mathbb{R}^{d,2}$, we can define the $d+1$-dimensional Anti-de Sitter space AdS_{d+1} using the cartesian coordinates for the embedding space $(X^0, X^1, \cdots X^d, , X^{d+1})$

$$AdS_{d+1} := \left\{ X \in \mathbb{R}^{d,2} \mid (X^0)^2 - \sum_{i=1}^{d} (X^i)^2 + (X^{d+1})^2 = a^2 \right\} \tag{1.1.2}$$

The corresponding metric is

$$ds^2 = -dX^0 dX^0 + \sum_{i=1}^{d} (dX^i)^2 - dX^{d+1} dX^{d+1} \tag{1.1.3}$$

We introduce the global coordinates system (τ, ρ, Ω_i), $i \in \{1, 2, \cdots, d\}$ by setting

$$X^0 = a\cosh(\rho)\cos(\tau), \quad X^i = a\sinh(\rho)\Omega_i, \quad X^{d+1} = a\cosh(\rho)\sin(\tau), \tag{1.1.4}$$

where Ω_i is the set of $d-1$ hypersphere defined as

$$\begin{aligned} \Omega_1 &= \cos(\theta_1) \\ \Omega_2 &= \sin(\theta_1)\cos(\theta_2) \\ \Omega_3 &= \sin(\theta_1)\sin(\theta_2)\cos(\theta_3) \\ &\vdots \\ \Omega_{d-1} &= \sin(\theta_1)\sin(\theta_2)\cdots\cos(\theta_{d-1}) \end{aligned} \tag{1.1.5}$$

The AdS_{d+1} metric in terms of global coordinates τ, ρ and Ω_i is given by

$$ds^2 = a^2\left(-\cosh^2(\rho)d\tau^2 + d\rho^2 + \sinh^2(\rho)d\Omega_{d-1}^2\right) \tag{1.1.6}$$

The conformal coordinates are obtained by setting $\tan(\alpha) = \sinh(\rho)$ in (1.1.6). The corresponding metric in conformal coordinates after a simple calculation gives

$$ds^2 = \frac{a^2}{\cos^2(\alpha)}\left(-d\tau^2 + d\alpha^2 + \sin^2(\alpha)d\Omega_{d-1}^2\right) \tag{1.1.7}$$

We can introduce another useful set of coordinates, the Poincare coordinates. First, define the light cone coordinates[7]

$$X^0 - X^d \equiv a^2 u, \quad X^0 + X^d \equiv a^2 v \tag{1.1.8}$$

and the other coordinates

$$x^i \equiv \frac{X^i}{au}, \quad t \equiv \frac{X^{d+1}}{au}. \tag{1.1.9}$$

Then the hyperboloid in (1.1.1) becomes

$$a^4 uv + a^2 u^2 \left(t^2 - \sum_{i=1}^{d-1} (x^i)^2\right) = a^2 \tag{1.1.10}$$

Combining (1.1.10) and (1.1.8) with (1.1.9) gives

$$X^0 = \frac{1}{2u}\left[1 + u^2\left(a^2 + \mathbf{x}^2 - t^2\right)\right], \tag{1.1.11}$$

$$X^i = aux^i, \quad i = 1, \cdots, d-1 \tag{1.1.12}$$

$$X^d = \frac{1}{2u}\left[1 + u^2\left(-a^2 + \mathbf{x}^2 - t^2\right)\right], \tag{1.1.13}$$

$$X^{d+1} = aut \tag{1.1.14}$$

where $\mathbf{x}^2 = \sum_{i=1}^{d-1}(x^i)^2$. Using the change of coordinate $z \equiv \frac{1}{u}$, we have

$$X^0 = \frac{1}{2z}\left(z^2 + a^2 + \mathbf{x}^2 - t^2\right), \tag{1.1.15}$$

$$X^i = \frac{ax^i}{z}, \quad i = 1, \cdots, d-1 \tag{1.1.16}$$

$$X^d = \frac{1}{2z}\left(z^2 - a^2 + \mathbf{x}^2 - t^2\right), \tag{1.1.17}$$

$$X^{d+1} = \frac{at}{z} \tag{1.1.18}$$

The AdS_{d+1} metric in terms of the coordinates $z, \mathbf{x}^2, t$ is

$$ds^2 = \frac{a^2}{z^2}\left(dz^2 + d\mathbf{x}\cdot d\mathbf{x} - dt^2\right) \tag{1.1.19}$$

Note that the coordinate z behaves as a radial coordinate and divides the hyperboloid (1.1.1) into two different regions called Poincare charts. In particular, we have from the change of coordinate $z = \frac{1}{u}$,

$$\frac{1}{z} = \frac{X^0 - X^d}{a^2} \tag{1.1.20}$$

The first chart corresponds to $z > 0$ where $X^0 > X^d$. This region covers one half of the hyperboloid (1.1.1). The second chart corresponds to $z < 0$, where $X^0 < X^d$ and this region covers the other half of the hyperboloid (1.1.1).

The $d+1$-dimensional Anti de Sitter space has isometry group $SO(2,d)$ with dimensions $\frac{1}{2}(d+1)(d+2)$. For example, the 5-dimensional AdS has isometry group $SO(2,4)$ consisting of 15 isometries. In the boundary theory (defined in Minkowski space), these isometries induce conformal symmetry with 15 generators: 4 special conformal transformations, 6 Lorentz transformations, 4 spacetime translations and 1 dilatation. The isometry group $SO(2,d)$ has maximal compact subgroup $SO(2) \times SO(d)$. In the global coordinates system (τ, ρ, Ω_i), the $SO(2)$ corresponds to the constant translation in the τ direction and the $SO(d)$ corresponds to rotations on the sphere S^{d-1}.

1.1.2 CFT

A Conformal Field Theory (CFT) is a field theory that is invariant under conformal transformations. A conformal transformation in $\mathbb{R}^d$ is a change of coordinates $x \to x'(x)$ such

that the metric in the new coordinates

$$g_{\mu\nu}(x) \to g'_{\mu\nu}(x') = \frac{\partial x^\alpha}{\partial x'^\mu}\frac{\partial x^\beta}{\partial x'^\nu} g_{\alpha\beta}(x) \tag{1.1.21}$$

is given by

$$g'_{\mu\nu}(x') = \Omega(x) g_{\mu\nu}(x); \quad \Omega(x) > 0 \tag{1.1.22}$$

Conformal transformations preserve angles but not distances. Consider an infinitesimal conformal transformation[8]

$$x^\mu \to x^\mu + \epsilon^\mu(x) \tag{1.1.23}$$

The metric changes to

$$g'_{\mu\nu} \to g_{\mu\nu} + (\partial_\mu \epsilon_\nu + \partial_\nu \epsilon_\mu) \tag{1.1.24}$$

In flat Minkowski space, $g_{\mu\nu} = \eta_{\mu\nu}$, conformal transformations obey

$$\partial_\mu \epsilon_\nu + \partial_\nu \epsilon_\mu = 2\omega(x)\eta_{\mu\nu} \tag{1.1.25}$$

The conformal Killing equation follows by taking the trace, to learn $\omega(x) = \frac{\partial\cdot\epsilon(x)}{d}$, so that

$$\partial_\mu \epsilon_\nu + \partial_\nu \epsilon_\mu = \frac{2}{d}\left(\partial \cdot \epsilon\right)\eta_{\mu\nu} \tag{1.1.26}$$

and $\Omega(x) = 1 + \frac{2}{d}\left(\partial \cdot \epsilon\right)$. Note that for $d = 2$, the conformal Killing equation becomes the Cauchy-Riemann equations

$$\partial_1 \epsilon_1 = \partial_2 \epsilon_2, \quad \partial_1 \epsilon_2 = -\partial_2 \epsilon_1 \tag{1.1.27}$$

For $d > 2$, we have the following solutions to the conformal Killing equations:

1. $\epsilon^\mu = a^\mu$ correspond to spacetime translations,
2. $\epsilon^\mu = \omega^\mu_\nu x^\nu$ correspond to rotations,
3. $\epsilon^\mu = \lambda x^\mu$, $(\lambda > 0)$ correspond to scale transformations or dilatations,
4. $\epsilon^\mu = b^\mu x^2 - 2x^\mu(b \cdot x)$ correspond to special conformal transformations.

The general solution to (1.1.26) is then[8, 9]

$$\epsilon^\mu = a^\mu + \omega^\mu_\nu x^\nu + \lambda x^\mu + b^\mu x^2 - 2x^\mu(b \cdot x) \tag{1.1.28}$$

where the parameters a^μ, ω^μ_ν, λx^μ and b^μ correspond respectively to translations, Lorentz rotations, dilatation and special conformal transformations. The tensor $\omega_{\nu\mu}$ is antisymmetric. There is a total of $\frac{(d+1)(d+2)}{2}$ parameters. The conformal transformations form the group $SO(d, 2)$ known as the conformal group. The corresponding generators of translations, Lorentz rotations, dilatation and special conformal transformations are denoted by P^μ, $M^{\mu\nu}$, D and K^μ respectively. Using (1.1.28) we can obtain differential operators that implement the conformal transformation $x^\mu \to x^\mu + \epsilon^\mu$. Concretely the differential operators which represent the generators of conformal transformations must obey

$$(ia_\nu P^\nu + i\omega_{\alpha\nu}M^{\alpha\nu} + i\lambda D + ib_\nu K^\nu)x^\mu = a^\mu + \omega^\mu_\nu x^\nu + \lambda x^\mu + b^\mu x^2 - 2x^\mu(b \cdot x) \tag{1.1.29}$$

It is now easy to see that we have the following differential operators

$$P^\mu = -i\partial^\mu \tag{1.1.30}$$
$$M^{\mu\nu} = -i\left(x^\mu\partial^\nu - x^\nu\partial^\mu\right) \tag{1.1.31}$$
$$D = ix_\mu\partial^\mu \tag{1.1.32}$$
$$K^\mu = -i\left(x^2\partial^\mu - 2x^\mu x\cdot\partial\right) \tag{1.1.33}$$

Now that we have reviewed AdS spaces and CFT theories, we will review how parameters are related on both sides of the correspondence.

1.1.3 Relation between parameters

String theory on $AdS_5 \times S^5$ has two parameters: a string coupling constant g_s and string length l_s. In addition to this, we have the curvature radius R of $AdS_5 \times S^5$. In $\mathcal{N} = 4$ super Yang-Mills theory, we have the rank N of the gauge group $U(N)$ and the gauge coupling constant g_{YM}. This constant is related to 't Hooft coupling $\lambda \equiv g_{YM}^2 N$. These parameters are related as follows

$$g_s = g_{YM}^2 = \frac{\lambda}{N} \qquad\qquad \frac{R^4}{l_s^4} = \lambda = g_{YM}^2 N \tag{1.1.34}$$

An important limit for the gauge theory is known as 't Hooft limit and has been discussed in [1]. 't Hooft showed that while taking N large and keeping $g_{YM}^2 N$ fixed, only planar Feyman diagrams contribute to the expansion. In this limit, the string coupling $g_s \to 0$ corresponding to a weak coupling limit of the string theory. Another important comment is that when $\lambda \ll 1$, we have $R \ll l_s$. This means that the curvature radius is much smaller than the string length. As a consequence, curvature corrections should be considered in this case. But when $\lambda \gg 1$, the curvature radius is very large compared to the string length and curvature correction can be neglected. At lower energies where type IIB string theory in $AdS_5 \times S^5$ is well approximated by supergravity, we must take $\lambda \gg 1$ which corresponds to the strong coupling limit of the CFT. Therefore, one can learn about a strongly coupled gauge theory (a theory where all the perturbative approaches fail) using a weakly coupled string theory and this is called strong/weak coupling duality. Since it is a duality between strongly coupled and weakly coupled theories, it is difficult to give a proof of it, but it is possible to check consequences of the duality on the two sides by comparing the physics from both sides. If the correspondence is true, then the symmetries enjoyed by the two theories should match, as well as all other physical quantities. All this amounts to the study of the AdS/CFT dictionary and we briefly introduce this in section 1.2.

1.2 AdS/CFT dictionary

The AdS/CFT duality states that the physics on the two sides of the correspondence is equivalent. This means that there is a one-to-one correspondence between physical quantities on both sides. Here we discuss the correspondence between symmetries and field/operators.

1.2.1 Matching symmetries

According to the duality, there is matching between symmetries on both sides of the theories. To clarify this, consider the duality between type IIB/$\mathcal{N}=4$ SYM. The $\mathcal{N}=4$ SYM theory is a theory with large symmetry namely super conformal invariance. In particular, the theory has Poincare invariance and scale invariance. The $\mathcal{N}=4$ appearing in the theory is the number of supersymmetries the theory has. AdS_5 is an AdS space in 5-dimensions. The S^5 is a 5-dimensional sphere. The isometries (symmetry) group of AdS_5 is $SO(2,4)$. This is simple to see by embedding the 5-dimensional AdS in a 6-dimensional flat space $\mathbb{R}^{4,2}$ with metric (1.1.3). Then the AdS_5 can be described as the hyperboloid (1.1.1). The symmetry group of S^5 is $SO(6)$. So the full bosonic symmetry group of $\mathrm{AdS}_5 \times S^5$ is $SO(2,4) \times SO(6)$. The 4-dimensional SYM theory also has $SO(2,4)$ symmetry realized as the conformal group. This group includes Poincare transformations, scale transformations as well as special conformal transformation. In addition, $\mathcal{N}=4$ SYM carries six real scalars fields ϕ^i, $i = 1, \cdots, 6$ associated with the group $SO(6) \approx SU(4)$ which corresponds to the R-symmetry group of the theory. The symmetry group of the bulk $\mathrm{AdS}_5 \times S^5$ agrees with the global symmetry of the boundary theory. The identification of the symmetry group of AdS with the conformal symmetry of the CFT suggests that the extra dimension of the bulk is associated with the energy scale of the boundary and this is referred to as the **scale/radius correspondence**. To be more precise, consider an AdS space in $d+1$ dimensions in Poincare coordinates with metric

$$ds^2 = \frac{R^2}{z^2}(dz^2 + \eta_{\mu\nu}dx^\mu dx^\nu) \tag{1.2.1}$$

where z is the extra dimension of the bulk AdS. A scale transformation $x^\mu \to \beta x^\mu$, $\mu = 0, \cdots, d$ leaves the theory invariant if the extra diemension in the bulk transforms as $z \to \beta z$. Under this transformation, the energies on the boundary rescale as $E \to \frac{E}{\beta}$. This suggests $\frac{1}{E} \sim z$. In particular, the boundary $z = 0$ of the bulk corresponds to the UV in the gauge theory.

1.2.2 Mapping between bulk fields and boundary operators

A most important aspect of the AdS/CFT dictionary is the mapping between fields in the bulk and operators on the boundary. The correspondence identifies a bulk field ϕ with a boundary operator $\mathcal{O}$ and this is called bulk field/boundary operator correspondence. An example of the correspondence between bulk field and boundary operator was given in [10] relevant to the case of type IIB string theory on $AdS_5 \times S^5$ and $\mathcal{N}=4$ super Yang-Mills theory in 4 dimensions. We first discuss the general context of the mapping and then consider how the correspondence relates the mass of a free scalar field to the scaling dimension of the boundary operator. Generally, for every field $\phi(x,z)$ in the bulk, we have a local gauge invariant operator $\mathcal{O}(x)$ in the gauge theory. z is the radial coordinate which vanishes at the boundary of the bulk. Consider an AdS_{d+1} spacetime and denote by $\phi_0(x)$ the restriction of ϕ to the boundary. Then, according to the correspondence, we have a coupling $\int_{S^d} \phi_0 \mathcal{O}$ where S^d is the boundary. The expectation value of the boundary operator is related to the asymptotic behaviour of the bulk field. One can also use symmetry to relate a bulk field to a boundary operator. An example is a conserved current on the boundary which has global

symmetry and it is coupled with the dynamics of a gauge field in the bulk[11]. Also, there is a map between the mass of the bulk field and the scaling dimension of the operator on the boundary. To clarify this, consider the mapping between a field ϕ in the bulk and an operator $\mathcal{O}$ in the boundary. According to AdS/CFT correspondence, the dynamics on both sides of the correspondence are identical and so we can write[10]

$$Z_{\text{boundary}} = Z_{\text{bulk}} \tag{1.2.2}$$

where Z is the partition function. In particular, for an operator $\mathcal{O}$ in the conformal field theory with scaling dimension Δ, the two point correlation function can be written as

$$\langle \mathcal{O}(x_1)\mathcal{O}(x_2)\rangle \sim \frac{1}{|x_1 - x_2|^{2\Delta}} \tag{1.2.3}$$

for two distinct points x_1 and x_2. Assume ϕ_0 is the boundary value of the field ϕ. Then the action of the bulk in terms of ϕ_0 results from the coupling between $\mathcal{O}$ and ϕ_0

$$\left\langle e^{\int d^d x \phi_0 \mathcal{O}} \right\rangle_{CFT} = Z_{\text{bulk}}(\phi_0) \tag{1.2.4}$$

A consequence of (1.2.4) is the formula

$$\Delta = \frac{d}{2} + \sqrt{\frac{d^2}{4} + m^2} \tag{1.2.5}$$

This is a relationship between the scaling dimension Δ of the operator $\mathcal{O}$ in the boundary and the mass m of the massive field in the bulk. In particular, for the correspondence between AdS_5 and $\mathcal{N} = 4$ SYM where we have $d = 4$, (1.2.5) becomes

$$\Delta(\Delta - 4) = m^2 \tag{1.2.6}$$

It is visible from (1.2.6) that there is a relationship between the mass m of the field in AdS_5 and the scaling dimension Δ of the operator $\mathcal{O}$ in $\mathcal{N} = 4$ SYM.

1.3 Black holes as fast scrambler

Over the last few years, theoretical physicists have studied the physics of black holes. Understanding the physics of black holes is one of most important applications of the AdS/CFT correspondence. A black hole is a region in space where gravitational forces are so strong that even light cannot escape. Gravity is so strong because matter has been compressed into a tiny space. From the point of view of general relativity, a mass that is sufficiently compact can deform spacetime, resulting in a black hole. One of the most important puzzles in theoretical physics in the past few years is called the black hole information loss paradox. The paradox was originally formulated by Stephen Hawking. Basically, Hawking showed that pure states will evolve into mixed states in the process of black hole formation and subsequent evaporation. This contradicts the dynamics of quantum mechanics which says that time evolution is unitary so that pure states must evolve into pure states. Since the

evolution in CFT is unitary we know that there must be an error in Hawking's argument, but even today it is not clear where that error is. From the perspective of quantum gravity and quantum information theory, studying scrambling is relevant for the so-called black hole information paradox. Black holes scramble (or thermalize) information at the fastest possible rate for any quantum field theory (QFT)[12]. Early investigations based on the dynamics of black holes revealed that fast scrambling is important to learn about the information that is released from the black hole [13]. The work from [14] suggested that the time necessary for a black hole to radiate the information that is stored in it corresponds to the time necessary to emit half of its entropy. In particular, the information that is stored in a black hole is quickly scrambled by the black hole's internal degrees of freedom. Based on the theory of quantum information and string theory, [12] formulate the following conjecture about fast scrambling:

- the time scale for the most rapid scramblers is logarithmic in the number of degree of freedom.
- Black holes are fast scramblers.

They also consider matrix model quantum mechanics proving that systems whose degrees of freedom are n by n matrices saturate the bound. In chapter 2, we study the thermalization time associated with black holes in general relativity using the $\mathcal{N} = 4$ super Yang-Mills theory.

1.4 Holography as quantum error correction code

Understanding holography using quantum error correcting codes has been a hot topic recently. The AdS/CFT correspondence is a holographic duality relating a bulk theory in $d+1$ dimensions on asymptotically AdS spacetime and a boundary theory in d dimensions. Remarkably, recent work has argued that information about the bulk is coded into the boundary in much the same way that information is coded into quantum error correcting codes. A fascinating ingredient of the duality is the relation between AdS geometry and CFT entanglement. In particular, Ryu and Takayanagi discussed the correspondence between area in the bulk and entanglement entropy on the boundary[15, 16]. Given a subregion $\mathcal{R}$ of the CFT, Ryu and Takayanagi proposed that the entanglement entropy of $\mathcal{R}$, to leading order, is given by

$$S(\mathcal{R}) = \frac{\text{Area}(\Gamma_{\mathcal{R}})}{4G} \tag{1.4.1}$$

where $\text{Area}(\Gamma_{\mathcal{R}})$ is the area of the minimal surface $\Gamma_{\mathcal{R}}$ in the bulk homologous to $\mathcal{R}$ and G is the Newton's constant. This formula provides the correspondence between the entanglement entropy of a subregion $\mathcal{R}$ in the CFT and the geometry of the dual AdS.

Operators in the bulk have different descriptions in the boundary. This leads to the question of which operator of the bulk can be reconstructed on a specific subregion of the boundary. This idea has been discussed in[17, 18] and it is formulated in the language of entanglement wedge reconstruction, which states that an operator in the bulk can be reconstructed on a subregion $\mathcal{R}$ of the boundary if and only if it is localized in the entanglement wedge $\varepsilon_{\mathcal{R}}$. The entanglement wedge $\varepsilon_{\mathcal{R}}$ is the domain surrounded by $\mathcal{R}$ and $\Gamma_{\mathcal{R}}$. A proposal

to explain the mapping between bulk and boundary as a quantum error correcting code was proposed in [19]. In this analysis, local operators in the bulk are interpreted as operators on a given subspace of states in the boundary, where the entanglement structure of the CFT operators are preserved from boundary erasure. With an appropriate code subspace, we discuss in section 3 that bilocal holography reproduces entanglement wedge reconstruction of holography.

1.5 Non-Perturbative String Theory from AdS/CFT

We end this introductory chapter with a few general questions that are closely related to the main goals of this thesis. $\mathcal{N} = 4$ super Yang-Mills theory is holographically dual to string theory on asymptotically $AdS_5 \times S^5$ spacetime[2, 10, 20]. This implies that all excitations appearing in the spectrum of string theory must appear in the conformal field theory (CFT) Hilbert space. The usual perturbative spectrum (which consists of supergravity excitations, as well as closed strings) is captured by the planar limit of the dual CFT[21]. There are also many non-perturbative objects, including branes[22, 23, 24, 25] and new spacetime geometries[26, 25, 27], an interesting example being spacetimes containing black holes, that must be found in the CFT Hilbert space[28, 29]. In Chapter 2 for example, we explore operators that are dual to new spacetime geometries. These non-perturbative configurations are dual to operators with a bare dimension that grows parametrically with N ($\sim N$ for branes or $\sim N^2$ for new spacetime geometries). To explain how this works, consider the half-BPS sector where a useful basis for the operators of the theory is given by the Schur polynomials. Consider a Schur polynomial labeled by a Young diagram consisting of a single column, $\chi_{(1^J)}(Z)$ of J boxes. For $J \sim O(1)$ the operator is dual to a collection of (point like) KK-gravitons. As J is increased to $J \sim O(\sqrt{N})$ long single trace operators dual to stringy states start to participate. Increasing J further to $O(N)$ we obtain a giant graviton brane. Thus, the dual to the single CFT operator $\chi_{(1^J)}(Z)$ transitions through different physical descriptions (particles, strings and branes) as the parameter J is varied. It is natural to ask how these different partial representations are combined into a single coherent description.

The character of the large N expansion changes as we transition between these different partial representations. For $J \ll \sqrt{N}$ we can take the usual 't Hooft limit and the large N theory is just the planar limit. As N goes to infinity and $J \gg \sqrt{N}$ one must sum much more than just the planar diagrams (see [24, 30] for clear and relevant discussions). For this reason we refer to these limits as large N but non-planar limits. In large N but non-planar limits one does not have the usual $1/N$ expansion. The ribbon graph expansion is not of much help because enormous combinatorial factors imply that the usual higher genus suppression is overwhelmed by the sheer number of diagrams of a given topology[24]. Different trace structures do mix and it is not at all clear how the large N expansion can usefully be organized. This is a key question that we wish to address, albeit in the limited setting of a specific example. A nice class of correlators that we will use to explore this issue are three point functions of $\frac{1}{2}$-BPS operators as well as extremal n-point functions of $\frac{1}{2}$-BPS operators. There are rigorous non-renormalization theorems[31] that prove that these correlators do not receive 't Hooft coupling corrections. Thus, they can be computed exactly, in the free field theory limit. Even this problem is one of considerable complexity, due to the very large dimensions of the operators. Fortunately, using techniques based on group representation

theory, this problem has been completely solved in [25, 43] for operators constructed using a single field (say Z) and in [44] for operators constructed using more than one matrix (see also [46, 47, 48]). Using these results it is possible to explain the structure of the $1/N$ expansion for some correlation functions of giant graviton branes [45]. This is a small first step towards defining the structure of the $1/N$ expansion in large N but non-planar limits.

Since $\hbar$ of the dual gravitational system is $1/N$, the different large N limits that can be taken lead to different classical configurations of the gravitational theory. This is inline with conventional wisdom: when performing a path integral quantization there are many possible saddle points so that typically a quantum system has many perturbative series, each associated to a different classical configuration. These series are the basic building blocks in many computations. Although summing a few terms gives a good approximation, these series are almost always divergent. One needs a theory that can organize these different series into a coherent description of the quantum system. This is precisely what the theory of resurgence does. The first step entails converting the divergent series into meaningful objects by Borel resummation in the perturbation parameter. Typically one considers a loop expansion and the small parameter is $\hbar$. The second step entails exhibiting a relation between the different series, which is manifested through the Stokes phenomenon[1]. This relation implies that, given a specific series, the discontinuities of its Borel transform encode the information about other series in the problem. In this way, one can (for example) synthesize the usual perturbative expansion, together with the expansions in the (typically many) different instanton sectors, to recover exact results. From this point of view, the Stokes lines of the perturbative expansion simply demarcate where contributions from other saddle points become dominant.

Given this discussion, it seems that resurgence has a crucial role to play in understanding the large N limit of Yang-Mills theories. Specifically, resurgence should be relevant to understand how the different representations (i.e. the different possible large N limits) fit together to provide a complete and coherent description. If the ideas of resurgence are relevant, there should be a Stokes phenomenon present as the parameter J (and not $\hbar$) is varied. As a first step in exploring this possibility, the paper [45] looks for and exhibits this Stokes phenomenon. The problem is approached using the exact WKB method[32]. The different perturbative series that appear are the WKB series around different classical trajectories. The basic objects are the (Borel resummed) perturbative series in $\hbar$. The series can be characterized by two types of data: their classical limit and their discontinuity structure[32, 33, 34], which is encoded in the action of the so-called Stokes automorphisms. A simple characterization of the Stokes discontinuities is in terms of Voros symbols, which are simply the exponent of the WKB series. The analysis of [45] starts with the observation that the (square of the) correlators we compute can be expressed in terms of the hypergeometric ${}_2F_1(a, b; c; x)$ function. This is a useful observation because the differential equation obeyed by the hypergeometric function is easily mapped into a Schrödinger equation, which can be approached using an exact WKB analysis. The relevant Schrödinger equation has $1/N$ playing the role of $\hbar$ so that the WKB expansion of the wave function of this Schrödinger equation gives the $1/N$ expansion of our correlator. Fortunately, the relevant Schrödinger

[1]The Stokes phenomenon is the basic fact that, in general, Borel resummations are discontinuous along rays in the complex plane. These rays are the Stokes and anti-Stokes lines.

equation has been studied in detail in [35, 36, 37, 38, 39]. In particular, the Voros symbols have been studied and their singularity structure in the WKB plane is well understood. The relevant WKB solutions have been proved to be Borel summable[40]. The solutions do exhibit Stokes phenomena in the parameter J and this has been studied in detail: the Stokes lines and Stokes regions for this equation can be described quite explicitly and connection formulas relating solutions in different Stokes domains are known. This implies that the singularities of the Borel transforms of the WKB solutions are well understood and that the Alien calculus for this problem is completely worked out[35, 36, 37, 38, 39]. These are the only ingredients needed to give the trans-series expansion for the hypergeometric function and hence of giant graviton correlators. For three point functions of operators dual to giant gravitons, that have a dimension of order N, [45] argues that the large N expansion takes the form (j_1 and j_2 are both strictly less than but of order 1)

$$\langle O_{A_{Nj_1}} O_{A_{Nj_2}} O_{A_{N(j_1+j_2)}} \rangle = e^{-Nj_1j_2} \sum_{n=1}^{\infty} c_n N^{-n} \tag{1.5.1}$$

A_{Nj_1} is a Young diagram with a single column of $j_1 N < N$ boxes, and $j_1 + j_2 \leq 1$. There is a similar result for the three point function of three dual giant gravitons. This is a non-perturbative result since the exponential factor can not be expanded in $1/N$. The exact correlator is therefore the product of a non-perturbative factor with a perturbative factor. The non-perturbative contribution has been explained using instanton configurations [41] in the tiny graviton theory. The tiny graviton matrix model[42] is a proposal for the discrete lightcone quantization of IIB string theory on the maximally supersymmetric ten-dimensional plane wave. It is a matrix quantum mechanics of $J \times J$ matrices. Instanton solutions of the model were studied in [41]. Remarkably, the instanton induced splitting and joining of giant gravitons developed in [41] is in complete agreement with the correlation functions of normalized Schur polynomials. It would be interesting to evaluate $\frac{1}{N}$ corrections in the tiny graviton theory and see if the subleading terms in (1.5.1) can be reproduced. Further, [45] argues that after the non-perturbative factor in (1.5.1) is removed, the correlator admits a $1/N$ expansion that is Borel summable. The Stokes lines across which the Borel sum has a discontinuity occur at the values of J at which we transition from one partial representation (as a brane) to another partial representation (as a string) of the holographic dual to the CFT operator. As we described above, the dual to a single CFT operator transitions through different physical descriptions (particles, strings and branes) as the dimension of the operator is varied. We vary the dimension smoothly and the variation of the CFT correlators is not singular at all. The reorganization of the $1/N$ expansion however changes discontinuously as a consequence of moving between the different descriptions. The results of [45] suggest that the transition between different representations are accompanied by a Stokes phenomena and it is natural to expect that resurgence will play a role when these different partial representations are combined into a single coherent description.

The paper [45] considers general extremal correlators between giant gravitons and between dual giant gravitons. The complete class of extremal correlation functions of Schur polynomials is much more general. It would also be interesting to study correlators involving operators with a dimension of order N^2, like those constructed in Chapter 2 of this thesis. These would have a gravitational interpretation in terms of physics in an LLM geometry[26],

so that one is probing a back reacted version of the $AdS_5 \times S^5$ spacetime. It is interesting to ask what the structure of the large N expansion in this case is? Once again the extremal correlation functions (corresponding to no excitation of the Gauss graph, in the language of Chapter 2) can be evaluated exactly. In simple examples [63] for well chosen backgrounds, the only effect on the extremal correlators is a renormalization $N \to N_{\text{eff}}$. The perturbative expansion in this LLM background becomes an expansion in $\frac{1}{N_{\text{eff}}^2}$, which suggests that the closed string coupling constant g_s has been renormalized. This same effect has also been observed beyond the half-BPS sector [64, 65, 66, 67]. Does this renormalization of N persist when non-perturbative corrections are considered? This could be probed by studying giant graviton correlators in the LLM background. If the closed string coupling is renormalized, then the tension of the D3-brane $\sim \frac{1}{g_s}$ should be renormalized and we do expect the renormalization of N to persist.

The true power of resurgence only comes into play when we have many non-perturbative sectors as well as a perturbative sector. Resurgence then relates the series in these different sectors (see [61] for recent results and references). Extremal giant graviton and dual giant graviton correlators have only a single sector. Further, the form of our extremal correlators makes it likely that we need to go beyond the half-BPS sector for correlators that have more than a single sector. The operators that we introduce in the next Chapter are natural candidates.

2 Scrambling in Yang-Mills

2.1 Introduction

Black holes in general relativity exhibit incredibly fast relaxation time scales. Since the AdS/CFT correspondence claims an equivalence between conformal field theories in d dimensions and theories of quantum gravity on negatively curved spacetimes[2, 10, 20], the mechanism behind these extremely rapid thermalization rates should be coded into the dynamics of large N and strongly coupled conformal field theories. Motivated by this issue we study scrambling and equilibration in $\mathcal{N} = 4$ super Yang-Mills theory, with gauge group $U(N)$. There are at least two features of our study that must be improved before we can make contact with the physics of black holes. First, operators in the conformal field theory corresponding to a black hole necessarily have a very large dimension $\Delta \sim N^2$. The generic operator is constructed using the complete collection of fields in the theory. Although our operators have a dimension of order N^2, they are special in that they are constructed using three complex adjoint scalars and two complex adjoint fermions. Second, the link to classical gravity emerges in the strong coupling limit of the field theory. Our analysis is limited to weak coupling. However, we will see that our simplified system is already interesting.

Recall that the AdS/CFT correspondence identifies the dimensions of operators in the conformal field theory with the energies of energy eigenstates in the dual gravitational theory. This has been pursued in exquisite detail in the planar limit of $\mathcal{N} = 4$ super Yang-Mills theory[70], where the identification of the dilatation operator D with a Hamiltonian is particularly fruitful because D is the Hamiltonian of an integrable spin chain. The energy of a spin chain state equals the dimension of the corresponding operator. The dynamics of the worldsheet string theory is also integrable [71] and there is an exact match between string theory energies and operator dimensions [72]. Although integrability allows us to go beyond weak coupling, the planar limit is not the correct arena for the questions we consider. Indeed, integrable systems do not thermalize in the conventional way: they do not thermalize to a Gibbs ensemble. Integrable systems thermalize into a "generalised Gibbs ensemble" due to the existence of many extensive conserved charges. This is well understood for integrable systems relaxing after a quantum quench[73]. Further, completely integrable models can never exhibit chaos, but the holographic dual to a black hole is expected to exhibit chaotic dynamics [74].

An interesting extension beyond the planar limit considers operators whose bare dimension grows parametrically with N as we take $N \to \infty$. The mixing problem of these heavy operators has new complications absent in the planar limit: single trace operators can and do mix so multi trace structures must be included in the problem and they all mix in a non-trivial way. A second complication is that the sheer number of non-planar diagrams is so big that it overcomes the usual higher genus suppression and we must sum more than just the planar diagrams [24, 75, 76]. The final complication arises because as the number of fields in the multi trace operator grows beyond N there are trace relations which express the equality of naively distinct multi trace structures[2]. Starting with [25] methods based on

[2]For example, invariants of a single matrix are written in terms of the eigenvalues of the matrix. Given N independent invariants, the eigenvalues and hence all invariants are determined. As a consequence, there

group representation theory were employed to address all three of these issues in a single complex matrix model. A linear basis for multi-matrix invariants, the restricted Schur polynomials, which we use in this work, is constructed in [44, 50] (see also [77]). Although we will not use them in our study, note that closely related bases were introduced and studied in [46, 47, 48, 78]. The restricted Schur polynomials are labeled by a collection of Young diagrams, one for each species of field appearing in the operator, plus one more denoted R for the complete collection of fields. They diagonalize the free field theory two point function, explicitly take all finite N trace relations into account and mix only weakly at one loop. Summing the complete set of ribbon graphs contributing to a free field theory correlator is reduced to rather straight forward manipulations in group theory: the computation of projection operators and matrices representing permutations, as well as commutators, products and traces of them.

Our focus is on operators constructed using $O(N^2)$ fields. The majority of the fields appearing in the operators we study are a single complex adjoint scalar (say ϕ_1). There are a smaller number of additional scalar (ϕ_2 and ϕ_3) as well as fermion (ψ_1 and ψ_2) fields, all transforming in the adjoint of $U(N)$. We will use n_i to denote the number of ϕ_i fields and m_i to denote the number of ψ_i fields. In the limit where the row lengths of the Young diagram R labeling the restricted Schur polynomials are all different, with the difference $\gg 1$ (called the displaced corners approximation [79, 80] because the corners on the right hand side of the Young diagram are well separated) the mixing problem simplifies dramatically. New symmetries appear and these naturally suggest that the state space can be labeled with a pair of Young diagrams (describing the ϕ_1 fields and one more, denoted R, for the complete collection of fields) and a graph for the remaining fields [80, 81]. The mixing problem can be diagonalized on the Young diagram labels, leaving a Hamiltonian describing dynamics on a graph[82, 83]. Vertices of the graph correspond to rows (for a short and wide diagram) or columns (for a tall and thin diagram) of the Young diagram R and hence they correspond to dual giant and giant graviton branes. As a consequence of the displaced corners condition the branes are separated in spacetime. Edges stretching between vertices correspond to open strings that stretch between branes. In a suitable adiabatic limit, reviewed in Appendix A, these modes are frozen, i.e. they do not evolve in time. Each brane can be excited, which is represented as a closed loop made out of a single edge attached to a given vertex. In the adiabatic limit these excitations of a particular brane are the only dynamical degrees of freedom. These degrees of freedom live at the vertices of the graph and they are able to hop to any other site as long as there is an edge in the graph that connects the two sites [82, 83].

Thus, the spin chain of the planar mixing problem is replaced by dynamics on a graph, when the mixing problem of heavy operators is considered. It is noteworthy that dynamics on a graph naturally emerges in this way. Indeed, models describing the dynamics on graphs were used to examine the fast scrambling conjecture[12], first in [84], which was followed by a number of interesting articles[85, 86, 87, 88, 89, 90][3]. The logic of [84] is elegant and

are relations between invariants expressed as a collection of terms that sum to zero. Each term is of a fixed degree in the matrix and different terms have different trace structures. An example of a relation of this type is provided by the Cayley-Hamilton Theorem and by the Mandelstam relations [205].

[3]These studies use an "interaction graph". Degrees of freedom live at the vertices of the interaction graph. The interaction graph has an edge between two vertices if and only if the Hamiltonian includes an interaction term for these degrees of freedom. There is a simple relation between the graph that emerges

worth summarizing. Consider a state of some subsystem S, and denote the complementary subsystem to S by S^c. By saying that information is scrambled we mean it is hidden in complicated correlations between subsystems S and S^c. Using this observation one can argue that scrambling subsystem S is the same as signaling to S^c. Thus, bounds on signaling are immediately bounds on scrambling. With this insight, [84] appeals to classic methods of Lieb-Robinson[91] which bound signaling by proving bounds on commutators $[O_A(t), O_B]$ where O_A and O_B are observables localized on disjoint subsystems A and B of a lattice spin system. In this way [84] bound the signaling time for Hamiltonians with dense two body interactions[4] to no faster than $O(\log n)$ with n the number of degrees of freedom. The resulting bound refers to the maximum degree D_V of any vertex of the interaction graph. D_V also appears in the assumption that each term in the Hamiltonian is bounded by c/D_V with c some constant that does not scale with the size of the system. The Lieb-Robinson bound then says that a suitably normalized commutator is bounded by $\sim \frac{1}{D_V} e^{8ct}$. Using this bound, its now possible to show that for times $\sim \log D_V$ the reduced density matrix on each site i is approximately a pure state. D_V is the maximum vertex degree, so we expect $D_V \sim n$. Since scrambling requires entanglement, this bounds the scrambling time to be at least $\sim \log n$.

In this chapter we study the dynamics of the Hamiltonian defined by the mixing problem for heavy operators, described by dynamics on a graph. The relevant Hamiltonian is described in Section 2.2. Our Hamiltonian describes the physics of bound states of giant gravitons and their excitations. The number of giants in the boundstate is large enough to backreact and produce a new spacetime geometry[26]. By choosing the right boundstate of giant gravitons excited in a particular way, we would produce operators dual to black holes. A black hole state would have a number of general features that one could look for[5]. First, the mass of the black hole in AdS translates, upon using the standard AdS/CFT dictionary, into a scaling dimension for operators that grows as $\Delta \sim N^2$. To explain the entropy of the black hole, the number of operators should be $\sim e^{bN^2}$ with b some constant that does not depend on N. We verify these expectations in Section 2.3. Each operator is labeled by a different graph and hence by a different Hamiltonian. By numerically generating the complete set of graphs for finite values of N (where numerical analysis is still possible), we give evidence that there is a "typical" graph and that almost every graph, at large N, looks like the typical graph. This typical graph defines a typical Hamiltonian and it is the dynamics of this typical Hamiltonian that we consider. In Section 2.4 we study scrambling, establishing a Lieb-Robinson bound which ensures that the system does not scramble faster than the bound implied by the fast scrambling conjecture. We also explore entanglement generation for the typical dynamics. The leads to a puzzle: the recurrence time is much smaller than we expect. In Section 2.5 we show for a conveniently chosen initial non-equilibrium state, that the system evolves to thermal equilibrium and we estimate the thermalization time scale. The puzzle of the recurrence time is also resolved: we argue that as far as the dynamics is concerned, the typical Hamiltonian is rather special and does not give a reliable description of the physics. Small fluctuations in the typical Hamiltonian are important and must be

from Yang-Mills theory, called a Gauss graph in [81] and the interaction graph: dropping the closed loops from the Gauss graph one obtains the interaction graph. We stick to this terminology in this article.

[4]Dense means the number of interacting pairs of degrees of freedom scales like n^2.

[5]For a very readable and informative discussion we recommend [28, 92, 93].

included. In Section 2.6 we discuss our results and outline some future directions.

2.2 Dynamics on Gauss graphs

As reviewed in Appendix A the dynamics we consider is of a system of bosons, hopping on a lattice. The lattice is defined by a directed graph $G = (V, E)$, where V is a set of vertices and E a set of directed edges. In what follows we always use $p = |V|$ to denote the total number of vertices. Since the edges are directed it makes sense to talk about edges departing from a vertex or edges arriving at a vertex. Not just any directed graph is allowed; at each vertex the number of arriving edges must equal the number of departing edges.

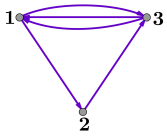
The bosons live at the vertices of the graph. Thus at each vertex $i \in V$ we have a bosonic Fock space $\mathcal{F}_i$. The full Fock space is a tensor product $\mathcal{F} \equiv \mathcal{F}_1 \otimes \mathcal{F}_2 \otimes \cdots \otimes \mathcal{F}_p$. Associated to the ith Fock space is a pair of oscillators $b_i, b_i^\dagger$ and a vacuum state $|0\rangle_i$. The oscillators $b_i, b_i^\dagger$ act as the identity on all $\mathcal{F}_j$ with $j \neq i$, and in the usual way on $\mathcal{F}_i$. The algebra of the bosonic operators is

$$[b_i, b_j^\dagger] = \delta_{ij} \tag{2.2.1}$$

The ith Fock space vacuum obeys $b_i|0\rangle_i = 0$ and the vacuum of the full Fock space $\mathcal{F}$ is given by

$$|0\rangle = |0\rangle_1 \otimes |0\rangle_2 \otimes \cdots \otimes |0\rangle_p \tag{2.2.2}$$

To write the Hamiltonian describing the dynamics of these bosons, it is useful to introduce the $p \times p$ matrix N_{ij}. The matrix elements N_{ij} count how many edges stretch between vertices i and j, regardless of orientation. As far as the Hamiltonian is concerned, we can ignore the orientation of edges which corresponds to treating G as an undirected graph. Thus, N_{ij} is a symmetric matrix with zeros on the diagonal, that completely determines the graph G. As an example, consider the following graph



$$N_{ij} = \begin{bmatrix} 0 & 1 & 3 \\ 1 & 0 & 1 \\ 3 & 1 & 0 \end{bmatrix} \tag{2.2.3}$$

In terms of this matrix, the Hamiltonian we study is given by

$$H = \frac{g_{YM}^2}{(4\pi)^2} \sum_{i,j=1, i\neq j}^{p} (\sqrt{r_i} - \sqrt{r_j})^2 N_{ij} + \frac{2g_{YM}^2}{(4\pi)^2} \sum_{i=1}^{p} \frac{r_i}{l_i} k_i \, b_i^\dagger b_i - \frac{2g_{YM}^2}{(4\pi)^2} \sum_{i,j=1, i\neq j}^{p} \sqrt{\frac{r_i r_j}{l_i l_j}} N_{ji} b_j^\dagger b_i \tag{2.2.4}$$

where

$$r_i = N + l_i \qquad k_i = \sum_{l=1, l\neq i}^{p} (N)_{il} \tag{2.2.5}$$

The parameters of the model are N, l_i, g_{YM}^2, p and the matrix N_{ij}. N sets the rank of the gauge group of the Yang-Mills theory and g_{YM}^2 is the coupling constant. We study the large

N limit, at weak 't Hooft coupling. The parameters l_i, $i = 1, 2, \cdots, p$ are positive integers of order $\sim N$. In the CFT they set the row lengths of Young diagram R labeling our operator. They are ordered so that $l_i > l_j$ if $j > i$. The displaced corners approximation requires that $|l_i - l_j| \gg 1$ for all $i \neq j$. In the holographic dual l_i is the angular momentum of the corresponding dual giant graviton. We are interested in the limit in which p goes to infinity. If we take $p = \epsilon N$ with $\epsilon \ll 1$, we can consider operators with differences in lengths of adjacent rows of R of order $\sim \epsilon^{-1} \gg 1$ which justifies the displaced corners approximation. In the next section we study the graphs relevant for our problem, thereby characterizing the matrices N_{ij}. We focus on graphs with number of edges $|E| \approx p^2 = \epsilon^2 N^2$. In this case, the bare dimension of our operator is $\Delta \sim \epsilon N^2$ and the number of fields scale as $n_1 \sim \epsilon N^2$ and $n_2 \sim n_3 \sim m_1 \sim m_2 \sim \epsilon^2 N^2$ as we take $N \to \infty$.

The spectrum of the Hamiltonian has an interesting structure. The first term in the Hamiltonian is an order ~ 1 number times the 't Hooft coupling $\lambda = g_{YM}^2 N$. This term is a constant, determined by the number of edges and the specific vertices the edges stretch between. The second term is a constant, equal to the total number of bosons hopping in the graph. Since the Hamiltonian preserves particle number we can restrict the dynamics to a subspace with fixed total number of particles. We work on the subspace with N_b bosons hopping on the graph. These first two terms give the largest contribution to the energy eigenvalues. The remaining terms give a much smaller correction to the first two terms. These small corrections resolve the degeneracies of the multiparticle Fock space. In Section 2.4.1 we estimate the size of the terms in the Hamiltonian. The first two terms are of size $\sim \lambda$, and that the remaining terms are of size $\sim \epsilon^2 \lambda$. The dimension of the multi particle Fock space grows very rapidly: for N_b bosons hopping on a graph with p vertices the dimension of the relevant subspace of Fock space is given by

$$dim_{p,N_b} = \frac{(p + N_b - 1)!}{N_b!(p-1)!} \tag{2.2.6}$$

The Hamiltonian we consider computes the one loop anomalous dimension E_1, which corrects the bare dimension, itself of order $E_0 = \epsilon N^2$. The pattern for the possible E_1 values present in the above spectrum, is a set of levels separated by gaps of order $\sim \lambda$, with each level a collection of an enormous numbers of nearly degenerate states, with splitting $\sim \epsilon^2 \lambda$. Using a measuring apparatus that can resolve energy differences $\sim N^2$, but not the much smaller scales $\sim \lambda$ or $\sim \epsilon^2 \lambda$ we would only resolve a coarse grained version of the physics. After coarse graining its not possible to distinguish between these almost degenerate states, so we naturally obtain macrostates with a large entropy. This is a promising start to explain the black hole entropy. One check of this idea is to count the total number of operators that can be defined. Since there is an operator associated to every graph (see Appendix A) the number of graphs should be large enough ($\sim e^{bN^2}$) for this idea to work.

An important technical comment is in order: the studies of the fast scrambling conjecture given in [84, 85, 87, 88] which were an important motivation for this study, make use of the assumption that the Hamiltonian (and other operators) have a finite norm. The Hamiltonian defined in (2.2.4), is unbounded. Thus, it seems that the methods of finite dimensional quantum mechanics can not be used and a careful treatment of the system with the methods of functional analysis [94] is necessary. This conclusion is too hasty and too pessimistic. The Hamiltonian in (2.2.4) conserves particle number. Thus, if we restrict to initial states

with finite particle number, the whole evolution happens in a finite dimensional subspace of the Fock space. In this case the Hamiltonian H and all relevant observables can be represented by bounded operators on this subspace so that we are back in the framework of finite dimensional quantum mechanics[95].

Our Hamiltonian is derived by evaluating the action of the dilatation operator on a specific class of heavy operators in $\mathcal{N} = 4$ super Yang-Mills. It is interesting to note that a closely related model was suggested and studied in [96] as a toy model of black hole dynamics. See also [97, 98] for related work.

2.3 Properties of Gauss Graphs

The graphs arising from the operator mixing problem of Yang-Mills theory were called Gauss graphs in [81]. Gauss graphs are graphs with directed edges and any number of vertices. In addition, at every vertex in the graph, the number of edges terminating on the vertex is equal to the number of edges departing from the vertex. We call this the Gauss constraint. By removing edges that have both endpoints at a single vertex (so these edges form a closed loop) we obtain the interaction graph. Edges of the interaction graph are always stretched between distinct vertices. A directed graph obeying the Gauss constraint is called a *balanced directed graph* [99] in the mathematics literature. In this section we describe an algorithm that can be used to generate the complete set of interaction graphs, given that each graph has p vertices and E edges. The number of interaction graphs grows extremely rapidly so that is makes sense to talk about the "typical graph". We characterize properties of the typical graph, using numerical results. For each interaction graph there is a Hamiltonian. By characterizing the typical graph we are characterizing the typical Hamiltonian. We can then study the scrambling time and relaxation rates of this typical Hamiltonian.

2.3.1 Generating interaction graphs

The key difficulty in generating interaction graphs entails respecting the Gauss constraint. Consider some interaction graph G. Our first observation is that any closed oriented path, made from edges belonging to G, respects the Gauss constraint. Deleting the edges that make up this path produces a new graph G', which itself also obeys the Gauss constraint, i.e. G' is also an interaction graph. We can now repeat the procedure: construct any closed path, made from edges belonging to G'. Delete this new path to find a new interaction graph G''. This procedure can be repeated until all edges in G have been deleted, and so G has been decomposed into a collection of closed paths. To generate the interaction graph G we follow the reverse process in which we "grow" G by dressing a bare set of vertices with closed oriented paths.

Its easy to understand why this decomposition is always possible: choose any given edge in the graph and consider the vertex that this edge ends on. The Gauss constraint guarantees that there is always an edge leaving this vertex, that can be joined with the edge we have to produce the second edge in the path. We can keep growing the path in this way. The growing process terminates when the last edge we consider can be joined with the first edge in the path, producing a closed path. The point is that the Gauss constraint implies that

any edges left after a closed path is deleted, belong to a closed path and hence as long as there are edges left, we can keep making closed paths.

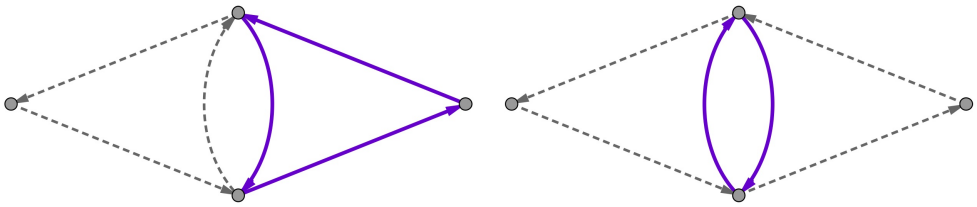


Figure 1: The interaction graph shown can be decomposed into two paths, each of length 3 as shown on the left, or into two paths, one of length 2 and one of length 4 as shown on the right.

The decomposition of an interaction graph into closed paths is not unique. Indeed, consider the example shown in Figure 1. The interaction graph shown, with a total of 6 edges, can be decomposed into two paths of length 3, or into one path of length 4 and one path of length 2.

N_E	N_G	N_C	F	N_G	N_C	F	N_G	N_C	F
2	6	0	0	10	0	0	15	0	0
3	8	0	0	20	0	0	40	0	0
4	27	6	0.22	85	0	0	315	0	0
5	48	24	0.5	224	24	0.11	744	0	0
6	112	64	0.57	660	180	0.27	2 770	120	0.04
7	192	144	0.75	1 640	720	0.44	9 120	1 440	0.16
8	378	291	0.77	4 095	2 285	0.56	29 100	8 370	0.29
9	624	536	0.86	9 360	6 260	0.67	86 600	36 120	0.42
10	1 092	954	0.87	20 910	15 470	0.74	247 176	130 566	0.53
11	1 728	1 584	0.92	44 220	35 520	0.80	671 160	417 960	0.62
12	2 802	2 593	0.93	90 945	76 825	0.84	1 752 230	1 223 520	0.70
13	4 248	4 032	0.95	179 820	158 340	0.88	4 396 200	3 338 760	0.76
14	6 516	6 216	0.95	346 320	313 380	0.90	10 655 670	8 604 660	0.81
15	9 528	9 216	0.97	646 860	598 680	0.93	24 983 264	21 132 744	0.85

Table 1: A table showing how many interaction graphs N_G with p vertices can be constructed using N_E edges. N_C of the graphs are connected. The fraction $F = \frac{N_C}{N_G}$ tells us the probability that a graph selected at random is connected. The first three columns have $p = 4$, the middle three columns have $p = 5$ and the last three columns have $p = 6$.

The algorithm we use to generate interaction graphs is as follows:

1. Partition the total number of edges E in the graph into a sum of path lengths in all possible ways. The Gauss constraint forces paths to have a length of at least 2. For example, a graph with $E = 4$ edges can be realized as two paths of length 2 or one path of length 4. We assume that the interaction graph has a total of p vertices and that these vertices are labeled as $1, 2, ..., p$.

2. Each path can be labeled with an ordered sequence of integers, which records the order in which the different vertices are traversed as one travels on the path. Each path visits

any given vertex at most once. Thus, the integers appearing in a given path label are distinct. In addition, since the path is closed, cyclic shuffling of the integers in the path does not lead to a new path. This makes it clear that the paths of length L can be labeled by permutations that are a single cycle of length L. We now need to sum over combinations of all possible paths consistent with the partition constructed in step 1.

3. The resulting list of interaction graphs will have some duplicates, since the decomposition of a given interaction graph into a collection of paths is not unique. The final step in the algorithm simple deletes the duplicate graphs.

For examples of the number of graphs obtained when using this algorithm, see Table 1. It is noteworthy that the number of interaction graphs grows very rapidly. For example, there are roughly 25 million interaction graphs with 15 edges and 6 vertices. Such enormous numbers justify a statistical approach to the problem.

Before leaving this subsection, we will explain how to count the number of interaction graphs, using methods from information theory used to count Markov types[100]. This counting will enable us to understand the number of interaction graphs as $N \to \infty$. Since the graph is a label for the operator, this will allow us to count the number of orthogonal[6] operators we have and thereby to verify that the growth is enough to explain the entropy of a black hole. Introduce the matrix E_{ij}, $i, j = 1, ..., p$. The off diagonal matrix elements E_{ij} denote the number of edges running from vertex i to vertex j. Clearly E_{ij} is not in general a symmetric matrix[7]. The diagonal matrix elements vanish $E_{ii} = 0$. Our task is to count the number of matrices obeying the equations

$$\sum_{i=1}^{p} E_{ij} = \sum_{i=1}^{p} E_{ji} \tag{2.3.1}$$

and

$$\sum_{i=1}^{p} \sum_{j=1}^{p} E_{ij} = N_E \tag{2.3.2}$$

The equation (2.3.1) is the Gauss constraint and (2.3.2) sets the number of edges in the graph. The number of solutions to (2.3.1) and (2.3.2) is the number of interaction graphs with p vertices and N_E edges, denoted N_{p,N_E}.

Let $\mathcal{E}$ be the set of all integer matrices obeying (2.3.1) and let $\mathcal{E}_{N_E}$ be the subset of matrices belonging to $\mathcal{E}$ that obeys (2.3.2). Given a pair of $p \times p$ matrices E and F, we define

$$F^{*E} \equiv \prod_{\substack{i,j=1 \\ i \neq j}}^{p} F_{ij}^{E_{ij}} \tag{2.3.3}$$

[6]By orthogonal operators, we mean operators which diagonalize the two point function. Thus they would be orthogonal in the Zamolodchikov norm of the conformal field theory.

[7]The relation between E_{ij} and the matrix N_{ij} appearing in (2.2.4) is $N_{ij} = E_{ij} + E_{ji}$.

We would like to evaluate the generating function

$$Z_{\text{Gauss}}(F) = \sum_{E\in\mathcal{E}} F^{*E} = \sum_{n_E\geq 0}\sum_{E\in\mathcal{E}_{n_E}} F^{*E} \tag{2.3.4}$$

Evaluating this generating function at $F_{ij} = z$ and using the obvious fact

$$\sum_{E\in\mathcal{E}_{n_E}} F^{*E} = \sum_{E\in\mathcal{E}_{n_E}} z^{\sum_{i=1}^p\sum_{j=1}^p E_{ij}} = \sum_{E\in\mathcal{E}_{n_E}} z^{n_E} = N_{p,N_E} z^{n_E} \tag{2.3.5}$$

we find

$$Z_{\text{Gauss}}(F_{ij} = z) = \sum_{n_E\geq 0} N_{p,N_E} z^{N_E} \tag{2.3.6}$$

We will now give a useful integral representation for $Z_{\text{Gauss}}(F)$ that uses nothing more than the residue theorem. First, introduce the diagonal matrix

$$D_X = \begin{bmatrix} x_1 & 0 & \cdots & 0 & 0 \\ 0 & x_2 & \cdots & 0 & 0 \\ \vdots & \vdots & \ddots & \vdots & \vdots \\ 0 & 0 & \cdots & x_{p-1} & 0 \\ 0 & 0 & \cdots & 0 & x_p \end{bmatrix} \tag{2.3.7}$$

which we will use below. Next, introduce the generating function

$$Z(F) = \sum_E F^{*E} \tag{2.3.8}$$

where the sum above is over all matrices E_{ij} with zeros on the diagonal and non-negative integers off the diagonal. There are two reasons for why it is useful to introduce this new generating function. First, it is a simple task to evaluate the sum and obtain an explicit answer

$$Z(F) = \prod_{\substack{i,j=1\\ i\neq j}}^p (1 - F_{ij})^{-1} \tag{2.3.9}$$

Second, it is possible to express $Z_{\text{Gauss}}(F)$ as a contour integral over $Z(F)$. To see this, note that the term that is independent of x_i, $i = 1, \cdots, p$ in

$$\begin{aligned} Z(D_X^{-1} F D_X) &= \sum_E \prod_{\substack{i,j=1\\ i\neq j}}^p F_{ij}^{E_{ij}} \prod_{k=1}^p x_k^{\sum_{l=1,l\neq k}^p E_{kl} - \sum_{l=1,l\neq k}^p E_{lk}} \\ &= \prod_{\substack{i,j=1\\ i\neq j}}^p \left(1 - F_{ij}\frac{x_i}{x_j}\right)^{-1} \end{aligned} \tag{2.3.10}$$

is obviously $Z_{\rm Gauss}(F)$. Thus we have

$$Z_{\rm Gauss}(F_{ij}=z)=\left(\frac{1}{2\pi i}\right)^p\oint\frac{dx_1}{x_1}\cdots\oint\frac{dx_p}{x_p}\prod_{\substack{i,j=1\\ i\neq j}}^{p}\left(1-z\frac{x_i}{x_j}\right)^{-1} \tag{2.3.11}$$

As an example, when $p=4$ we find

$$\begin{aligned} Z_{\rm Gauss}(F_{ij}=z) &= \frac{z^8-2z^7+3z^6+2z^5-2z^4+2z^3+3z^2-2z+1}{(1-z)^9(z+1)^5\left(z^2+1\right)\left(z^2+z+1\right)^2} \\ &= 1+6z^2+8z^3+27z^4+48z^5+112z^6+192z^7+378z^8+624z^9+1092z^{10} \\ &\quad +1728z^{11}+2802z^{12}+4248z^{13}+6516z^{14}+9528z^{15}+O(z^{16}) \end{aligned} \tag{2.3.12}$$

which nicely confirms our numerical results in Table 1. For $p=5$ we have

$$Z_{\rm Gauss}(F_{ij}=z)=\frac{n(z)}{(1-z)^{16}(1+z)^8(1+z^2)^2(1+z+z^2)^4(1+z+z^2+z^3+z^4)} \tag{2.3.13}$$

where

$$\begin{aligned} n(z) &= z^{20}-3z^{19}+7z^{18}+3z^{17}+2z^{16}+17z^{15}+35z^{14}+29z^{13}+45z^{12}+50z^{11}+72z^{10} \\ &\quad +50z^9+45z^8+29z^7+35z^6+17z^5+2z^4+3z^3+7z^2-3z+1 \end{aligned} \tag{2.3.14}$$

Expanding (2.3.13) we again confirm the results in Table 1.

Starting from (2.3.11) we can now explore the growth of the number of interaction graphs as we take $p\to\infty$. Setting $x_i=e^{i\theta_i}$ we have

$$Z_{\rm Gauss}(F_{ij}=z)=\left(\frac{1}{2\pi}\right)^p\int_{-\pi}^{\pi}d\theta_1\cdots\int_{-\pi}^{\pi}d\theta_p\prod_{\substack{i,j=1\\ i\neq j}}^{p}\left(1-ze^{i(\theta_i-\theta_j)}\right)^{-1} \tag{2.3.15}$$

The integrand is invariant under the simultaneous shift $\theta_i\to\theta_i-a$, $i=1,2,\cdots,p$. Using this symmetry to carry out the integral over θ_1 we obtain

$$\begin{aligned} Z_{\rm Gauss}(F_{ij}=z) &= \left(\frac{1}{2\pi}\right)^{p-1}\int_{-\pi}^{\pi}d\theta_2\cdots\int_{-\pi}^{\pi}d\theta_p\prod_{i=2}^{p}\left(1-ze^{i\theta_i}\right)^{-1}\left(1-ze^{-i\theta_i}\right)^{-1} \\ &\quad\times\prod_{\substack{i,j=2\\ i\neq j}}^{p}\left(1-ze^{i(\theta_i-\theta_j)}\right)^{-1} \end{aligned} \tag{2.3.16}$$

In terms of the function

$$L(z,\theta_2,\cdots,\theta_p)=\sum_{i=2}^{p}\log\left[\left(1-ze^{i\theta_i}\right)\left(1-ze^{-i\theta_i}\right)\right]+\sum_{\substack{i,j=2\\ i\neq j}}^{p}\log\left[1-ze^{i(\theta_i-\theta_j)}\right] \tag{2.3.17}$$

we can write the number of interaction graphs as

$$N_{p,N_E}=\frac{1}{i\,(2\pi)^p}\oint\frac{dz}{z^{1+N_E}}\int_{-\pi}^{\pi}d\theta_2\cdots\int_{-\pi}^{\pi}d\theta_p e^{-L(z,\theta_2,\cdots,\theta_p)} \tag{2.3.18}$$

To determine the asymptotic behavior of this integral we will use a saddle point evaluation as usual. Using the equivalent form

$$L(z,\theta_2,\cdots,\theta_p)=\sum_{i=2}^{p}\log\left[1-2z\cos\theta_i+z^2\right]+\frac{1}{2}\sum_{\substack{i,j=2\\ i\neq j}}^{p}\log\left[1-2z\cos(\theta_i-\theta_j)+z^2\right] \tag{2.3.19}$$

it is simple to verify that $L(z,\theta_2,\cdots,\theta_p)$ assumes its minimum value at $\theta_2=\cdots=\theta_p=0$. An equally simple computation shows that, at this minimum, $L(z,\theta_2,\cdots,\theta_p)+(N_E+1)\log z$ is minimized at

$$z=\frac{N_E+1}{p^2-p+N_E+1} \tag{2.3.20}$$

Setting $p=\epsilon N$ and $N_E=\epsilon^2N^2$ and working to leading order in the saddle point approximation, we find at large N that

$$N_{p,N_E}\sim e^{2\epsilon^2N^2\log(2)} \tag{2.3.21}$$

Assuming that the interaction graphs do indeed label microstates of a black hole, this is the correct growth to reproduce the expected black hole entropy.

2.3.2 Characterizing interaction graphs

Given this algorithm we can now easily generate collections of graphs, and then use these to numerically characterize the properties of interaction graphs. We would like to employ the notion of *typicality*. Something is typical if it happens in the vast majority of cases: the typical lottery ticket loses, after 1000 coin flips we typically find the ratio of the number of heads to the number of tails is close to 1 and so on. We would like to characterize the typical interaction graph.

Our goal now is to make the above intuitive notions mathematically precise. For useful background see [101]. What does it mean for an interaction graph to be typical? Consider an element x of a set S, $x\in S$. Typicality is a relational property of x, which x possesses with respect to S. Typicality refers to an attribute P and a (probability) measure for this attribute μ_P. For our discussion, S is the set of all interaction graphs, with a given number of vertices p and edges E, denoted $S_{p,E}$. As discussed in the previous section, we can consider $p\sim\epsilon N$. Thus, at large N we know that p is enormous and the number of interaction graphs explodes. We will also assume that we are in the "dense graph" regime specified by allowing the total number of edges to scale as $E\sim p^2\sim\epsilon^2N^2$. Thus, we are interested in characterizing the typical graph in the set S_{p,p^2} of interaction graphs.

We will define the measure μ_P simply by counting. This assumes that every graph is equally likely. In this case the probability μ_P that a given graph has property P is simply given by counting the number of graphs with property P and then dividing by the total number of graphs. When μ_P tends towards 1, P becomes a property of a typical graph. In what follows we are interested in determining some of the properties of a typical graph in S_{p,p^2}.

One interesting attribute P is whether or not the graph is connected. For a Hamiltonian defined using a disconnected graph, the bosons hopping on the graph are confined to a given connected component. A state that is not initially entangled can never build up entanglement between Hilbert spaces defined on vertices of different disconnected components of the graph. Its only on a connected graph that an initial state that is not entangled can evolve into a maximally entangled state, entangling all of the Hilbert spaces defined at the different vertices. The trend shown in Table 1 is exactly what one expects: for a fixed number of vertices, as the number of edges increases the probability that the graph is connected (denoted by F in Table 1) increases. Our numerical results imply that just as E approaches p^2, this probability of being connected approaches 1[8]. With this numerical evidence, we assume in what follows that the typical graph in S_{p,p^2} is connected.

As discussed in the introduction, when deriving the Lieb-Robinson bound for dynamics on a graph an important parameter which enters the bound is the maximum degree D_V of any vertex in the graph[9]. Thus, a second interesting attribute P for the questions we consider is the maximum degree D_V. In Figure 2 we have given histograms for the different values of D_V on the sets $S_{5,E}$. In this case, the largest value D_V can attain is 4, when a given vertex connects to all of the remaining vertices. The first histogram has $E = 6$ edges. There are significant fractions of graphs with all possible allowed values $D_V = 1, 2, 3, 4$. As E increases a definite pattern emerges: $D_V = 4$ becomes the most probable value for $E \geq 12$ edges. The largest value shown is $E = 16$ edges. It is clear that by the time we reach $E = p^2 = 25$ edges, the overwhelming majority of graphs will have $D_V = 4 = p - 1$. Based on this numerical evidence, we assume in what follows that the typical graph in S_{p,p^2} has $D_V = p - 1$. Since we work at large p we simplify this to $D_V = p$.

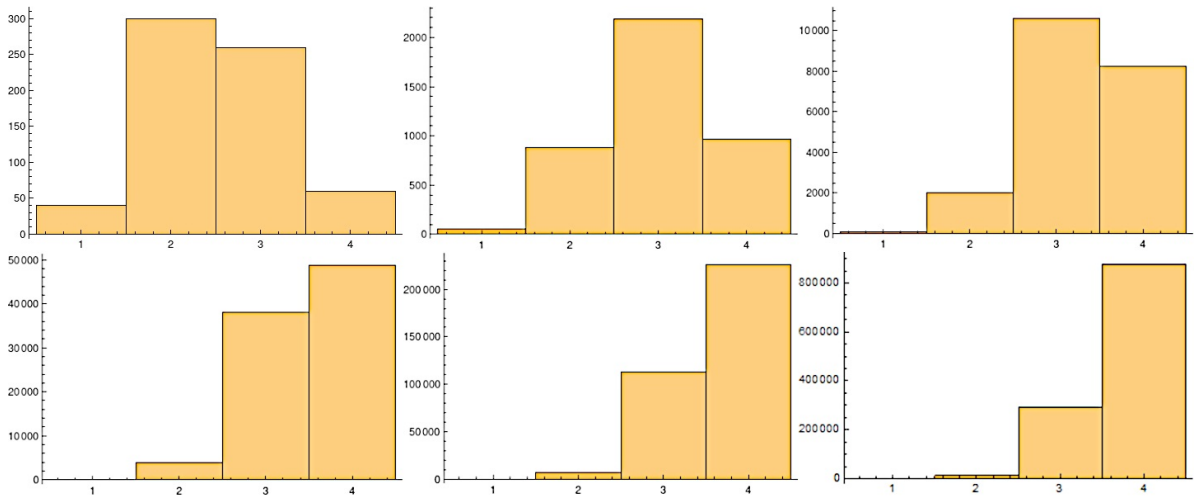


Figure 2: The above plots show histograms of the maximum vertex degree D_V, for Gauss graphs with 5 vertices and $E = 6, 8, 10, 12, 14$ and 16 edges.

[8]For $p = 4$ and $E = 20$ we find that a graph is connected with probability 0.99.

[9]Our graphs can have multiple edges between a given pair of vertices. D_V counts how many other vertices V is connected to and not the number of edges with an endpoint on V

It is interesting to ask how this typical value of D_V is reached. It maybe that most graphs have a single vertex with a large value for D_V and the remaining vertices have much smaller values for their degree. In this case, since there are p vertices, we will find that the average vertex degree stays close to 1. The opposite extreme is that the degree of all vertices is increasing roughly equally, so that most graphs in S_{p,p^2} have an average vertex degree which is close to the maximum value of $p-1$. Numerically we find that the average vertex degree is an increasing function with the number of edges E (see Figure 4) and that when $E \sim p^2$ we find an average value close to the maximum allowed value. Of course we can not probe large values of p (already $p = 6$ requires very long run times), but this conclusion makes sense: nothing has introduced an asymmetry between the p vertices, so we would expect the degree of each vertex to be roughly equal. Thus, from now on we assume that most vertices in a typical graph in S_{p,p^2} have the maximum degree.

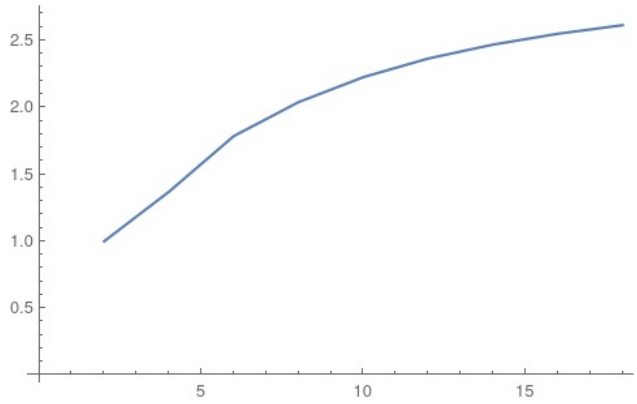


Figure 3: The above plots show the average vertex degree for graphs with $p = 4$ vertices versus the number of edges E. For $E = 16$ the average vertex degree is 2.55. This indicates that most vertices that have been averaged over must assume the maximum value of $p-1 = 3$.

The conclusions we have reached in this section regarding the typical interaction graph have a number of interesting implications. Recall that each vertex in the graph is a giant graviton brane and each edge is an open string excitation of the brane. By characterizing the typical graph we are learning about the typical excited state of this p giant graviton system. The typical state of a system of p giant graviton branes, excited by stretching p^2 open strings between the branes, has roughly the same number of open strings endpoints glued to each brane. In terms of the Gauss graph operators, the differences between the row lengths of R and those of r are roughly constant, equal to p. This is good news: if one simply piled all the excitations into a small number of rows of R[10] one might imagine a situation in which Young diagram R satisfies the distant corners approximation, but the approximation breaks down for r. This might invalidate the derivation given in [83] which assumes that the corners of both R and r are distant. Fortunately this does not happen for the typical graph which justifies the distant corners approximation.

Many proposed quantum mechanical models of black holes include highly non-local interactions. A good example is the SYK model [102, 103, 104] which is a lattice model with

[10]This would correspond to piling many edges onto one vertex of the interaction graph.

all-to-all interactions. Since each vertex of a typical graph of S_{p,p^2} has a mean vertex degree which is close to the maximum value, we find that the generic Hamiltonian defined by the mixing problem for heavy operators, has all-to-all interactions.

2.4 Scrambling on typical graphs

In this section we would like to explore how quickly entanglement is generated by the typical graph Hamiltonian. We restrict ourselves to the subspace of Fock space with a definite number N_b of bosons. Towards this end, in the next section we will formulate a Lieb-Robinson bound for the typical graph Hamiltonian. The bound limits the growth of commutators $[O_i(0), O_j(t)]$ where $O_i \in \mathcal{F}_i$ so that we are bounding the growth of operators [105]. The growth of operators is a reliable probe of scrambling[106, 84, 107, 108]. To obtain our bounds, we use arguments of [109], used to derive Lieb-Robinson bounds for general harmonic systems on general lattices. Information that has been scrambled is stored in the complicated correlations between many different subsystems. Consequently, scrambling is intimately related to the generation of entanglement. With this motivation, we consider in Section 2.4.2 a toy model for our system, simple enough that we can compute the Von Neumann entropy as a function of time, using the reduced density matrix of a given Fock space $\mathcal{F}_i$ and starting from an initially unentangled state. Although this explicitly shows the generation of entanglement in the system, it also poses a puzzle: the recurrence time associated with the typical Hamiltonian is much smaller than expected.

2.4.1 Lieb-Robinson bound for typical graph dynamics

Trade the oscillator operators $b_i, b_i^\dagger$ for a pair of Hermittian operators, α_i and β_i given by

$$\alpha_i = \frac{b_i + b_i^\dagger}{\sqrt{2}} \qquad\qquad \beta_i = \frac{b_i - b_i^\dagger}{i\sqrt{2}} \tag{2.4.1}$$

This is a complete set of operators in the sense that if for any operator O we have

$$[\alpha_i, O] = 0 \qquad [\beta_i, O] = 0 \tag{2.4.2}$$

then O is a multiple of the identity operator. Rewriting the Hamiltonian in terms of the α_i, β_i operators, we obtain the following result

$$H = H_0 + \frac{1}{2}\sum_{i,j=1}^{p} \alpha_i M_{ij} \alpha_j + \frac{1}{2}\sum_{i,j=1}^{p} \beta_i M_{ij} \beta_j \tag{2.4.3}$$

where H_0 is an additive constant equal to

$$H_0 = \frac{2g_{YM}^2}{(4\pi)^2}\sum_{i,j=1}^{p} (\sqrt{r_i} - \sqrt{r_j})^2 N_{ij} - \frac{g_{YM}^2}{4\pi^2}\sum_{i=1}^{p} \frac{r_i k_i}{l_i} \tag{2.4.4}$$

and the matrix M_{ij} is given by

$$M_{ij} = \frac{2g_{YM}^2}{(4\pi)^2}\frac{r_i k_i}{l_i}\delta_{ij} - \frac{2g_{YM}^2}{(4\pi)^2}\sqrt{\frac{r_i r_j}{l_i l_j}} N_{ij} \tag{2.4.5}$$

Recall that r_i, l_i and k_i were introduced in Section 2.2. A simple computation shows that

$$\begin{aligned} \alpha_i(t) &= e^{iHt}\alpha_i e^{-iHt} \\ &= [\cos(Mt)]_{kj}\,\alpha_j + [\sin(Mt)]_{kj}\,\beta_j \end{aligned} \tag{2.4.6}$$

$$\begin{aligned} \beta_i(t) &= e^{iHt}\beta_i e^{-iHt} \\ &= [\cos(Mt)]_{kj}\,\beta_j - [\sin(Mt)]_{kj}\,\alpha_j \end{aligned} \tag{2.4.7}$$

Using these results we immediately obtain the following commutators

$$\begin{aligned} i\,[\alpha_k(t),\beta_j] &= -\cos(Mt)_{kj} \qquad i\,[\alpha_k(t),\alpha_j] = \sin(Mt)_{kj} \\ i\,[\beta_k(t),\alpha_j] &= \cos(Mt)_{kj} \qquad i\,[\beta_k(t),\beta_j] = \sin(Mt)_{kj} \end{aligned} \tag{2.4.8}$$

To proceed we would like to estimate the size of terms of the form $(M^n)_{kj}$. Recall that $p = \epsilon N$. From our analysis of the typical graph, we know that all vertex degrees are close to the maximal value of p, which implies that matrix elements N_{ij} are typically non-zero and order 1. Consequently, the size of the off diagonal elements of M_{ij} are

$$-\frac{2g_{YM}^2}{(4\pi)^2}\sqrt{\frac{r_i r_j}{l_i l_j}}N_{ij} \sim -\frac{2g_{YM}^2}{(4\pi)^2}\sqrt{\frac{r_i r_j}{l_i l_j}} = -\frac{2\epsilon\lambda}{p(4\pi)^2}\sqrt{\frac{r_i r_j}{l_i l_j}} \equiv \frac{\epsilon\lambda c_{ij}}{p} \tag{2.4.9}$$

where

$$c_{ij} = -\frac{2\epsilon\lambda}{(4\pi)^2}\sqrt{\frac{r_i r_j}{l_i l_j}} \tag{2.4.10}$$

is a small number, independent of N. For the diagonal elements of M_{ij}, we use the fact that for the typical graph we have k_i = the degree of the ith vertex = p independent of i and hence these matrix elements are of size

$$\frac{2g_{YM}^2}{(4\pi)^2}\frac{r_i k_i}{l_i} = \frac{2\epsilon\lambda}{(4\pi)^2}\frac{r_i}{l_i} \equiv \epsilon\lambda c_i \tag{2.4.11}$$

which is independent of N. Using these results, we can bound the size of $|(M^n)_{ij}|$, for $i \neq j$. Choose the constant $c > 0$ to be larger than $|c_{ij}|$ for all i, j and larger than $|c_i|$ for all i. We will illustrate the computation with two examples and then state the general rule. For $n = 1$ we are talking about an off diagonal element so that

$$M_{ij} = \frac{\lambda\epsilon c_{ij}}{p} \qquad \Rightarrow \qquad |M_{ij}| < \frac{c\lambda\epsilon}{p} \tag{2.4.12}$$

For $n = 2$ we have a product of two matrices. There is a single index summed. Thus, we have $p-2$ terms which are off diagonal and two terms that are the product of an off diagonal element with a diagonal element, so that

$$|(M^2)_{ij}| = \left|\sum_{\substack{k=1\\k\neq i,j}}^{p}\frac{c_{ik}c_{kj}\epsilon^2\lambda^2}{p^2} + \frac{c_{ij}\epsilon^2\lambda^2}{p}(c_{ii}+c_{jj})\right|$$

$$
\begin{aligned}
&< \sum_{\substack{k=1 \\ k\neq i,j}}^{p} \frac{|c_{ik}|\,|c_{kj}|\,\epsilon^2\lambda^2}{p^2} + \frac{|c_{ij}|\,(|c_{ii}|+|c_{jj}|)\,\epsilon^2\lambda^2}{p} \\
&< (p-2)\frac{c^2\epsilon^2\lambda^2}{p^2} + 2\frac{c^2\epsilon^2\lambda^2}{p} = 3\frac{c^2\epsilon^2\lambda^2}{p} + O\left(\frac{1}{p^2}\right)
\end{aligned} \tag{2.4.13}
$$

We drop the p^{-2} term. Proceeding in this way its easy to see that

$$
|(M^n)_{ij}| < (2n+1)\frac{c^n\epsilon^n\lambda^n}{p} \tag{2.4.14}
$$

Consequently, for example, we can estimate

$$
\begin{aligned}
|i[\alpha_k(t),\beta_j]| = |\cos(Mt)_{kj}| &< \sum_{n=0}^{\infty} \frac{t^{2n}}{(2n)!}|(M^{2n})_{kj}| \\
&< \sum_{n=0}^{\infty} \frac{t^{2n}\epsilon^{2n}\lambda^{2n}}{(2n)!}\frac{c^{2n}}{p}(2n+1) \\
&= \frac{\cosh(c\epsilon\lambda t) + c\epsilon\lambda t\sinh(c\epsilon\lambda t)}{p}
\end{aligned} \tag{2.4.15}
$$

The right hand side becomes of order 1 when $e^{c\epsilon\lambda t} \sim p$ i.e. when $t \sim \frac{\log p}{\epsilon\lambda c}$. At this time scale, the bounds for all of the commutators in (2.4.8) are order 1.

Define the amount of time t_{sig} as the smallest time needed to signal from site j to site k. This implies that for suitable operators O_j acting on $\mathcal{F}_j$ and O_k acting on $\mathcal{F}_k$ we have

$$
\langle\psi(0)|[O_j(0), O_k(t_{\text{sig}})]|\psi(0)\rangle > \delta \tag{2.4.16}
$$

with δ some $O(1)$ number. The Lieb-Robinson bound then forces

$$
t_{\text{sig}} > \frac{\log p}{\epsilon\lambda c} \tag{2.4.17}
$$

This logarithmic scaling of signaling implies a logarithmic scaling of the scrambling time. Thus, our Hamiltonian does not scramble in a time less than $\sim \log p$ consistent with the fast scrambling conjecture [12].

2.4.2 Entanglement Generation

Recall that the matrix M_{ij} for the typical interaction graph is given by

$$
M_{ij} = v_i v_j\left(\delta_{ij} - \frac{1}{p}\right) \qquad v_i = \sqrt{\frac{2\lambda\epsilon}{(4\pi)^2}}\sqrt{\frac{r_i}{l_i}} \tag{2.4.18}
$$

where ϵ, λ are both fixed and much smaller than 1 as we take $N \to \infty$. The ratios $\frac{r_i}{l_i}$ are larger than 1 and fixed as we take $N \to \infty$. We will now make a simplifying assumption, that will yield a problem that is simple enough to solve. We assume that the v_i's are so similar that we can simply set them to be equal to v. There are examples for which this

is indeed an accurate assumption, but this is besides the point. We make the assumption because it leads to a simple model that nevertheless captures the scaling with p of matrix elements of the Hamiltonian and it also captures the all-to-all interactions property of the typical Hamiltonian. In this case M has the following form

$$M = v^2(1+\frac{1}{p})\mathbf{1} + v^2 K = v^2(1+\frac{1}{p})\mathbf{1} + v^2 \begin{bmatrix} -\frac{1}{p} & -\frac{1}{p} & -\frac{1}{p} & \cdots & -\frac{1}{p} & -\frac{1}{p} \\ -\frac{1}{p} & -\frac{1}{p} & -\frac{1}{p} & \cdots & -\frac{1}{p} & -\frac{1}{p} \\ -\frac{1}{p} & -\frac{1}{p} & -\frac{1}{p} & \cdots & -\frac{1}{p} & -\frac{1}{p} \\ \vdots & \vdots & \vdots & \ddots & \vdots & \vdots \\ -\frac{1}{p} & -\frac{1}{p} & -\frac{1}{p} & \cdots & -\frac{1}{p} & -\frac{1}{p} \\ -\frac{1}{p} & -\frac{1}{p} & -\frac{1}{p} & \cdots & -\frac{1}{p} & -\frac{1}{p} \end{bmatrix} \tag{2.4.19}$$

where $\mathbf{1}$ is the $p \times p$ identity matrix. Starting from the initial state

$$|\psi(0)\rangle = b_i^\dagger |0\rangle \tag{2.4.20}$$

it is straight forward to find the probability that we have a particle on site i at time t

$$|\langle 0|b_i|\psi(t)\rangle|^2 = \frac{p^2 + 2(p-1)\cos(pv^2t) - 2p + 2}{p^2} \equiv p_i(t) \tag{2.4.21}$$

The reduced density matrix obtained by tracing over all Fock spaces $\mathcal{F}_j$, $j \neq i$ acts on the two dimensional subspace of $\mathcal{F}_i$ with basis $\{|0\rangle, b_i^\dagger|0\rangle\}$. The reduced density matrix is given by

$$\rho_i(t) = \begin{bmatrix} 1 - p_i(t) & 0 \\ 0 & p_i(t) \end{bmatrix} \tag{2.4.22}$$

and the corresponding Von Neumann entropy is

$$\begin{aligned} S_i &= -\mathrm{Tr}\ (\rho_i \log \rho_i) \\ &= -\frac{2(p-1)\cos(v^2t) + p^2 - 2p + 2}{p^2} \log\left(\frac{2(p-1)\cos(v^2t) + p^2 - 2p + 2}{p^2}\right) \\ &\quad + \frac{2(p-1)(1-\cos(v^2t))}{p^2} \log\left(\frac{2(p-1)(1-\cos(v^2t))}{p^2}\right) \end{aligned} \tag{2.4.23}$$

The above plot shows that entanglement is generated and it exhibits the recurrence time of $T_r = 2\pi/v^2$. At time T_r the entanglement entropy returns to zero and the curve repeats. This recurrence time is much smaller than expected and it casts a doubt on the model. Typically the recurrence is doubly exponential in the size of the system [110, 111, 112]. This suggests a recurrence time of $\sim \exp\exp p$. In the next section we will consider equilibration for dynamics described by the typical Hamiltonian, which will lead to an explanation for this tiny recurrence time.

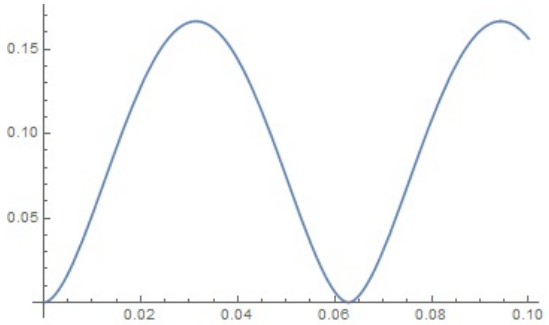


Figure 4: The above plot shows the Von Neumann entropy versus v^2t, for $p = 100$.

2.5 Equilibration during intervals

The classical idea of equilibration involves evolution towards thermal equilibrium. A closed finite dimensional quantum system evolving unitarily has recurrent and time reversal invariant dynamics. It can never come to equilibrium in the classical sense, so we must relax the above classical notion. At quantum level, equilibration will mean that a quantity, initialised at a non-equilibrium value, evolves towards the equilibrium value and then stays close to it for an extended time[11]. This leads to two natural notions of equilibration (see [95]):

1. **Equilibration on average:** A time dependent observable equilibrates on average if its value is for most times during the evolution close to some equilibrium value.

2. **Equilibration during intervals:** A time dependent property equilibrates during a (time) interval if its value is close to some equilibrium value for all times in that interval.

Results establishing equilibration during intervals imply bounds on the time it takes to equilibrate. These time scales are of central interest to us, so we use the second notion above. The conditions under which equilibration during intervals of quadratic bosonic Hamiltonians[12] can be guaranteed has been studied in [113, 114]. Since our system is a quadratic bosonic Hamiltonian, these results are immediately applicable.

We will study a subsystem, given for simplicity by a single site. The rest of the system behaves like a heat bath allowing the subsystem to reach a state that maximizes its entropy. Our strategy is to start the entire lattice system in an initial non-equilibrium state and then to demonstrate that the state of a single site evolves to the equilibrium state, that is, the state that maximizes the entropy.

To carry out the computation, we need to know something about the state that maximizes the entropy. The state (density operator ρ) that maximizes the entropy

$$H(\rho) = -\mathrm{Tr}\,(\rho \log \rho) \tag{2.5.1}$$

for given mean and second moments[13], is a Gaussian state [115]. Instead of discussing the density operator itself, it is useful to study the characteristic function $\chi(\beta)$. The characteristic function contains all the information necessary to reconstruct the density matrix so

[11] This requires a measure that quantifies how close the value of an obervable is to its "equilibrium value".

[12] Hamiltonians that are quadratic polynomials in the bosonic creation and annihilation operators.

[13] Define $b(\alpha) = \sum_{i=1}^{l}(\alpha_i b_i^\dagger - \alpha_i^* b_i)$. We call $\langle b(\alpha)\rangle$ the mean and $\langle b(\alpha)b(\alpha')\rangle$ the correlation matrix or the second moment.

that it is an alternative description of the system. The characteristic function is given by the expectation value of the Weyl operators, defined by

$$D(\beta) = e^{\sum_{i=1}^{p} \beta_i b_i^\dagger - \beta_i^* b_i} \tag{2.5.2}$$

A density operator ρ is called Gaussian if its quantum characteristic function has the form

$$\mathrm{Tr}\,(\rho\, V(z)) = e^{im\cdot\beta - \frac{1}{2}\beta^*\cdot\alpha\cdot\beta} \tag{2.5.3}$$

with m_i, α_{ij} constants independent of β_i, β_i^*. To see why Gaussian states maximize the entropy, recall that given any density matrix ρ, there is a Gaussian density matrix $\tilde{\rho}$ with the same mean and second moments[116]. Consider the quantity

$$H(\tilde{\rho}) - H(\rho) = \mathrm{Tr}\ (\rho(\log\rho - \log\tilde{\rho})) + \mathrm{Tr}\ ((\rho - \tilde{\rho})\log\tilde{\rho}) \tag{2.5.4}$$

The first term on the right hand side is the relative entropy, which is non-negative[117]. The second term on the right hand side vanishes because (i) $\log\tilde{\rho}$ is a quadratic polynomial in $b_i, b_i^\dagger$ and (ii) ρ and $\tilde{\rho}$ have the same first and second moments. This proves that

$$H(\tilde{\rho}) - H(\rho) \geq 0 \tag{2.5.5}$$

which proves the statement.

We now study the reduced density matrix for a singe site. The environment E is all sites except for site i. The reduced density matrix

$$\rho_i = \mathrm{Tr}_{\,E}(|\phi\rangle\langle\phi|) \tag{2.5.6}$$

is an operator acting in the Hilbert space associated to the ith site. Put m bosons on each site so that the initial state is

$$|\phi\rangle = |m\rangle^{\otimes p} \qquad |m\rangle^{\otimes p} = \prod_{i=1}^{p} \frac{(b_i^\dagger)^m}{\sqrt{m!}}|0\rangle_i \tag{2.5.7}$$

Notice that this initial state is not entangled and is nothing like the maximally entangled equilibrium state. We will evaluate the characteristic function

$$\chi_i(\alpha, t) = \mathrm{Tr}\ \left(\rho_i(t)\, e^{\alpha b_i^\dagger - \alpha^* b_i}\right) = \langle\phi|e^{\alpha b_i^\dagger(t) - \alpha^* b_i(t)}|\phi\rangle \tag{2.5.8}$$

From (2.4.6) and (2.4.7) we have

$$b_i(t) = (e^{-itM})_{ij} b_j \equiv U_{ij} b_j \qquad\qquad b_i^\dagger(t) = (e^{itM})_{ji} b_j^\dagger = U_{ji}^* b_j^\dagger \tag{2.5.9}$$

M is a symmetric matrix so U is also symmetric. Using the initial state

$$\chi_i(t) = \langle\phi|e^{\sum_{j=1}^{p}(\alpha U_{ij} b_j - \alpha^* U_{ij}^* b_j^\dagger)}|\phi\rangle = \prod_{j=1}^{p}{}_j\langle m|e^{\alpha U_{ij} b_j - \alpha^* U_{ij}^* b_j^\dagger}|m\rangle_j \tag{2.5.10}$$

we can evaluate each factor in this product. First, using the Baker-Campbell-Haussdorf formula [118] it is simple to verify that (no sum on j)

$$e^{\alpha U_{ij} b_j - \alpha^* U_{ij}^* b_j^\dagger} = e^{\alpha U_{ij} b_j} e^{-\alpha^* U_{ij}^* b_j^\dagger} e^{-\frac{|\alpha|^2}{2}|U_{ij}|^2} \tag{2.5.11}$$

Using this identity we easily find

$$\begin{aligned}
{}_j\langle m|e^{\alpha U_{ij} b_j - \alpha^* U_{ij}^* b_j^\dagger}|m\rangle_j &= {}_j\langle m|e^{\alpha U_{ij} b_j} e^{-\alpha^* U_{ij}^* b_j^\dagger}|m\rangle_j e^{-\frac{|\alpha|^2}{2}|U_{ij}|^2} \\
&= \sum_{k=0}^{m}\sum_{l=0}^{m} \frac{(\alpha U_{ij})^k (-\alpha^* U_{ij}^*)^l}{k!l!} \frac{m!}{\sqrt{(m-k)!(m-l)!}} {}_j\langle m-k|m-l\rangle_j e^{-\frac{|\alpha|^2}{2}|U_{ij}|^2} \\
&= \sum_{k=0}^{m} \frac{(-|\alpha|^2|U_{ij}|^2)^k}{k!k!} \frac{m!}{(m-k)!} e^{-\frac{|\alpha|^2}{2}|U_{ij}|^2} \\
&= L_m(|\alpha|^2|U_{ij}|^2) e^{-\frac{|\alpha|^2}{2}|U_{ij}|^2}
\end{aligned} \tag{2.5.12}$$

where $L_m(\cdot)$ is a Laguerre polynomial. Thus, we find

$$\chi_i(t) = \prod_{j=1}^{p} L_m(|\alpha|^2|U_{ij}|^2) e^{-\frac{|\alpha|^2}{2}|U_{ij}|^2} \tag{2.5.13}$$

We want to prove that, at late times, the characteristic function becomes a Gaussian, i.e. that at late times we have

$$\chi_i(t) = e^{-c\alpha^2} \tag{2.5.14}$$

where c is a constant (independent of α). Consider

$$\log \chi_i(t) = -\sum_{j=1}^{p} \frac{|\alpha^2|}{2}|U_{ij}|^2 + \sum_{j=1}^{p} \log L_m(|\alpha|^2|U_{ij}|^2) \tag{2.5.15}$$

Expand the log

$$\sum_{j=1}^{p} \log L_m(|\alpha|^2|U_{ij}|^2) = \sum_{j=1}^{p} \left(1 - L_m(|\alpha|^2|U_{ij}|^2)\right) + \sum_{j=1}^{p}\sum_{k=2}^{\infty} \frac{\left(1 - L_m(|\alpha|^2|U_{ij}|^2)\right)^k}{k} \tag{2.5.16}$$

and use the expansion of the Laguerre polynomials

$$L_m(x) = \sum_{n=0}^{m} \frac{m!}{(m-n)!n!n!}(-x)^n = 1 - mx + O(x^2) \tag{2.5.17}$$

If we can argue that $x = |\alpha|^2|U_{ij}|^2$ is small for late times t, then we can set

$$\sum_{j=1}^{p} \log L_m(|\alpha|^2|U_{ij}|^2) = \sum_{j=1}^{p} m|\alpha|^2|U_{ij}|^2 \tag{2.5.18}$$

and consequently

$$\log \chi_i(t) = -\sum_{j=1}^{p} \frac{|\alpha^2|}{2} |U_{ij}|^2 - \sum_{j=1}^{p} m\, |\alpha|^2 |U_{ij}|^2 \tag{2.5.19}$$

which would establish the result. Determining how rapidly $|\alpha|^2|U_{ij}|^2$ approaches zero will tell us how quickly the system equilibrates.

Why should $|\alpha|^2|U_{ij}|^2$ get small for large t? The matrix M_{ij} is real and symmetric, so that it can be diagonalized. Denote the eigenvectors and eigenvalues of M_{ij}, labeled by $k = 1, \cdots p$, as $(\eta_k)_i$ and λ_k respectively. In terms of these eigenvectors and eigenvalues we have

$$U_{ij} = \sum_{k=1}^{p} (\eta_k)_i\, e^{-i\lambda_k t}\, (\eta_k^*)_j \tag{2.5.20}$$

so that

$$|U_{ij}|^2 = \sum_{k=1}^{p} \sum_{l=1}^{p} (\eta_k)_i\, e^{-i\lambda_k t}\, (\eta_k^*)_j\ (\eta_l^*)_i\, e^{i\lambda_l t}\, (\eta_l)_j \tag{2.5.21}$$

There are two sums above which become infinite sums at large N. If the eigenvalues are distinct, we are adding terms with different rapidly oscillating phases for large t, so that there will be many cancellations and we expect the sum is small. To formulate a precise argument we need to know the λ_k and $(\eta_k)_i$. We have not managed to solve for the eigenvectors and eigenvalues of M in general, but can do so for the toy model we introduced in Section 2.4.2. In this case M has the following form

$$M = v^2(1 + \frac{1}{p})\mathbf{1} + v^2 K \tag{2.5.22}$$

where $\mathbf{1}$ is the $p \times p$ identity matrix. Everything is an eigenvector of the identity matrix, so we need only find the eigenvectors and eigenvalues of K. Notice that K has rank one. Recall that the rank of K is the dimension of the vector space spanned by its columns. Since all of the columns of K are identical they span a one dimensional space. The rank is also equal to the number of non-zero eigenvalues, so K has only one non-zero eigenvalue equal to -1. The corresponding eigenvector $|k = -1\rangle$ has every component equal to 1

$$|k = -1\rangle = \frac{1}{\sqrt{p}} \begin{bmatrix} 1 \\ \vdots \\ 1 \end{bmatrix} \tag{2.5.23}$$

The remaining K eigenvectors span the subspace orthogonal to $|k = -1\rangle$ and have K eigenvalue equal to zero. Thus, $|k = -1\rangle$ is an eigenvector of M with eigenvalue equal to $\frac{1}{p}$ while any vector orthogonal to $|k = -1\rangle$ is also an eigenvector of M with eigenvalue equal to $1 + \frac{1}{p}$. In this case the eigenvalues are not distinct and terms in (2.5.21) will not in general cancel. Thus we don't expect $|\alpha|^2|U_{ij}|^2$ to becomes small for large t and hence the

system will not equilibrate. To get some insight into what is going on, consider an initial state, with excitations localized on a pair of lattice sites i and j, given by

$$|\psi\rangle = \frac{1}{\sqrt{2}}\left(b_i^\dagger - b_j^\dagger\right)|0\rangle \tag{2.5.24}$$

We easily find

$$H|\psi\rangle = \left(H_0 + v^2 + \frac{v^2}{p}\right)|\psi\rangle + \frac{v^2}{\sqrt{2}}\sum_{k=1}^{p}(K_{ki} - K_{kj})b_k^\dagger|0\rangle \tag{2.5.25}$$

The second term in the last line above allows excitations to move from their original lattice site to a new lattice site. However the two contributions cancel so that $|\psi\rangle$ is an eigenstate and the excitation does not disperse - it remains localized on sites i and j. The excitation can move to every other site with exactly equal hopping strength, so that in the end the excitations are blocked from moving anywhere and are instead localized. This is rather generic: all states in the Hilbert space orthogonal to the state

$$|k=-1\rangle = \frac{1}{\sqrt{p}}\sum_{i=1}^{p} b_i^\dagger|0\rangle \tag{2.5.26}$$

are eigenstates of the Hamiltonian and hence do not evolve in time[14]. The intuitive picture behind equilibration is as follows [119]: as time evolves, the system becomes correlated. From each site a wave front moving at the speed of sound for the lattice emerges, carrying information. The cumulative effect is an effective averaging process: information stored at one site becomes spread across the entire lattice. In our case, since the wave fronts are blocked from moving, we should not expect the system to equilibrate.

The spectrum of the typical Hamiltonian gives us an explanation for why we found such a small recurrence time. In the large p limit there is a single energy eigenvalue equal to $\frac{v^2}{p} = 0 + O(p^{-1})$ and $p-1$ energy eigenvalues equal to $v^2 - \frac{v^2}{p} = v^2 + O(p^{-1})$. The energy of these degenerate states is the only energy in the problem and it clearly sets the recurrence time we found. To get such a simple spectrum things must be fine tuned. Random deviations from this typical Hamiltonian will lift the degeneracy leading to a spectrum that is more realistic as we will soon see.

So, the Hamiltonian associated to the typical interaction graph exhibits localization. However, even small fluctuations about this typical configuration should disrupt the localization. Lets again look at a simple example. Choose a matrix M_{ij} which opens up a "conducting path" that passes through each vertex of the graph, as follows

$$M = v^2(1+\frac{1}{p})\mathbf{1} + v^2K + v^2\begin{bmatrix} -\frac{2}{p} & \frac{1}{p} & 0 & \dots & 0 & \frac{1}{p} \\ \frac{1}{p} & -\frac{2}{p} & \frac{1}{p} & \dots & 0 & 0 \\ 0 & \frac{1}{p} & -\frac{2}{p} & \dots & 0 & 0 \\ \vdots & \vdots & \vdots & \ddots & \vdots & \vdots \\ 0 & 0 & 0 & \dots & -\frac{2}{p} & \frac{1}{p} \\ \frac{1}{p} & 0 & 0 & \dots & \frac{1}{p} & -\frac{2}{p} \end{bmatrix} = v^2(1+\frac{1}{p})\mathbf{1} + v^2K + v^2L$$

[14]At large p the Hamiltonian becomes a projector onto the space orthogonal to the $|k=-1\rangle$ so that the result of applying the Hamiltonian to any state is an eigenstate.

This is a small change to the typical Hamiltonian: we have only changed order p matrix elements out of a total of p^2 matrix elements, and we have only adjusted each element by an amount $\sim p^{-1}$. The form of matrix L was chosen so that we can again solve for the eigenvectors and eigenvalues of M exactly. First note that $[L, K] = 0$ so that L and K can be simultaneously diagonalized. A simple computation shows that the eigenvectors and eigenvalues of L are given by

$$(\eta_k)_l = \frac{e^{ikl}}{\sqrt{p}} \qquad \lambda_k = \frac{2\cos(k) - 2 + p - p\delta_{k,0}}{p} v^2 \qquad\qquad k = \frac{2n\pi}{p}$$

with $n = 0, 1, 2, \cdots, p-1$. The eigenstate with $n = 0$ is the eigenstate of K with eigenvalue -1. Using these eigenvalues and eigenvectors we have

$$\begin{aligned} U_{ij} &= \sum_{n=0}^{p-1} e^{i\frac{2\pi n}{p}(i-j)} e^{-i\frac{2\cos(\frac{2n\pi}{p})+p-p\delta_{k,0}-2}{p} v^2 t} = U(i-j) \\ &\sim i^{i-j} e^{-iv^2} \times \frac{1}{2\pi i^{i-j}} \int_0^{2\pi} d\phi e^{-i\frac{2}{p}\cos(\phi)v^2 t} e^{i(i-j)\phi} \\ &= i^{i-j} J_{i-j}(\frac{2v^2 t}{p}) \end{aligned} \tag{2.5.27}$$

where $J_l(x)$ is the Bessel function. This is the kind of result we want because we know that $|J_l(x)| < x^{-\frac{1}{3}}$ for all $x \geq 0$ [120]. Thus, for times such that

$$\frac{2v^2 t_{\text{eq}}}{p} \sim 1 \qquad \Rightarrow \qquad t_{\text{eq}} \sim \frac{p}{2v^2} \tag{2.5.28}$$

the matrix elements U_{ij} are becoming small enough to neglect and the density matrix is approaching a Gaussian state. Thus, the system evolves to the state of maximum entropy and we come to equilibrium. Notice that this time is much much smaller than the enormous recurrence time. The system now remains at equilibrium until we get close to the recurrence time. Notice that t_{eq} is significantly larger than the scrambling time.

2.6 Discussion

We have studied the one loop mixing problem for operators with a large enough bare dimension that they could be dual to black holes or new spacetime geometries. This mixing problem is significantly more complicated than the planar mixing problem. Despite this, a remarkably simple description emerges. The dilatation operator defines dynamics on a graph of the type that has recently been suggested as models for quantum dynamics of black holes [84, 85, 87, 88, 89, 90]. It is intriguing to see simple dynamics on graphs emerging naturally from the mixing problem of very large dimension operators in Yang-Mills theory.

Each operator has a number of labels, one of which is the interaction graph. Operators only mix if they have the same interaction graph label. We have carried out a careful counting of the interaction graphs and find that the number of graphs matches the entropy of a black hole suggesting that we might think of these operators as dual to a black hole microstate. By numerically generating lists of graphs we have characterized the "typical

interaction graph" and the dynamics associated to it. We find a lattice model defined on p sites with $p \sim O(N)$ and with all-to-all interactions. Despite this non-locality, we have proved that the scrambling time is bounded consistent with the fast scrambling conjecture. By considering a specific example, we have also given evidence that the system equilibrates in a time scale $t \sim \frac{p}{\lambda}$ where $p \sim N$.

The idea that gravitational dynamics should emerge from the sector of heavy operators in the Yang-Mills theory has been pursued in [121, 122, 123, 124, 125, 126]. Our study is a continuation of these ideas.

There are a number of interesting directions that could now be pursued. Our analysis has all been limited to weak coupling. To make contact with black hole physics we need to make progress in understanding the strong coupling limit of the theory, which is presently a formidable problem. However, one might look for BMN like [21] limits or for observables that are protected by super symmetry, which has not yet been considered in the setting of heavy operators. A more manageable problem is to generalize our analysis to generic operators constructed using all of the fields in the field theory. By using only complex scalar fields ϕ_i and not $\phi_i^\dagger$, we naturally construct operators that have dimension close to their R-charge. By including enough $\phi_i^\dagger$ fields we would be able to construct operators with the quantum numbers expected for near extremal or even Schwarzschild black holes. This generalization should be a straight forward technical exercise. The spectrum we have computed may find application in the arguments of [127] which explore how the thermodynamics of small black holes is recovered from the dual conformal field theory. Our considerations of equilibration made use of two specific examples and a specific initial condition. Clearly a lot more is needed to properly understand the equilibration of our system and the associated time scales. It would also be interesting to explore situations in which we need to correct the distant corners approximation, which are required when the giant gravitons become coincident in space time. Thermal averages in the Yang-Mills theory involve averages over the complete ensemble of graphs. Corrections to the distant corners approximation would allow transitions between different graphs and the number of particles hopping on the graph would no longer be conserved.

Finally, our goal was to gain some insights into the mechanism behind extremely rapid black hole thermalization rates which must be present in the dynamics of large N Yang-Mills theories. Since our study has reduced to simple dynamics on graphs, perhaps the most important lesson to be drawn is that the "toy models" considered in [84, 85, 87, 88, 89, 90] may in fact be better than one might have expected. The description in terms of a graph certainly carries over to the case that more fields are included, but its validity at strong coupling is yet to be established.

3 Quantum Error Correction and Holographic Information from Bilocal Holography

3.1 Introduction

Holography, as embodied in the AdS/CFT correspondence[2, 10, 20], is a profound new discovery about nature that is still poorly understood. The correspondence describes a duality between a quantum gravitational theory in asymptotically AdS spacetime and a conformal field theory in one fewer spatial dimensions. A question that has been surprisingly fruitful, goes under the name "subregion duality". Subregion duality asks what region of the bulk AdS spacetime is dual to a subregion of the conformal field theory. Questions of this type have lead to an appreciation that quantum error correction plays a role in holography[128, 129, 130], and also to the notion of the holography of information[131, 132, 133, 134, 135, 136, 137], which adds to our understanding of how information is coded into the bulk gravitational theory. Our goal in this chapter is to describe a simple setting in which these ideas can be probed and scrutinized.

We study the free $O(N)$ vector model in $2+1$ dimensions, described by the action

$$S = \int d^3x \sum_{a=1}^{N} \left(\frac{1}{2} \partial_\mu \phi^a \partial^\mu \phi^a \right) \tag{3.1.1}$$

This theory is holographically dual [138, 139] to higher spin gravity in AdS_4 [140, 141, 142]. As usual the single trace operators of the CFT give the single particle spectrum of the dual gravity. The single trace operators consist of a single primary of spin 0 and dimension $\Delta = 1$

$$O_{\Delta=1}(t, \vec{x}) = \sum_{a=1}^{N} \phi^a(t, \vec{x}) \phi^a(t, \vec{x}) \tag{3.1.2}$$

and a tower of conserved higher spin currents, each of spin s and dimension $\Delta = s + 1$

$$\begin{aligned} J_s(t, \vec{x}, \alpha) &= J_{\mu_1 \mu_2 \cdots \mu_s}(t, \vec{x}) \alpha^{\mu_1} \alpha^{\mu_2} \cdots \alpha^{\mu_s} \\ &= \sum_{a=1}^{N} \sum_{k=0}^{s} \frac{(-1)^k \ : (\alpha \cdot \partial)^{s-k} \phi^a(t, \vec{x}) \ (\alpha \cdot \partial)^k \phi^a(t, \vec{x}) :}{k!(s-k)! \Gamma(k + \frac{1}{2}) \Gamma(s - k + \frac{1}{2})} \end{aligned} \tag{3.1.3}$$

where α^μ is a polarization tensor that we can take to be null. The three point functions of these spinning primaries reproduce the detailed prediction of the cubic higher spin gravity [143] at leading order in the gravitational coupling.

Bilocal holography [144, 145, 146, 147, 148, 149, 150], a constructive approach to holography, can be used to construct the holographic dual to this free CFT. There are two basic ingredients that go into bilocal holography, both of which have a transparent physical motivation:

1. Perform a change of variables in the path integral from the original field $\phi^a(t,\vec{x})$ to a gauge invariant bilocal field $\sigma(t,\vec{x}_1,\vec{x}_2)$. This change of field variable reorganizes the dynamics so that the loop expansion parameter for the bilocal field theory is $\frac{1}{N}$, matching expectations for the loop expansion of the dual holographic theory.

The bilocal field given by

$$\sigma(t,\vec{x}_1,\vec{x}_2)=\sum_{a=1}^{N}\phi^a(t,\vec{x}_1)\phi^a(t,\vec{x}_2) \tag{3.1.4}$$

is the complete set of equal time $O(N)$ invariant variables. Notice that this change of field variables naturally leads to a higher dimensional theory: the original field $\phi^a(t,\vec{x})$ is defined in a $2+1$ dimensional spacetime, whereas the bilocal is defined in a $4+1$ dimensional spacetime. This change of field variables has an important consequence: the original field $\phi^a(t,\vec{x})$ transforms in a short irreducible representation $V_{\frac{1}{2},0}$ of the conformal group $\mathrm{SO}(2,3)$ constructed on top of a primary field of dimension $\Delta=\frac{1}{2}$ and spin $s=0$. In contrast to this, the bilocal fields transform in the tensor product $V_{\frac{1}{2},0}\otimes V_{\frac{1}{2},0}$. The generators of conformal transformations, obtained by using the standard co-product, are representations of this tensor product. The tensor product reduces as follows[151]

$$V_{\frac{1}{2},0}\otimes V_{\frac{1}{2},0}=V_{1,0}\oplus\bigoplus_{s=2,4,6,\cdots}V_{s+1,s} \tag{3.1.5}$$

Each term in the direct sum on the right hand side corresponds to a field in the higher spin theory [140]. Quite independent of this observation, it is natural to interpret each term in the direct sum as a distinct field. To develop this point of view we should change basis for the Lie algebra of $\mathrm{SO}(2,3)$. This motivates the second step in bilocal holography

2. Performs a change of variables from the CFT bilocal coordinates (which label points in a $1+4$ dimensional spacetime) to coordinates for an $\mathrm{AdS}_4\times\mathrm{S}^1$ (which is also a $1+4$ dimensional spacetime). This change of coordinates takes us from a basis of generators (denoted collectively as $L^A_{\otimes}$) for $\mathrm{SO}(2,3)$ naturally describing the LHS of (3.1.5) to a basis of generators (denoted collectively as $L^A_{\oplus}$)naturally describing the RHS.

This second point is highly non-trivial and is discussed in detail in the original works [145, 149], as well as in Appendix B. The compact space S^1 which has made an appearance, turns out to be a nice way to organize the complete set of fields in higher spin gravity, very much in harmony with the ideas in [144]. We do not know a proof that the change of basis required by (3.1.5) can always be accomplished with a change of coordinates, but for the case of lightcone quantization [145] this is straight forward to demonstrate as reviewed in Appendix B. In a light front quantization equal x^+ slices are used to define the Hilbert space. The light cone coordinates are given by $x^\pm=x^1\pm x^0=x^1\pm t$. The coordinate x^2, which is transverse to the light cone will simply be denoted as x in what follows. The relevant bilocal is given by

$$\sigma(x^+,x_1^-,x_1,x_2^-,x_2)=\sum_{a=1}^{N}\phi^a(x^+,x_1^-,x_1)\phi^a(x^+,x_2^-,x_2) \tag{3.1.6}$$

These two steps completely determine the bilocal field theory. For another approach, related to bilocal holography, see [152].

This construction of bilocal field theory is entirely motivated from the CFT and has not taken as input, any information from the dual higher spin gravity. It is interesting to ask if the bilocal field theory reproduces any features of the dual gravitational description. In Section 3.2, following [145, 149], we verify that the CFT equations of motion for the elementary field ϕ^a imply equations for the bilocal that reproduce the bulk equations of motion for the complete set of fields of higher spin gravity, and that the complete set of single trace CFT primaries are recovered from the boundary value of the bilocal field. This proves that bilocal holography, without any input from the dual higher spin gravity, achieves the desired bulk reconstruction. Using this bulk reconstruction we are able to tackle the central question of which subregion of the bulk spacetime (if any) is dual to a given subregion of the conformal field theory? This is the subject of Section 3.3. The subregion of the boundary CFT is obtained by restricting the coordinate x transverse to the lightcone, to an interval. Using bilocal fields living on this interval, we can reconstruct the bulk fields within a region of the bulk bounded by an extremal surface. On the face of it, this appears to mesh nicely with ideas that have appeared in the entanglement wedge reconstruction [153, 154, 155, 156]. Entanglement wedge reconstruction tells us what part of the bulk is encoded in a given subregion of the boundary: only bulk operators lying in the entanglement wedge of the boundary subregion can be reconstructed. However, using the values of the fields that have been reconstructed, it is not possible to distinguish bulk fields with different spins. To distinguish different spin components, even the reconstruction of fields at a single bulk point requires the complete boundary region. There is no redundancy in how bulk information is coded into the boundary. At the level of the complete CFT Hilbert space and the complete bulk AdS Hilbert space, AdS/CFT is a one-to-one mapping between the states of the two Hilbert spaces.

This is puzzling since recent insights [128, 129, 130] appear to have demonstrated and then exploited the fact that there is a certain redundancy in the bulk reconstruction. An important ingredient in the quantum error correction approach to holography is the code subspace. The code subspace is a construction that allows the description of effective field theory around a given classical background. Any low energy observer does not have access to infinite energy and they can act with, at most, a finite number of fields in the theory. These limitations can be built in as cutoffs, on both the momentum and the occupation number. In this way the Hilbert space which a low energy observer accesses can be constructed by acting on the relevant background state with a set of effective fields. This formulation of effective field theory is state dependent [157] since it requires a reference state. The resulting description is closely related to the construction of the little Hilbert space of states around black hole states given in [158, 157], or equivalently, it is the code subspace of [128]. For an explicit construction of the code subspace starting from an LLM reference state, see [126]. In Section 3.4 we consider how restricting to a finite energy code subspace affects our bulk reconstruction. It is only after restricting the complete bulk AdS Hilbert space to the code subspace that reconstruction of local bulk operators using a subregion of the boundary is possible. In this case only a finite number of modes are excited, bulk information is encoded redundantly on the boundary and the quantum error correction picture emerges. The illustrative examples considered in [128] find a concrete realization in the bilocal holography

description. Further, we find a natural emergence of the bit thread description of entanglement entropy developed in [159, 160, 161]. We are also able to demonstrate entanglement wedge reconstruction using bilocal holography.

Another puzzle which catalyzed significant progress is the monogamy problem: modes just inside and modes just outside the horizon of a black hole must be entangled for a smooth horizon geometry. Further, the Page curve demonstrates that modes just outside the horizon are entangled with modes far from the hole. This is already a paradox because the monogamy of entanglement forbids entanglement between the modes just outside the horizon and both modes just inside the horizon and modes far from the hole. One plausible resolution to this paradox, called the holography of information, claims that in fact the modes inside the black hole are not distinct degrees of freedom from the modes far from the black hole. What is the mechanism for such an identification? This holographic nature of the gravitational degrees of freedom only plays a role at late times when the state is a complicated state with many degrees of freedom at many different locations in spacetime (the emitted Hawking radiation) excited. We argue that bilocal holography offers a natural mechanism for the holography of information: very complicated states in the gravity have more degrees of freedom excited than there are independent degrees of freedom in the CFT. This implies that there are relations between the gravitational degrees of freedom. These are the analog of trace relations for matrix theories, except that here the relations are between degrees of freedom at different locations in the bulk AdS spacetime. We explain in particular, in Section 3.5, that these relations naturally relate degrees of freedom localized at the boundary to degrees of freedom deep in the bulk AdS. For ideas along these lines see also [162, 163, 152]. We present our conclusions and discuss our results in Section 3.6.

Finally, note that bilocal holography is a special case of collective field theory [164, 165]. The goal of collective field theory was always to change to invariant variables in order to obtain a loop expansion in $\frac{1}{N}$. This is a powerful insight which goes well beyond vector models. In particular, we should expect an analogous construction for $\mathcal{N} = 4$ super Yang-Mills theory. The key obstacle is that there is not yet a manageable description for the invariant variables for matrix theories. We will comment more on this possibility in Section 3.6.

3.2 Bilocal Bulk Reconstruction

In this section we review bilocal holography as developed in [144, 145, 146, 147, 148, 149, 150]. The main novelty in our discussion is a mixed position space/momentum space description, which will be useful when we discuss subregion duality in later sections. Apart from this new representation, this section is a review of material developed in [144, 145, 146, 147, 148, 149, 150]. The key goal of this section is to explain how bilocal holography solves the bulk reconstruction problem.

A general formalism for changing to invariant variables in field theory, known as collective field theory, has been developed in [164, 165]. We use these general results in what follows. The change to bilocal variables is accomplished using the chain rule

$$\pi^a(t,\vec{x}) \;=\; -i\frac{\delta}{\delta\phi^a(t,\vec{x})}$$

$$
\begin{aligned}
&= -i \int d^2y \int d^2z \; \frac{\delta\sigma(t,\vec{z},\vec{y})}{\delta\phi^a(t,\vec{x})} \; \frac{\delta}{\delta\sigma(t,\vec{z},\vec{y})} \\
&= \int d^2y \int d^2z \; \frac{\delta\sigma(t,\vec{z},\vec{y})}{\delta\phi^a(t,\vec{x})} \, \Pi(t,\vec{z},\vec{y})
\end{aligned} \tag{3.2.1}
$$

After changing to the bilocal variables (3.1.4) the CFT Hamiltonian

$$
H = \int d^2x \sum_{a=1}^{N} \left(-\frac{1}{2} \frac{\delta}{\delta\phi^a(\vec{x})} \frac{\delta}{\delta\phi^a(\vec{x})} + \frac{1}{2} \vec{\nabla}\phi^a \cdot \vec{\nabla}\phi^a \right) \tag{3.2.2}
$$

becomes

$$
\begin{aligned}
H &= 2\mathrm{Tr}(\Pi\sigma\Pi) + \frac{1}{2} \int d^2x \left(-\vec{\nabla}_x \cdot \vec{\nabla}_x \sigma(x,y) \right) \Big|_{x=y} \\
&\quad + \frac{N^2}{8} \mathrm{Tr}(\sigma^{-1}) - \frac{N}{2} \mathrm{Tr}(\sigma^{-1}) \int dx \delta(0) + \frac{1}{2} \mathrm{Tr}(\sigma^{-1}) \left(\int dx \delta(0) \right)^2
\end{aligned} \tag{3.2.3}
$$

where we are using a natural bilocal notation. In this notation, for example,

$$
\mathrm{Tr}(\Pi\sigma\Pi) = \int d^2x \int d^2y \int d^2z \; \Pi(t,\vec{x},\vec{y}) \sigma(t,\vec{y},\vec{z}) \Pi(t,\vec{z},\vec{x}) \tag{3.2.4}
$$

The second line in (3.2.3) arises from a non-trivial Jacobian resulting from the change of variables. The Jacobian, which is a non-linear contribution, generates an infinite sequence of interaction vertices even for the free vector model. The last two terms in (3.2.3) are counter terms that cancel divergences that appear when the $\frac{1}{N}$ expansion is carried out. The second and third terms of (3.2.3) define an effective potential

$$
V = \frac{1}{2} \int d^2x \left(-\vec{\nabla}_x \cdot \vec{\nabla}_x \sigma(x,y) \right) \Big|_{x=y} + \frac{N^2}{8} \mathrm{Tr}(\sigma^{-1}) \tag{3.2.5}
$$

This potential plays an important role when the $\frac{1}{N}$ expansion is developed. We start by determining the "classical" large N configuration σ_0 by solving

$$
\frac{\delta V}{\delta\sigma(t,\vec{x},\vec{y})} \Big|_{\sigma=\sigma_0} = 0 \tag{3.2.6}
$$

We then expand about the leading solution as

$$
\begin{aligned}
\sigma(t,\vec{x},\vec{y}) &= \sigma_0(t,\vec{x},\vec{y}) + \frac{1}{\sqrt{N}} \eta(t,\vec{x},\vec{y}) \\
\Pi(t,\vec{x},\vec{y}) &= \sqrt{N} \pi(t,\vec{x},\vec{y})
\end{aligned} \tag{3.2.7}
$$

It is the fluctuations $\eta(t,\vec{x},\vec{y})$ and $\pi(t,\vec{x},\vec{y})$ which are identified with bulk AdS fields. They are a set of conjugate variables and obey the equal time commutation relation

$$
[\eta(t,\vec{x},\vec{y}), \pi(t,\vec{x}',\vec{y}')] = i\delta(\vec{x}-\vec{x}')\delta(\vec{y}-\vec{y}') \tag{3.2.8}
$$

This commutation relation is exact. We know that the bilocal collective field theory will reproduce the CFT correlators to all orders in the $1/N$ expansion, since we have simply

performed a change of variables. This has been confirmed in detail in [166, 167], by generating the loop expansion for the bilocal field theory and showing that it reproduces the $1/N$ expansion of the original vector model. The non-trivial thing about the change of variables is that the loop expansion in the original variables is an expansion in $\hbar$, whereas the loop expansion in the bilocal variables is an expansion in $1/N$.

The discussion above has been general. Now we specialize to light front quantization. The fluctuation around the bilocal field (3.1.6) is denoted $\eta(x^+, x_1^-, x_1, x_2^-, x_2)$. Bulk AdS fields are identified with the fluctuation $\eta(x^+, x_1^-, x_1, x_2^-, x_2)$. To spell out this mapping between bulk and boundary fields, we provide (i) a coordinate transformation between the coordinates of the bilocal field, and coordinates for the bulk $AdS_4 \times S^1$ spacetime and (ii) an explicit mapping between the fluctuation $\eta(x^+, x_1^-, x_1, x_2^-, x_2)$ and the bulk $AdS_4 \times S^1$ field $\Phi(X^+, X^-, X, Z, \theta)$. As mentioned in the introduction, this mapping is determined by the requirement that the basis for the Lie algebra is transformed from the direct product basis appearing on the LHS of (3.1.5) to the direct sum basis appearing on the right hand side of (3.1.5). In this section we simply state the resulting map. The reader wanting the details can find them in Appendix B.

The coordinate transform between bilocal coordinates and those of $AdS_4 \times S^1$ is conveniently developed in a mixed position space/momentum space representation, obtained by Fourier transforming with respect to x_1^- and x_2^-. The bilocal field is now a function of x^+ as well as p_1^+, x_1, p_2^+ and x_2. The bulk AdS spacetime has Poincare coordinates X^0, X^1, X^2 and Z. Move to light cone coordinates $X^\pm = X^0 \pm X^1$ and use the notation $X \equiv X^2$. After Fourier transforming with respect to X^-, the AdS coordinates are X^+, P^+, X, Z. There is also an angle θ, which is a coordinate for S^1. The coordinate transform relating the CFT coordinates $x^+, p_1^+, x_1, p_2^+, x_2$ to the $AdS_4 \times S^1$ coordinates X^+, P^+, X, Z, θ identifies $x^+ = X^+$ and

$$\begin{aligned} x_1 &= X + Z \tan\left(\frac{\theta}{2}\right) & x_2 &= X - Z \cot\left(\frac{\theta}{2}\right) \\ p_1^+ &= P^+ \cos^2\left(\frac{\theta}{2}\right) & p_2^+ &= P^+ \sin^2\left(\frac{\theta}{2}\right) \end{aligned} \tag{3.2.9}$$

The inverse transformation is

$$\begin{aligned} X &= \frac{p_1^+ x_1 + p_2^+ x_2}{p_1^+ + p_2^+} & Z &= \frac{\sqrt{p_1^+ p_2^+}(x_1 - x_2)}{p_1^+ + p_2^+} \\ P^+ &= p_1^+ + p_2^+ & \theta &= 2\tan^{-1}\left(\sqrt{\frac{p_2^+}{p_1^+}}\right) \end{aligned} \tag{3.2.10}$$

This map is non-trivial and it plays an important role in bilocal holography. As we explain in Appendix B, it is determined by CFT kinematics.

We will now explain the role of the coordinate θ, which parametrizes an S^1. This extra coordinate collects the complete set of four dimensional higher spin fields into a single five dimensional field. The AdS_4 higher spin fields with spin $2s$, denoted as $\Phi_{2s}(X^+, X^-, X, Z)$, are obtained by developing $\Phi(X^+, X^-, X, Z, \theta)$ in an expansion as follows

$$\Phi(X^+, X^-, X, Z, \theta) = \sum_{s=0}^{\infty} \cos(2s\theta)\ \Phi_{2s}(X^+, X^-, X, Z) \tag{3.2.11}$$

We are now ready so state the mapping between bulk and boundary fields. The map between bilocal fields of the CFT and the higher spin bulk fields happens on a single time (x^+) slice

$$\Phi\left(X^+, X^-, X, Z, \theta\right) = \int_{-\infty}^{\infty} dx_1^- \int_{-\infty}^{\infty} dx_2^- \; 2\pi i \sin\theta \delta'(X^- - x_1^- \cos^2\frac{\theta}{2} - x_2^- \sin^2\frac{\theta}{2}) \times \eta\left(X^+, x_1^-, X + Z\tan\frac{\theta}{2}, x_2^-, X - Z\cot\frac{\theta}{2}\right) \tag{3.2.12}$$

where the prime on the delta function denotes a derivative with respect to X^-. We can rewrite this map in terms of the Fourier transformed bilocal

$$\eta\left(X^+, x_1^-, X + Z\tan\frac{\theta}{2}, x_2^-, X - Z\cot\frac{\theta}{2}\right) = \int \frac{dp_1^+}{2\pi} \int \frac{dp_2^+}{2\pi} e^{-ip_1^+ x_1^- - ip_2^+ x_2^-} \times \eta\left(X^+, p_1^+, X + Z\tan\frac{\theta}{2}, p_2^+, X - Z\cot\frac{\theta}{2}\right) \tag{3.2.13}$$

to obtain

$$\Phi\left(X^+, X^-, X, Z, \theta\right) = \int_{-\infty}^{\infty} \frac{dp_1^+}{2\pi} \int_{-\infty}^{\infty} \frac{dp_2^+}{2\pi} \; (2\pi)^2 (p_1^+ + p_2^+) \sin\theta e^{-i(p_1^+ + p_2^+)X^-} \times \delta(p_2^+ \cos^2\frac{\theta}{2} - p_1^+ \sin^2\frac{\theta}{2}) \eta\left(X^+, p_1^+, X + Z\tan\frac{\theta}{2}, p_2^+, X - Z\cot\frac{\theta}{2}\right) \tag{3.2.14}$$

This is an off shell mapping between CFT fields and bulk AdS fields. This interpretation is a simple consequence of the fact that the original integration variables for the path integral are the CFT fields ϕ^a, while after the change of variables we integrate over the bilocals. A simple rewriting gives

$$\Phi(X^+, p^+, X, Z, \theta) = 2\pi p^+ \sin\theta \; \eta(X^+, p^+\cos^2\frac{\theta}{2}, X + Z\tan\frac{\theta}{2}, p^+\sin^2\frac{\theta}{2}, X - Z\cot\frac{\theta}{2}) \tag{3.2.15}$$

The basic result proved in Appendix B, says

$$L^A_{\oplus}\Phi(X^+, p^+, X, Z, \theta) = 2\pi p^+ \sin\theta \; L^A_{\otimes}\eta(X^+, p^+\cos^2\frac{\theta}{2}, X + Z\tan\frac{\theta}{2}, p^+\sin^2\frac{\theta}{2}, X - Z\cot\frac{\theta}{2}) \tag{3.2.16}$$

where the notation for the generators of the conformal group, $L^A_{\otimes}$ and $L^A_{\oplus}$ was defined in point 2 in the introduction.

Both the change of coordinates (3.2.9) and the operator mapping (3.2.14) are motivated entirely from the CFT. Consequently, evidence that bilocal holography solves the bulk reconstruction problem is tremendously compelling. The usual approach to reconstruction [168, 169, 170] constructs the bulk operators by perturbatively solving the bulk equations of motion, understood as operator equations in the CFT, using the extrapolate dictionary [171] to set boundary conditions. We will now argue that, upon using the bilocal map, the

CFT equations of motion imply the bulk equations of motion. Further, the complete set of single trace primaries in the CFT are recovered in the $Z \to 0$ limit from the bulk AdS field $\Phi(X^+, X^-, X, Z, \theta)$.

The CFT equation of motion is the equation of motion for a free massless scalar

$$\left(\frac{\partial}{\partial x^+}\frac{\partial}{\partial x^-} + \frac{\partial^2}{\partial x^2}\right)\phi^a(x^+, x^-, x) = 0 \tag{3.2.17}$$

This holds at the full quantum level, inside correlation functions, up to contact terms as usual. After Fourier transforming to momentum space

$$\phi^a(x^+, p^+, x) = \int \frac{dp^+}{2\pi}\, e^{-ip^+x^-}\phi^a(x^+, x^-, x) \tag{3.2.18}$$

the equation of motion is written as

$$i\frac{\partial}{\partial x^+}\phi^a(x^+, p^+, x) = \frac{1}{p^+}\frac{\partial^2}{\partial x^2}\phi^a(x^+, p^+, x) \tag{3.2.19}$$

Consequently, the leading large N bilocal equation of motion, again up to contact terms, is

$$i\frac{\partial}{\partial x^+}\sigma(x^+, p_1^+, x_1, p_2^+, x_2) = \left(\frac{1}{p_1^+}\frac{\partial^2}{\partial x_1^2} + \frac{1}{p_2^+}\frac{\partial^2}{\partial x_2^2}\right)\sigma(x^+, p_1^+, x_1, p_2^+, x_2) \tag{3.2.20}$$

Since this equation is linear, it must be obeyed by both σ_0 and η. Consequently, we have

$$i\frac{\partial}{\partial x^+}\eta(x^+, p_1^+, x_1, p_2^+, x_2) = \left(\frac{1}{p_1^+}\frac{\partial^2}{\partial x_1^2} + \frac{1}{p_2^+}\frac{\partial^2}{\partial x_2^2}\right)\eta(x^+, p_1^+, x_1, p_2^+, x_2) \tag{3.2.21}$$

Now, using (3.2.9) and (3.2.10) to change coordinates, it is a simple application of the chain rule to prove that

$$\begin{aligned} &i\frac{\partial}{\partial x^+}\eta(x^+, p_1^+, X + Z\tan\frac{\theta}{2}, p_2^+, X - Z\cot\frac{\theta}{2}) \\ &= \frac{1}{p_1^+ + p_2^+}\left(\frac{\partial^2}{\partial X^2} + \frac{\partial^2}{\partial Z^2}\right)\eta(x^+, p_1^+, X + Z\tan\frac{\theta}{2}, p_2^+, X - Z\cot\frac{\theta}{2}) \end{aligned} \tag{3.2.22}$$

Using the above CFT equation of motion, it is simple to see that

$$\begin{aligned} \frac{\partial}{\partial X^+}\frac{\partial}{\partial X^-}\Phi\left(X^+, X^-, X, Z, \theta\right) &= -\int_{-\infty}^{\infty} dp_1^+ \int_{-\infty}^{\infty} dp_2^+\ \sin\theta(p_1^+ + p_2^+)e^{-i(p_1^+ + p_2^+)X^-} \\ &\times\delta(p_2^+\cos^2\frac{\theta}{2} - p_1^+\sin^2\frac{\theta}{2})\left(\frac{\partial^2}{\partial X^2} + \frac{\partial^2}{\partial Z^2}\right)\eta\left(x^+, p_1^+, X + Z\tan\frac{\theta}{2}, p_2^+, X - Z\cot\frac{\theta}{2}\right) \\ &= -\left(\frac{\partial^2}{\partial X^2} + \frac{\partial^2}{\partial Z^2}\right)\Phi\left(X^+, X^-, X, Z, \theta\right) \end{aligned} \tag{3.2.23}$$

so that

$$\left(\frac{\partial}{\partial X^+}\frac{\partial}{\partial X^-} + \frac{\partial^2}{\partial X^2} + \frac{\partial^2}{\partial Z^2}\right)\Phi\left(X^+, X^-, X, Z, \theta\right) = 0 \tag{3.2.24}$$

This is the equation of motion obtained for an arbitrary symmetric higher spin field in light cone gauge in AdS_4 [172].

To complete the demonstration of bulk reconstruction, we must show that the complete set of single trace primaries can be obtained from the boundary behavior $Z \to 0$ of the bulk fields $\Phi_{2s}\left(X^+, X^-, X, Z\right)$. A simple computation gives

$$\begin{aligned}\Phi_{2s}\left(X^+, X^-, X, Z\right)\Big|_{Z=0} &= \frac{2}{\pi}\int_0^\pi d\theta \cos(2s\theta)\Phi\left(X^+, X^-, X, 0, \theta\right) \\ &= \int_0^\pi d\theta \cos(2s\theta)\int_{-\infty}^{\infty}\frac{dp_1^+}{2\pi}\int_{-\infty}^{\infty}\frac{dp_2^+}{2\pi}\ 8\pi(p_1^+ + p_2^+)\sin\theta e^{-i(p_1^+ + p_2^+)X^-} \\ &\quad \times\delta(p_2^+\cos^2\frac{\theta}{2} - p_1^+\sin^2\frac{\theta}{2})\eta\left(X^+, p_1^+, X, p_2^+, X\right) \end{aligned} \tag{3.2.25}$$

Using the delta function to perform the integral over θ, we find

$$\begin{aligned}\Phi_{2s}\left(X^+, X^-, X, 0\right) &= \int_{-\infty}^{\infty}\frac{dp_1^+}{2\pi}\int_{-\infty}^{\infty}\frac{dp_2^+}{2\pi}\cos\left(4s\arctan\sqrt{\frac{p_2^+}{p_1^+}}\right)\ 16\pi e^{-i(p_1^+ + p_2^+)X^-} \\ &\quad \eta\left(X^+, p_1^+, X, p_2^+, X\right) \\ &= 16\pi\int_{-\infty}^{\infty}\frac{dp_1^+}{2\pi}\ e^{-ip_1^+X^-}\phi^a(X^+, p_1^+, X)\ \times \\ &\quad \int_{-\infty}^{\infty}\frac{dp_2^+}{2\pi}\ e^{-ip_2^+X^-}\phi^a(X^+, p_2^+, X)\ \cos\left(4s\arctan\sqrt{\frac{p_2^+}{p_1^+}}\right) \end{aligned} \tag{3.2.26}$$

Now, we note that

$$(p_1^+ + p_2^+)^s\ \cos\left(2s\arctan\sqrt{\frac{p_2^+}{p_1^+}}\right) = \Gamma\left(\frac{1}{2}\right)s!\Gamma\left(s+\frac{1}{2}\right)\sum_{k=0}^{s}\frac{(-1)^k(p_1^+)^{s-k}(p_2^+)^k}{\Gamma\left(s-k+\frac{1}{2}\right)\left(\Gamma\left(k+\frac{1}{2}\right)k!(s-k)!\right)} \tag{3.2.27}$$

which implies that

$$\frac{\partial^s}{\partial X^{-s}}\Phi_s(X^+; X^-, X, 0) = 16\pi\Gamma\left(\frac{1}{2}\right)s!\Gamma\left(s+\frac{1}{2}\right)\sum_{k=0}^{s}\frac{(-1)^k\partial_-^{s-k}\phi^a(X^+, X^-, X)\partial_-^k\phi^a(X^+, X^-, X)}{\Gamma\left(s-k+\frac{1}{2}\right)\Gamma\left(k+\frac{1}{2}\right)k!(s-k)!} \tag{3.2.28}$$

We have recovered the conserved higher spin current of spin s, given in (3.1.3). For $s = 0$ we simply obtain the $\Delta = 1$ scalar of spin zero. This gives a primary state from each single trace conformal multiplet. The complete set of states in the multiplet can be obtained by acting with generators of the conformal algebra. This demonstrates that the complete set of single trace primaries is obtained from the boundary behavior $Z \to 0$ of the bulk fields $\Phi_{2s}\left(X^+, X^-, X, Z\right)$.

The equation of motion for the original CFT field (3.2.19), when applied to a bilocal field within a correlator, naturally gives rise to contact terms that encode corrections that are subleading at large N. After changing variables to the bilocal field, the subleading terms are generated by an infinite sequence of vertices that arise upon expanding the Jacobian about

the leading configuration. These interactions should be reproduced by a fully gauge fixed version of Vasilliev's higher spin theory [140, 141, 142]. This seems hard to test explicitly, given the complexity of Vasiliev theory. However we know that the vertices generated by the Jacobian are exactly the interactions needed to reproduce the correlators of the CFT, to all orders in $\frac{1}{N}$, because correctly changing integration variables in the path integral does not change the value of correlation functions. Assuming the vector model/higher spin duality, this is evidence that the $\frac{1}{N}$ correction to the bilocal equations of motion will agree with the higher order corrections to the higher spin equations of motion, extending agreement beyond the leading order at large N. In this sense, the reconstruction of bilocal holography goes well beyond that of [168, 169, 170] which is perturbative by construction. This completes our demonstration that bilocal holography, without any input from the dual higher spin gravity, achieves the correct bulk reconstruction.

3.3 Subregion duality

Which subregion of the CFT (if any) is dual to a given subregion of the bulk spacetime? This deceptively simple question has motivated enormous progress: it lead to the discovery that there is some arbitrariness in the mapping between the CFT and the dual AdS theory, elegantly described as the statement that the bulk-to-boundary map in AdS/CFT defines a quantum error correcting code [128, 129, 130]. This discovery was an important ingredient needed to answer the question posed by subregion duality [154, 155, 173, 156]: the bulk region encoded in an arbitrary boundary region $\mathcal{R}$ is the entanglement wedge of $\mathcal{R}$[174]. The entanglement wedge of boundary region $\mathcal{R}$ is the bulk region located in a single time slice, bounded by $\mathcal{R}$ itself and its Ryu-Takayanagi (RT) surface [175, 176], which is the minimal area bulk surface anchored to the boundary of $\mathcal{R}$. Entanglement wedge reconstruction[154, 155, 173, 156, 177, 178, 179, 153, 180] provides a boundary operator acting only on the boundary subregion $\mathcal{R}$ for each bulk operator acting on the entanglement wedge of $\mathcal{R}$. In this section using bilocal holography, we consider the subregion duality problem. We focus on the subregion defined by restricting x to an interval. Bilocal fields restricted to this interval correspond to bulk fields within the entanglement wedge of the interval. These bulks fields are a linear combination of AdS_4 fields, with arbitrary even integer spin. As we explain in detail, to distinguish the different spin components, even the reconstruction of fields at a single bulk point requires the complete boundary region. Consequently, using the values of the fields that have been reconstructed, it is not possible to distinguish bulk fields with different spins. At the level of the complete CFT Hilbert space and the complete bulk AdS Hilbert space, AdS/CFT is a one-to-one mapping between the states of the two Hilbert spaces. There is no redundancy in how bulk information is coded into the boundary. In the next section we reconsider the subregion duality problem, after properly accounting for the limitations faced by any low energy observer. In this case the map provided by bilocal holography does indeed define a quantum error correcting code.

Our strategy entails considering localized CFT excitations and determining where they map to in the dual bulk spacetime. Given the form of the bilocal map, it is most instructive to consider bilocal excitations at time x^+, with the first excitation localized at (x_1, p_1^+) and the second at (x_2, p_2^+). The two excitations in the bilocal are described as wavepackets, tightly peaked at x_1 and x_2 along the spatial direction x transverse to the light cone, but

because they have a definite value for p^+, completely smeared along the x^- direction. The map (3.2.9) - (3.2.10) mixes spacetime coordinates and momenta, so its not entirely obvious where the CFT excitations are located in the bulk. Note the easily verified identity

$$\left(X - \frac{x_1 + x_2}{2}\right)^2 + Z^2 = \left(\frac{x_1 - x_2}{2}\right)^2 \tag{3.3.1}$$

which is a direct consequence of the map (3.2.10). This identity implies the excitation sits on a semicircle in the X, Z plane, in the bulk. The semicircle has radius $(x_1 - x_2)/2$ and center at $X = (x_1 + x_2)/2$ and $Z = 0$. To locate the excitation on this semicircle, we can specify an angle θ as follows

$$\tan\theta = \frac{Z}{X - \frac{x_1+x_2}{2}} = \frac{2\sqrt{p_1^+ p_2^+}}{p_1^+ - p_2^+} \tag{3.3.2}$$

where the last equality is easily obtained from the map (3.2.10). Using double angle trignometric identities it is simple to verify that the angle θ we have just defined is the angle θ appearing in the map.

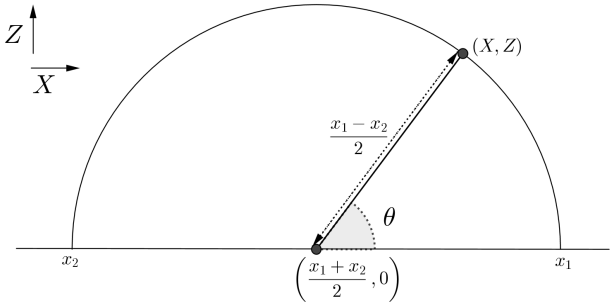


Figure 5: The bilocal describing a pair of excitations localized at (x_1, p_1^+) and (x_2, p_2^+) correspond to a bulk excitation localized at (X, Z) as shown. This figure lives on a constant $x^+ = X^+$ slice. The angle θ is related to p_1^+ and p_2^+ according to (3.3.2).

If we study excitations confined to a strip subregion of the CFT, defined by $x^+ = 0$, $-\infty \leq x^- \leq \infty$ and $-L \leq x \leq L$ then the corresponding bulk excitations can be located at any θ, X^-, but are confined to the semicircle

$$X^2 + Z^2 \leq L^2 \qquad -\infty \leq X^- \leq \infty \qquad 0 \leq \theta \leq \pi \tag{3.3.3}$$

of the (X, Z) plane and are at $X^+ = 0$. The semicircle bounding the region in which the bulk excitations are located has an attractive interpretation. The metric of AdS_4, written using lightcone coordinates on the Poincare patch, is given by

$$ds^2 = \frac{dX^+ dX^- + dX^2 + dZ^2}{Z^2} \tag{3.3.4}$$

The induced metric on a constant X^+ slice is thus given by

$$ds^2 = \frac{dX^2 + dZ^2}{Z^2} \tag{3.3.5}$$

Now consider a region $\mathcal{E}_{\mathcal{R}}$ of the (X, Z) plane stretching from the boundary at $Z = 0$ to a curve $Z = Z(X)$. The area of this region is given by

$$\mathcal{A} = \int dX \frac{\sqrt{Z'^2 + 1}}{Z} \qquad Z' = \frac{dZ}{dX} \tag{3.3.6}$$

Minimizing the area we find[15]

$$\frac{dZ}{dX} = \frac{\sqrt{R^2 - Z^2}}{Z} \tag{3.3.7}$$

which is solved by $X^2 + Z^2 = R^2$. This demonstrates that bulk excitations are restricted to region $\mathcal{E}_R$ bounded by the boundary of AdS and an extremal surface. Thus, $\mathcal{E}_{\mathcal{R}}$ is nothing but the entanglement wedge!

The above result suggests that we are recovering the entanglement wedge reconstruction. This conclusion is however, too hasty: recall that the bulk field $\Phi(X^+, X^-, X, Z, \theta)$ defined in the bilocal map is a mixture of fields of any even spin. The bulk fields reconstructed from the CFT subregion do not allow us to distinguish these different spin components. To obtain fields of a definite spin we need to compute the integral

$$\int_0^\pi d\theta \ \Phi(X^+, X^-, X, Z, \theta) \cos(2s\theta) \tag{3.3.8}$$

As $\theta \to 0$ we must have $\frac{x_1+x_2}{2} \to -\infty$ and to get $\theta = \pi$ we must have $\frac{x_1+x_2}{2} \to \infty$. Thus, as θ ranges from 0 to π, x ranges over the entire boundary.

In conclusion, even to reconstruct the complete set of higher spin fields at just a single point in the bulk, we require the entire boundary. This is not unexpected: since AdS/CFT is an isomorphism between two theories, it is highly unlikely that a given subregion of the CFT is dual to a given subregion of the bulk spacetime. Within bilocal holography, we see explicitly that this is not the case: AdS/CFT provides only a global map between bulk and boundary states.

3.4 Code Subspace and Quantum Error Correction

A crucial ingredient in proposals for the role of quantum error correction in holography and entanglement wedge reconstruction, are that we restrict ourselves to the code subspace of the full Hilbert space. The code subspace provides a correct description of effective field theory around a given classical background. Any given observer can not access the complete Hilbert space. For example, they can't access infinite energy states and can only act with a subset of all the fields in the theory. This is what the code subspace accounts for. The code subspace is closely related to how the little Hilbert space of states, nearby a reference state, is built in the work of Papadodimas and Raju [158, 157].

[15]Instead of minimizing this area functional, we have used the usual trick of writing down the conserved quantity implied by the fact that $\mathcal{A}$ is independent of X. We have set the conserved quantity equal to R^{-1} which is constant. This is why we obtain a first order equation.

3.4.1 Quantum Error Correction

We will follow the prescription for the code subspace given in [128]. One starts by choosing a finite set of local bulk operators $\varphi_i(X^\mu)$, realized in the CFT using the representation provided by bilocal holography. The code subspace $\mathcal{H}_C$ is the linear span of states of the form

$$|\Omega\rangle, \qquad \varphi_i(X^\mu)|\Omega\rangle, \qquad \varphi_i(X_1^\mu)\varphi_j(X_2^\mu)|\Omega\rangle, \cdots \tag{3.4.1}$$

$|\Omega\rangle$ is the ground state of the system. The range of i, which determines the number of fields we act with and the number of points where the operators are located, is bounded by a fixed finite number.

Restricting to the code subspace has far reaching consequences. By assumption, at any given bulk point, we have a linear combination of a finite number of AdS_4 fields, with known spins. To separate the components of a given spin we don't need to use (3.3.8) so that θ need not run continuously from 0 to π. Given a sum of a finite number of fields of known spins, we can solve for each component given the sum at a finite number of θ's. By choosing different bilocal fields, we obtain distinct semicircles giving the value of the bulk field $\Phi(X^+, X^-, X, Z, \theta)$ for a sufficiently large number of values of θ. An example is shown in Figure 6 below. Consequently from a given subregion $\mathcal{R}$ of the CFT we can reconstruct the fields that belong to the code subspace in the bulk region corresponding to the entanglement wedge $\mathcal{E}_\mathcal{R}$.

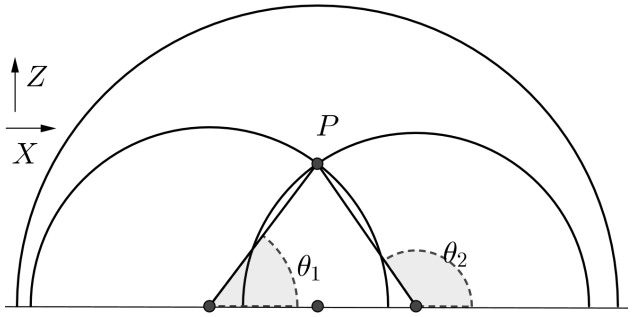


Figure 6: It is possible to choose distinct bilocals from the subregion $\mathcal{R}$ that correspond to different semicircles passing through point P. This allows us to obtain the value of the bulk field $\Phi(X^+, X^-, X, Z, \theta)$ at P for a number of distinct θ.

The properties that motivated the quantum error correction formulation of holography are now easy to demonstrate. To see how a single bulk operator corresponds to multiple boundary operators, constructed using different subregions, consider Figure 7 below. In subregion A we reconstruct the values of $\Phi(X^+, X^-, X, Z, \theta)$ at angles $\theta_i < \frac{\pi}{2}$, while in subregion B we reconstruct at angles $\theta_i > \frac{\pi}{2}$. This demonstrates an ambiguity in the bulk reconstruction, since the bulk field is coded into different subregions of the CFT.

From Figure 8 below it is clear the bulk field at the point P can not be reconstructed using either of the subregions A or B. However, if bilocals from the union $A \cup B$ are used, we can construct the bulk field at point P. The new bilocals, not present in either A or B,

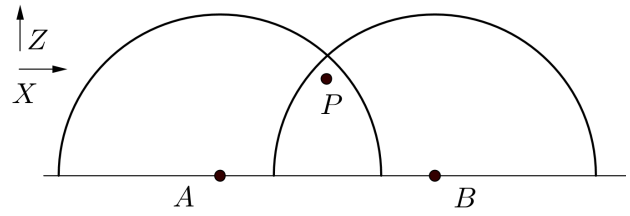


Figure 7: The fields at point P can be reconstructed using bilocals taken from region A or region B. It is however not possible to reconstruct the bulk fields at point P using bilocals from the intersection $A \cap B$.

are bilocals with one point in A and one in B. These bilocals are separated enough that they reach deep enough into the bulk to reconstruct P; they represent information that is shared non-locally between the two boundary subregions.

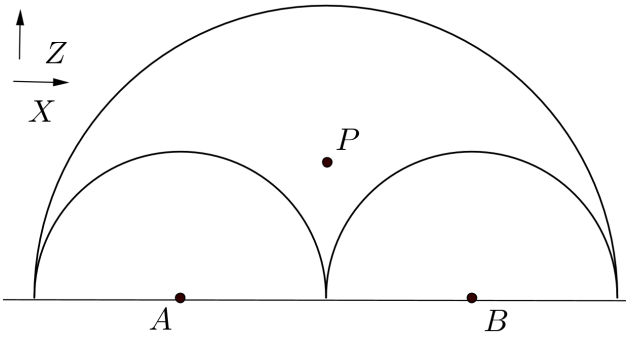


Figure 8: It is not possible to reconstruct the bulk operator at P if we restrict to either subregion A or B. The reconstruction is however possible if bilocals from $A \cup B$ are used.

3.4.2 Entanglement Entropy and Bit Threads

Another observable, associated to a subregion A of the CFT, is the entanglement entropy $S(A)$. An important formula describing this observable is the RT formula, which states that entanglement entropy of a region in the boundary CFT is determined by a geometric extremization problem in the bulk [175, 176]. The RT formula states that the entropy of a spatial region A on the boundary CFT is given by

$$S(A) = \frac{1}{4G_N}\text{area}(m(A)) \tag{3.4.2}$$

where $m(A)$ is a minimal hypersurface in the bulk, homologous to A. The RT formula holds for a conformal field theory dual to a state represented by a classical spacetime with a time-reflection symmetry. Since our bulk spacetime is time independent AdS_4, we are always within this regime of validity. Denote a Cauchy slice in the geometry by $\mathcal{M}$. We can ensure

that $\mathcal{M}$ is a compact manifold with a boundary by introducing a cutoff "near" the conformal boundary. The CFT lives on the boundary of $\mathcal{M}$.

The Riemannian version of the max flow-min cut theorem can be used to rewrite the RT formula in terms of the maximal flow of a vector field v^μ, through any surface homologous to A[159]. (See [160] for a nice discussion of the proof of the required theorem.) The integral curves of any vector field are oriented and locally parallel. Following [161] it is useful to generalize the notion of integral curves of a vector field, by dropping these two conditions. This gives the concept of a bit thread: bit threads are unoriented curves, that pass through a given neighborhood, at different angles and are even allowed to intersect. A thread configuration is a set of unoriented curves on $\mathcal{M}$, such that threads end only on the boundary of $\mathcal{M}$ and the thread density is nowhere larger than $1/4G_N$.

How should we think about bit threads? In what follows we argue that bit threads have a natural interpretation within bilocal holography. The bilocal field creates gauge invariant excitations, which are naturally entangled as a result of the sum over the color index

$$\sigma(x^+, x_1^-, x_1, x_2^-, x_2)|0\rangle = \sum_{a=1}^{N} \phi^a(x^+, x_1^-, x_1)\phi^a(x^+, x_2^-, x_2)|0\rangle \tag{3.4.3}$$

A gauge invariant pair of modes in the vacuum is naturally entangled in this way. The entanglement entropy of subregion A receives contributions from entangled pairs, which entangle a mode in A with a mode in its complement $\bar{A}$. Consider a pair of modes which are entangled, with one of the pair localized at position (x_1^-, x_1) in A and the other at (x_2^-, x_2) in $\bar{A}$. This entangled pair will have contributions from all possible p_1^+ and p_2^+ values. Consequently, the bilocal map implies that the bulk degree of freedom is smeared over the semicircle with center $\frac{1}{2}(x_1+x_2)$ and radius $\frac{1}{2}(x_1-x_2)$. Thus, in the bulk these entangled pairs are represented by semicircles which end at the two modes being entangled. The semicircles indicate where the corresponding bulk modes are smeared. This is precisely what a bit thread is: the bit threads connecting A to $\bar{A}$ are manifestations of the entanglement between A and $\bar{A}$. We can visualize each bit thread as a "channel" allowing a bit of (quantum) information to be communicated between different regions on the spatial boundary. Recall that a thread configuration, by definition, is a set of unoriented curves on $\mathcal{M}$, such that threads end only on the boundary of $\mathcal{M}$ and the thread density is nowhere larger than $1/4G_N$. The semicircles of the bilocal holography, which end on points in the CFT clearly do end on the boundary of $\mathcal{M}$. In addition, since these threads end on degrees of freedom in the CFT, the density of threads is naturally restricted by the holographic bound which dictates that the boundary theory has only one bit of information per Planck area.

As a final piece of evidence in favor of our interpretation, the paper [181] constructs explicit examples of flows v^μ for a number of geometries including empty AdS. The fact that the family of integral curves is given by a two parameter family of semicircles is in harmony with our interpretation[16].

This bit thread perspective gives an attractive and intuitive interpretation to the RT formula. As an example of the utility of the bit thread perspective[159, 161] recall that given

[16]Our geometry obtained by setting x^+ = constant is naturally related to the case of AdS_3 of [181]. Choosing an entangling regions given by an interval is then naturally related to the sphere discussion of Section 2.1.1 of [181].

a disjoint spatial region A of the boundary CFT, the minimal hypersurface homologous to A will not always vary continuously even as A is varied continuously. Bit threads do vary continuously as a function of A. It is satisfying to see the accord between bit threads and how a gauge invariant entangled pair is represented in the bulk using bilocal holography.

3.4.3 Entanglement Wedge Reconstruction

We end this section considering the problem of entanglement wedge reconstruction, within bilocal holography, in the empty AdS geometry. The problem is to construct any bulk operator Φ_a supported in the entanglement wedge a of A from boundary observables O_A, living on the subregion A of the CFT. Building on earlier work [153] showing the equality of bulk and boundary relative entropies a rather precise and elegant characterization of entanglement wedge reconstruction was developed in [155]. For an arbitrary state, we restrict to a subregion by tracing over the complement to this subregion. Given the equality of bulk and boundary relative entropies, a natural way forwards is to phrase entanglement wedge reconstruction as a universal recovery channel that undoes the effect of the partial trace. It is non-trivial [155] to prove that there is a universal recovery channel that can recover from the noise introduced by restricting from the entire bulk to subregion a. In the case of bilocal holography, things are simpler, as a consequence of the fact that the map from CFT bilocals $\eta(x^+, p_1^+, x_1, p_2^+, x_2)$ to bulk fields $\Phi(X^+, X^-, X, Z, \theta)$ given in (3.2.14) is so simple. A short computation shows

$$\begin{aligned}\eta(x^+, p_1^+, x_1, p_2^+, x_2) &= \int_{-\infty}^{\infty} dx^- \frac{e^{i(p_1^+ + p_2^+)x^-}}{2\sqrt{p_1^+ p_2^+}} \\ &\times \Phi\left(x^+, x^-, \frac{p_1^+ x_1 + p_2^+ x_2}{p_1^+ + p_2^+}, \frac{\sqrt{p_1^+ p_2^+}(x_1 - x_2)}{p_1^+ + p_2^+}, 2\tan^{-1}\sqrt{\frac{p_2^+}{p_1^+}}\right) \quad (3.4.4)\end{aligned}$$

Now, by convention take $x_1 > x_2$. If we set

$$\alpha = \frac{p_1^+}{p_1^+ + p_2^+} \qquad \beta = \frac{p_2^+}{p_1^+ + p_2^+} \quad (3.4.5)$$

then we have $\alpha + \beta = 1$ and $0 \leq \alpha, \beta \leq 1$. The $Z = \sqrt{\alpha\beta}(x_1 - x_2)$ coordinate is zero when either $\alpha = 0$ or $\beta = 0$, and it takes a maximum value of $\frac{1}{2}(x_1 - x_2)$ at $\alpha = \frac{1}{2} = \beta$. The $X = \alpha x_1 + \beta x_2$ coordinate ranges from x_2 when $\beta = 1$ and $\alpha = 0$, to x_1 when $\alpha = 0$ and $\beta = 1$. This proves that a bilocal with points x_1, x_2 inside A is reconstructed using bulk fields within a.

3.5 Non-localities from large N

The modes across the horizon of a black hole must be entangled if the horizon geometry is to be smooth. Further, for old black holes the Page curve implies that modes just outside the hole must be entangled with modes that were emitted earlier and are now far from the hole. Given that entanglement is monogamous, this represent a paradox [182, 183, 184] (see also [185]). Three possible resolutions to this paradox are

1. Fuzzballs [186, 187, 188, 189].

2. Firewalls [182, 183, 184].

3. Holography of information [158].

The first proposal resolves the paradox by cutting spacetime off at the black hole horizon, so that there are no modes inside the horizon. The second proposal relaxes entanglement between modes just inside and outside the hole, at the cost of large energy densities at the horizon, i.e. a wall of fire. The third proposal resolves the paradox by identifying modes inside the hole with the radiation modes in the distant region, far from the hole. In this section we explain how bilocal holography provides a mechanism to realize the holography of information scenario.

According to the quantum error correcting framework for holography, bulk information is coded into boundary degrees of freedom, in a redundant way. Could this redundancy explain why degrees of freedom inside the black hole are identified with degrees of freedom of the radiation far from the hole? Probably not. The redundancy in the quantum error correcting description arises both because information about the bulk is encoded non-locally into the boundary and because we are focusing on a subspace, the code subspace, that a low energy observer has access to. The holography of information is a property of the full unitary evolution in a black hole background, using the complete Hilbert and not the code subspace. To understand the holography of information, one has to explain non-local redundancies present in the complete bulk Hilbert space. Where do these non-localities come from?

The central hypothesis of bilocal holography is that a gauge fixed version of the gravitational dual is obtained by a change to gauge invariant variables in the CFT. We will argue that the CFT does not have enough independent degrees of freedom to produce a local field theory in higher dimensions, so that the holographic theory necessarily has non-local redundancies. We will show that these redundancies imply identifications between degrees of freedom at the boundary and degrees of freedom that can be arbitrarily deep in the AdS bulk, which is very reminiscent of the holography of information. Both the CFT and the higher dimensional gravitational theory have an infinite number of degrees of freedom, making a comparison difficult. To make the discussion well defined, discretize space $(x^-, x) \to (x_i^-, x_i)$ to obtain a lattice with L sites. The original fields $\phi^a(x^+, x_i^-, x_i)$ give at most NL independent[17] degrees of freedom, while the bilocal $\sigma(x^+, x_i^-, x_i, y_j^-, y_j)$ gives L^2 degrees of freedom. For $L > N$ not all the degrees of freedom in the bilocal can be independent. These redundancies will show up in complicated states, with more than $\sim 2N$ modes excited to produce the state. Clearly, this is a finite N effect. An example of a complicated state is the state of an old black hole, which has an atmosphere of excited quanta produced by Hawking radiation.

We can describe these redundancies in enough detail to see that they imply identifications between degrees of freedom deep in the bulk and degrees of freedom located close to the boundary. To simplify the discussion, switch to the mixed position/momentum description, evaluate all bilocals at the same momentum $p_1^+ = p_2^+ = p^+$ and discretize the spatial coordinate transverse to the light cone $\sigma(x^+, p^+, x_i, p^+, y_j)$. The simplest case is when $N = 1$. In

[17]Gauge invariance will reduce the number of physical degrees of freedom to less than NL so this upper bound is strict.

this case it is clear that

$$\sigma(x^+,p^+,x_1,p^+,y_1)\sigma(x^+,p^+,x_2,p^+,y_2)=\sigma(x^+,p^+,x_1,p^+,y_2)\sigma(x^+,p^+,x_2,p^+,y_1) \quad (3.5.1)$$

This constraint between the bilocal degrees of freedom can be written as

$$\det M=0 \qquad M=\begin{bmatrix}\sigma(x^+,p^+,x_1,p^+,y_1) & \sigma(x^+,p^+,x_1,p^+,y_2)\\ \sigma(x^+,p^+,x_2,p^+,y_1) & \sigma(x^+,p^+,x_2,p^+,y_2)\end{bmatrix} \quad (3.5.2)$$

which simply expresses the fact that the 2×2 matrix M has rank 1. In the general case where we have N components, this constraint can be written as $\det M=0$ where

$$M=\begin{bmatrix}\sigma(x^+,p^+,x_1,p^+,y_1) & \sigma(x^+,p^+,x_1,p^+,y_2) & \cdots & \sigma(x^+,p^+,x_1,p^+,y_{N+1})\\ \sigma(x^+,p^+,x_2,p^+,y_1) & \sigma(x^+,p^+,x_2,p^+,y_2) & \cdots & \sigma(x^+,p^+,x_2,p^+,y_{N+1})\\ \vdots & \vdots & \ddots & \vdots\\ \sigma(x^+,p^+,x_{N+1},p^+,y_1) & \sigma(x^+,p^+,x_{N+1},p^+,y_2) & \cdots & \sigma(x^+,p^+,x_{N+1},p^+,y_{N+1})\end{bmatrix} \quad (3.5.3)$$

expressing the fact that the $N+1\times N+1$ dimensional matrix M has rank N.

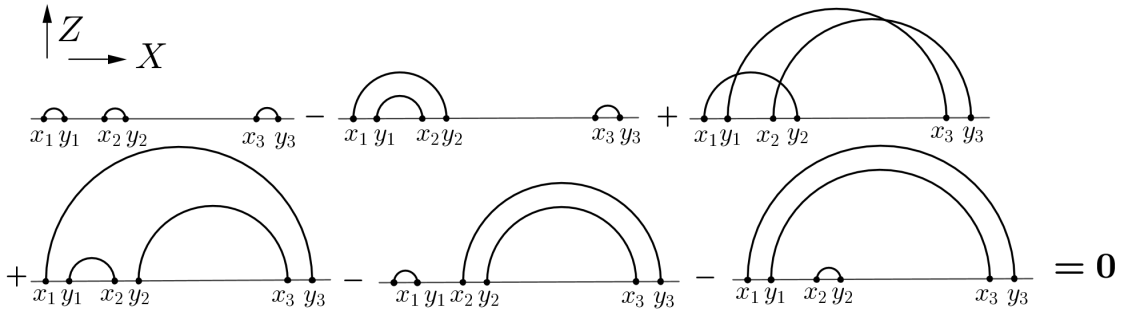


Figure 9: Constraints that arise when $N=2$.

We can study the above constraint for some interesting choices of the points x_i and y_i. $N=2$ is already an instructive example. Choose four points x_i and y_i for $i=1,2$ clustered in a small region and two more points for $i=3$, close to each other, but well separated from the first four points. The constraint, written diagrammatically, is shown in Figure 9. The bulk operator corresponding to each bilocal is located on the semicircle shown. Since all light cone momenta are equal $\theta=\pi$ and each bulk operator is located on the semicircle at the point which is deepest in the bulk. The first two diagrams in Figure 9 correspond to three operators located near the boundary. Choosing the points x_1,x_2,y_1,y_2 to be arbitrarily close to each other, and choosing the points x_3,y_3 to be arbitrarily close to each other, these operators are arbitrarily close to the boundary. The remaining four diagrams correspond to two operators located deep in the bulk and an operator located near the boundary. Making the separation between location of the four points x_1,x_2,y_1,y_2 and the location of the two points x_3,y_3 arbitrarily large, the operators that explore the bulk are arbitrarily deep in the bulk. This demonstrates non-local identifications between degrees of freedom at the boundary and degrees of freedom arbitrarily deep in the AdS bulk.

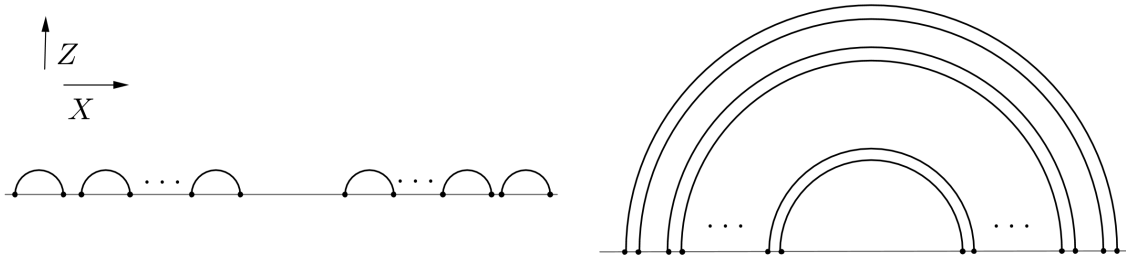


Figure 10: Two of the diagrams participating in the constraint that arises for general N.

For general N the relations are more complicated, but the conclusion is unchanged. For example, two of the diagrams participating in the constraint that arises from considering $N+1$ pairs of points are shown in Figure 10. The first diagram is again associated with degrees of freedom that are localized at the boundary whilst the second describes degrees of freedom localized arbitrarily deep in the bulk.

3.6 Conclusions

Bilocal holography gives an explicit mapping between the degrees of freedom of a CFT and its gravitational dual. We have discussed the example of bilocal holography, relating the free $O(N)$ vector model and its dual higher spin gravity in AdS_4 spacetime. The map between degrees of freedom is one-to-one at large N and there is no ambiguity in the map.

To describe effective field theory relevant for a low energy observer, one introduces a code subspace. The code subspace accounts for the fact that a low energy observer only has access to a subspace of the full Hilbert space. There is a redundancy in how the states of the code subspace are encoded in the CFT and in this way we can see how the quantum error correction description of holography is recovered from bilocal holography. Further, by inverting the operator mapping we prove entanglement wedge reconstruction. The bilocal of the boundary theory maps into a line in the bulk with endpoints given by the bilocal coordinates, in a way that is reminiscent of the bit threads description of entanglement.

At finite N bilocal holography predicts a genuine redundancy of the gravitational degrees of freedom: complicated states in the gravity dual can have more degrees of freedom excited than there are independent degrees of freedom in the CFT. In this case, there will be relations between naively independent degrees of freedom in the gravitational theory. We gave a rudimentary analysis of this issue and argued that the relations which appear naturally relate degrees of freedom localized at the boundary with degrees of freedom deep in the bulk of AdS. This has important implications for how information is coded into the gravitational theory.

There are a number of ways in which the analysis presented in this chapter can be extended. A simple extension would be to repeat the analysis using the canonical map developed in [149]. Another interesting extension would be to explore the Wilson-Fisher fixed point conformal field theory. For results in this direction see [190]. A much more interesting analysis would be to apply the ideas of bilocal holography (i.e. of collective field

theory [164, 165]) to theories of matrices. The number and type of gauge invariants that can be constructed is much richer, but the ideas would be the same: one first changes to invariant variables and then defines a coordinate transformation that will naturally adapt the generators to the direct sum of representations that appear in a given multi-local gauge invariant.

4 Conclusion

In this thesis, we have studied in chapter 2, operators that have a very large dimension of order N^2 again in $\mathcal{N} = 4$ super Yang-Mills theory. We have argued that these operators have properties which make them a possible dual to black holes. The one loop mixing problem of these operators determines dynamics on a graph. We have found that the number of interaction graphs grows fast enough to account for the entropy of a black hole. We characterized the typical interaction graph and studied the associated dynamics. Additionally, we have shown that the scrambling time corresponds to fast scrambling and the time scale for the system to equilibrate is $t \sim \frac{p}{\lambda}$ with $p \sim N$ giving the number of vertices in the interaction graph.

In chapter 3 we studied bilocal holography, relevant for the duality between the $O(N)$ vector model CFT and higher spin gravity in AdS. There is a one to one correspondence between degrees of freedom of the two theories. With an appropriate code subspace, our results show that bilocal holography reproduces a holographic quantum error correcting code. The code gives a geometric map between the bulk Hilbert space of the entanglement wedge and a boundary subspace of Hilbert space. We have also shown that operators in the entanglement wedge of the bulk can be reconstructed on a given subspace of the boundary.

A Gauss Graph Hamiltonian from Yang-Mills

In this section we review the results of [82, 83], where the Hamiltonian we study (2.2.4) was derived. We consider the mixing problem for operators belonging to the su(2|3) sector of the theory. Truncation to this subsector is consistent to all orders of perturbation theory[191]. We choose this sector because it is the maximal closed subsector with finitely many fields. The fact there are finitely many fields simplifies the analysis and it is possible to obtain explicit formulas for the action of the dilatation operator.

A basis for these operators is given by the restricted Schur polynomials. The relevant restricted Schur polynomials are labeled by 6 Young diagrams and some multiplicity labels. We study operators with $\Delta \sim N^2$ that are holographically dual to a system of giant gravitons. Operators with p long columns (rows) are dual to a system of p (dual) giant gravitons[18]. These operators mix with each other, but not with operators labeled by Young diagrams of a different shape. We take $n_1 \sim \epsilon N$ with $\epsilon \ll 1$. There are bosonic ϕ_2, ϕ_3 excitations, as well fermionic (ψ_1 and ψ_2) excitations. Limit the number of excitations by requiring $n_2 \sim n_3 \sim m_1 \sim m_2 \sim \epsilon^2 N^2$. We use a collective label $N_A = (n_2, n_3, m_2, m_2)$ to refer to the number of excitations.

We will now explain why our operators are labeled by Young diagrams. To construct all possible gauge invariant operators, we can take a product of an arbitrary number of fields and then contract all row indices with all column indices to obtain a gauge invariant operator. We can specify which row indices are to be computed with which column indices by giving a permutation. So we could label our operators with a permutation. Alternatively, by taking a Fourier transform on the group, we can trade the permutation for the label of an irreducible representation, that is, for a Young diagram[19]. This introduces the Young diagram R which has as many boxes as fields used to construct the operator, i.e. it has $n_1+n_2+n_3+m_1+m_2$ boxes. For operators dual to giant gravitons[197], the Young diagram R has a small number of long columns and for operators dual to dual giant gravitons[22, 23], the Young diagram R has a small number of long rows[24, 25, 27]. We will consider operators with a total of p long rows.

The construction described so far is redundant. Distinct permutations used to construct the gauge invariant operator might only differ by swapping two fields of a given species. Since our fields are bosons or fermions, swapping these fields does not lead to a new operator. Consequently, we need to remove this redundancy. This is done by projecting so that the collection of fields of a given species is in a definite representation of the permutation group - so we get one more Young diagram for each species of field[20]. Since we have five different types of fields, this makes a total of 6 Young diagrams. Each box in the Young diagram R corresponds to a field, and we can specify how many fields of each species appear in a given

[18] Branes connected by an open string described using a spin chain have been considered in [192, 193, 194, 195, 196].

[19] This discussion is not quite the whole story. We should have one Young diagram for the row indices and one for the column indices. Projecting to the singlet then forces these two to agree.

[20] Recall that the permutation group swapping indices of all fields has appeared. R is a representation of this group. The representations for each species are a representation of the subgroup which swaps only indices of fields that are the same species. The representation of the subgroup can be embedded into R in more than one way and this is why we need multiplicity labels.

row of R. This specifies the excitations of each dual giant graviton brane.

The operators that are obtained by this construction have orthogonal two point functions in the free field theory[44], provide a complete linear basis for local gauge invariant operators [50] and they mix only weakly when interactions are turned on [80]. The Hamiltonian we study is derived by evaluating the action of the one loop dilatation operator in the su(2|3) sector, which is given by [198, 199]

$$\begin{aligned} D = \; - \; & \frac{2g_{YM}^2}{(4\pi)^2}\left(\sum_{i>j=1}^{3}\mathrm{Tr}\left([\phi_i,\phi_j]\left[\partial_{\phi_i},\partial_{\phi_j}\right]\right)+\sum_{i=1}^{3}\sum_{a=1}^{2}\mathrm{Tr}\left([\phi_i,\psi_a]\left[\partial_{\phi_i},\partial_{\psi_a}\right]\right)\right. \\ + \; & \left.\mathrm{Tr}\left(\{\psi_1,\psi_2\}\left\{\partial_{\psi_1},\partial_{\psi_2}\right\}\right)\right) \end{aligned} \tag{A.0.1}$$

on restricted Schur polynomials. It is useful to introduce the notation

$$D \equiv -\frac{2g_{YM}^2}{(4\pi)^2}\sum_{A>B=1}^{5} D_{AB} \tag{A.0.2}$$

where D_{AB} mixes fields of species A and B. A major simplification in this computation follows by noting that at large N, corners on the right hand side of the Young diagram are well separated. This is the displaced corners limit [79, 80]. The action of the symmetric group simplifies in this limit and there are new symmetries: swapping the row or column indices of fields that belong to a given species and sit in the same row of R is a symmetry. To use these new symmetries we refine the number of fields of a species N_A to produce a p dimensional vector $\vec{N}_A$, with each component recording how many fields are in a given row. For example, the number of ϕ_2 fields n_2 is refined to produce $\vec{n}_2$, and the group swapping ϕ_2 fields in a given row, the enhanced symmetry of the displaced corners limit, is[21]

$$H_{\vec{n}_2} = S_{(n_2)_1} \times S_{(n_2)_2} \times \cdots \times S_{(n_2)_p} \tag{A.0.3}$$

In this limit, the number of restricted Schur polynomials matches the order of the double coset, indicating that we can organize the local operators using the double coset [81]. The four double cosets relevant for labeling our operators are

$$A \;\; \leftrightarrow \;\; \sigma_A \in H_{\vec{N}_A} \setminus S_{N_A}/H_{\vec{N}_A} \tag{A.0.4}$$

These double cosets are the crucial ingredient needed to make the connection to physics on a graph. Indeed, the collection of graphs with n edges and p vertices, and with number of edges terminating at each vertex recorded in $\vec{n}$ is described by a double coset [200]. By this connection each element of a double coset is described by a graph, so that we can label our operators by a graph. Diagonalizing $D_{\phi_1,A} \in \{D_{\phi_1\phi_2}, D_{\phi_1\phi_3}, D_{\phi_1\psi_1}, D_{\phi_1\psi_2}\}$ first, the resulting eigenoperators are the Gauss graph operators [80, 81], labeled by two Young diagrams (the R and r_1 labels of the restricted Schur polynomial) and a graph (which takes the place of four Young diagrams). Vertices of graphs correspond to rows/columns of r_1, i.e. each vertex

[21] We divide on the left to account for the symmetry associated with the row indices and on the right to account for the symmetry associated with column indices. See (A.0.4).

corresponds to a giant graviton brane. Each A field type is a species of edge in the graph and there is an edge for each field. Edges are directed. We give the complete graph as a graph for each A, specified by four elements $\vec{\sigma}$, one of each of the four double cosets in (A.0.4). These are the graphs that we call Gauss graphs.

Intuitively its clear why the graph provides a useful description: it naturally accounts for the symmetries of the displaced corners limit. Recall that each row of R corresponds to a vertex and each edge in the graph corresponds to a field in the operator. The symmetry of swapping row indices of fields in a given row is now the symmetry of swapping endpoints of edges that end on the same vertex (an obvious symmetry of the graph) while the symmetry of swapping column indices of fields is the symmetry of swapping start points of edges that start on the same vertex.

The elements of the double cosets in (A.0.4) correspond to the graphs we consider. Vertices can be dressed by closed edges with ends attached to the same vertex or by edges between two distinct vertices. Fermi statistics forbids two or more parallel edges (edges with the same orientation and endpoints) of the same fermion species [201]. We refined N_A to produce a vector $\vec{N}_A$. To describe the graph refine $\vec{N}_A$ to produce a matrix $(N_A)_{i\to j}$ whose elements describe the number of edges running from vertex i to vertex j. In terms of this matrix, the Gauss Law constraint is $\sum_{k\neq i}(N_A)_{i\to k} = \sum_{k\neq i}(N_A)_{k\to i}$. The transformation from restricted Schur basis to Gauss graph basis is derived in [202]. After the transformation, the dilatation operator is most naturally written as a system of particles hopping on a lattice, with lattice sites given by vertices of the Gauss graph [82]. Closed edges forming loops at a vertex translate into particles at that site. The hopping strength is determined by the number of edges of all other species stretched between the vertices. There are two distinct species of bosons, for ϕ_2, ϕ_3, and two distinct species of fermions, for ψ_1, ψ_2.

To simplify the discussion that follows, we will consider only the bosonic sector of the theory. The bosons are described by oscillators

$$\big[a_{ij}, \bar{a}_{kl}\big] = \delta_{il}\delta_{jk} \qquad\qquad \big[b_{ij}, \bar{b}_{kl}\big] = \delta_{il}\delta_{jk} \tag{A.0.5}$$

with all other commutators vanishing. The Fock space vacuum $|0\rangle$ obeys $a_{ij}|0\rangle = 0 = b_{ij}|0\rangle$ for $i, j = 1, 2, \cdots, p$. our final result for the Hamiltonian of the lattice model, arising from the one loop dilation operator, is

$$\begin{aligned} H &= \frac{2g_{YM}^2}{(4\pi)^2}\sum_{A=1}^{4}\sum_{i>j=1}^{p}(\hat{N}_A)_{ij}\left(\sqrt{N+l_{R_i}}-\sqrt{N+l_{R_j}}\right)^2 \\ &\quad +\frac{2g_{YM}^2}{(4\pi)^2}\sum_{A=1}^{3}\sum_{B=1+A}^{4}\sum_{i,j=1}^{p}\sqrt{\frac{(N+l_{R_i})(N+l_{R_j})}{l_{R_i}l_{R_j}}}\Bigg(-(\hat{N}_B)_{ji}(\bar{a}_A)_{jj}(a_A)_{ii}-(\hat{N}_A)_{ji}(\bar{a}_B)_{jj}(a_B)_{ii} \\ &\quad +2\delta_{ij}\Big(\sum_{l\neq i}(\hat{N}_A)_{i\to l}+(\bar{a}_A)_{ii}(a_A)_{ii}\Big)\Big(\sum_{l\neq i}(\hat{N}_B)_{i\to l}+(\bar{a}_B)_{ii}(a_B)_{ii}\Big)\Bigg) \end{aligned} \tag{A.0.6}$$

In the above formula, l_{R_i} is the length of the ith row of Young diagram R.

Thus, in this non-planar limit the operator mixing problem translates into dynamics on an emergent lattice, described by a graph. We consider states with definite $(\hat{N}_A)_{i\to j}, (\hat{N}_A)_{ij}$ for $i \neq j$ eigenvalues. These are constants of the motion. We can replace the operators

$(\hat{N}_A)_{i\to j}, (\hat{N}_A)_{ij}$, for $i \neq j$ by fixed non-negative integers $(N_A)_{i\to j}, (N_A)_{ij}$ for each state. To simplify the problem we consider operators without fermionic excitations

$$(\hat{m}_1)_{ij} = 0 = (\hat{m}_2)_{ij} \tag{A.0.7}$$

Edges between vertices are given by the ϕ_2 field, so that

$$(\hat{n}_3)_{ij} = 0 \qquad i \neq j \tag{A.0.8}$$

Excitations localized to a vertex are all given by ϕ_3 fields so that

$$(\hat{n}_2)_{ii} = 0 \tag{A.0.9}$$

Setting $(n_2)_{ij} = N_{ij}$, $r_i = N + l_{R_i}$, $k_i = \sum_{j\neq i, j=1}^{p} N_{ij}$ and renaming $l_{R_i} \to l_i$ $b_{ii} \to b_i$ and $\bar{b}_{ii} \to b_i^\dagger$ our Hamiltonian becomes

$$H = \frac{g_{YM}^2}{(4\pi)^2} \sum_{i,j=1}^{p} N_{ij} \left(\sqrt{r_i} - \sqrt{r_j}\right)^2 - \frac{2g_{YM}^2}{(4\pi)^2} \sum_{i,j=1, i\neq j}^{p} \sqrt{\frac{r_i r_j}{l_i l_j}} N_{ji} b_j^\dagger b_i + \frac{2g_{YM}^2}{(4\pi)^2} \sum_{i=1}^{p} \frac{k_i r_i}{l_i} b_i^\dagger b_i \tag{A.0.10}$$

This is the one loop correction to the dimension. To get the total dimension of the operator we would sum this with the bare dimension, given by $\Delta_0 = n_1 + n_2 + n_3 + \frac{3}{2}(m_1 + m_2)$.

B Coordinate Transformation

An important component of bilocal holography is the relation between the CFT and AdS coordinates given in (3.2.9) and (3.2.10). This mapping of the coordinates is determined entirely by the symmetries of the problem as we explain in this section. The basic idea is the following: each scalar field $\phi^a(x)$ transforms in the short representation $V_{\Delta,s}$ of $SO(2,3)$ constructed on the primary of dimension $\Delta = \frac{1}{2}$ and spin $s = 0$. The bilocal transforms in the tensor product $V_{\frac{1}{2},0} \otimes V_{\frac{1}{2},0}$, which is reducible

$$V_{\frac{1}{2},0} \otimes V_{\frac{1}{2},0} = V_{1,0} \oplus \bigoplus_{s=2,4,6,\cdots} V_{s+1,s} \tag{B.0.1}$$

The original bilocal coordinates are the natural set of coordinates to describe the tensor product on the LHS of (B.0.1), while the AdS coordinates are natural to describe the RHS.

We will start with a trivial toy model to illustrate the idea and then verify the origin of the transformation (3.2.9).

B.1 Motivational Example

Consider the tensor product of two spin $\frac{1}{2}$-particles. This decomposes into the triplet and the singlet

$$\frac{1}{2} \otimes \frac{1}{2} = 1 \oplus 0 \tag{B.1.1}$$

In the basis natural for the LHS of (B.1.1), we have the z component of spin (for example) given by the standard co-product

$$J^z = \Delta(\frac{1}{2}\sigma^3) = \frac{1}{2}\sigma^3 \otimes \mathbf{1} + \mathbf{1} \otimes \frac{1}{2}\sigma^3 \tag{B.1.2}$$

where $\mathbf{1}$ is a 2×2 identity matrix and σ^3 is a Pauli matrix. In the basis natural for the RHS of (B.1.1), the z component of spin is given by

$$J^z = J_1^z \oplus J_0^z \tag{B.1.3}$$

where J_1^z is a 3×3 matrix with eigenvalues equal to $-1, 0, 1$ and J_0^z is a 1×1 matrix with eigenvalue equal to 0. In moving from the basis which is natural for the LHS of (B.1.1) to the basis which is natural for the RHS, we see that the generators are transformed. We will see exactly the same features in the vector model. The transformation between the bases natural for the two sides of (B.1.1) is accomplished by the change of coordinates given in (3.2.9) and (3.2.10).

B.2 Conformal Transformations

The generators of conformal transformations for the bilocal $\sigma(x^+, x_1^-, x_1, x_2^-, x_2)$ are obtained using the standard coproduct

$$\Delta(L) = L \otimes 1 + 1 \otimes L \tag{B.2.1}$$

where L is a generator acting on the field $\phi^a(x^+, x^-, x)$. This is the direct product representation i.e. the analog of the LHS of (B.1.1) and it is the representation naturally derived from the CFT. A complete basis for so$(2,3)$ is

$$\begin{aligned}
P^+ &= p_1^+ + p_2^+ \\
P^x &= \frac{\partial}{\partial x_1} + \frac{\partial}{\partial x_2} \\
P^- &= -\frac{1}{2p_1^+}\frac{\partial^2}{\partial x_1^2} - \frac{1}{2p_2^+}\frac{\partial^2}{\partial x_2^2} \\
J^{+-} &= x^+ P^- + \frac{\partial}{\partial p_1^+}\, p_1^+ + \frac{\partial}{\partial p_2^+}\, p_2^+ \\
J^{+x} &= x^+ \left(\frac{\partial}{\partial x_1} + \frac{\partial}{\partial x_2}\right) - x_1 p_1^+ - x_2 p_2^+ \\
J^{-x} &= -\frac{\partial}{\partial p_1^+}\frac{\partial}{\partial x_1} - \frac{\partial}{\partial p_2^+}\frac{\partial}{\partial x_2} + \frac{x_1}{2p_1^+}\frac{\partial^2}{\partial x_1^2} + \frac{x_2}{2p_2^+}\frac{\partial^2}{\partial x_2^2} \\
D &= x^+ P^- - \frac{\partial}{\partial p_1^+} p_1^+ - \frac{\partial}{\partial p_2^+} p_2^+ + x_1\frac{\partial}{\partial x_1} + x_2\frac{\partial}{\partial x_2} + 1 \\
K^+ &= -\frac{1}{2}\left(-2x^+\left(\frac{\partial}{\partial p_1^+} p_1^+ + \frac{\partial}{\partial p_2^+} p_2^+\right) + x_1^2 p_1^+ + x_2^2 p_2^+\right) + x^+ D \\
K^- &= \frac{3}{2}\left(\frac{\partial}{\partial p_1^+} + \frac{\partial}{\partial p_2^+}\right) + p_1^+\frac{\partial^2}{\partial {p_1^+}^2} + p_2^+\frac{\partial^2}{\partial {p_2^+}^2} - x_1\frac{\partial}{\partial x_1}\frac{\partial}{\partial p_1^+} - x_2\frac{\partial}{\partial x_2}\frac{\partial}{\partial p_2^+} + \frac{x_1^2}{4p_1^+}\frac{\partial^2}{\partial x_1^2} + \frac{x_2^2}{4p_2^+}\frac{\partial^2}{\partial x_2^2}
\end{aligned}$$

$$
\begin{aligned}
K^x &= -\frac{1}{2}\left(-2x^+\left(\frac{\partial}{\partial x_1}\frac{\partial}{\partial p_1^+}+\frac{\partial}{\partial x_2}\frac{\partial}{\partial p_2^+}\right)+x_1^2\frac{\partial}{\partial x_1}+x_2^2\frac{\partial}{\partial x_2}\right)\\
&\quad +x_1\left(-x^+\frac{1}{2p_1^+}\frac{\partial^2}{\partial x_1^2}-\frac{\partial}{\partial p_1^+}p_1^++x_1\frac{\partial}{\partial x_1}+\frac{1}{2}\right)+x_2\left(-x^+\frac{1}{2p_2^+}\frac{\partial^2}{\partial x_2^2}-\frac{\partial}{\partial p_2^+}p_2^++x_2\frac{\partial}{\partial x_2}+\frac{1}{2}\right)
\end{aligned}
\tag{B.2.2}
$$

The analog of the RHS of (B.1.1) is provided by the generators for completely symmetric tensor fields in light cone gauge in AdS, which have been worked out by Metsaev in [172]. Notice that this representation, since it is determined by the transformation of the bulk fields, is the natural representation for the bulk gravitational description. We now want to argue that the change of coordinates (3.2.9) followed by a simple similarity transform, takes us from the above generators (natural for CFT) to those of [172] (natural for AdS). After changing coordinates using (3.2.9), we obtain the following generators

$$
\begin{aligned}
P^+ &= p^+\\
P^x &= \frac{\partial}{\partial x}\\
P^- &= -\frac{1}{2p^+}\left(\frac{\partial^2}{\partial x^2}+\frac{\partial^2}{\partial z^2}\right)\\
J^{+-} &= x^+P^- -\left(-\frac{1}{p^+}-\frac{\partial}{\partial p^+}\right)p^+\\
J^{+x} &= -p^+x+x^+\frac{\partial}{\partial x}\\
J^{-x} &= \left(-\frac{\partial}{\partial p^+}-\frac{1}{p^+}\right)\frac{\partial}{\partial x}-xP^-+\frac{1}{p^+}\left(\frac{\partial}{\partial\theta}+\cot(\theta)\right)\frac{\partial}{\partial z}\\
D &= x^+P^-+x\frac{\partial}{\partial x}+z\frac{\partial}{\partial z}+p^+\left(-\frac{\partial}{\partial p^+}-\frac{1}{p^+}\right)\\
K^+ &= -\left(x^+\left(-\frac{1}{p^+}-\frac{\partial}{\partial p^+}\right)+\frac{1}{2}(x^2+z^2)\right)p^++x^+D\\
K^- &= -\left(x^+\left(-\frac{1}{p^+}-\frac{\partial}{\partial p^+}\right)+\frac{1}{2}(x^2+z^2)\right)P^-+\left(-\frac{1}{p^+}-\frac{\partial}{\partial p^+}\right)D\\
&\quad +\frac{1}{p^+}\left(x\frac{\partial}{\partial z}-z\frac{\partial}{\partial x}\right)\left(\frac{\partial}{\partial\theta}+\cot\theta\right)+\frac{1}{p^+}\left(\frac{\partial}{\partial\theta}+\cot\theta\right)^2\\
K^x &= -x^+\left(-\frac{1}{p^+}-\frac{\partial}{\partial p^+}\right)\frac{\partial}{\partial x}-\frac{1}{2}(x^2+z^2)\frac{\partial}{\partial x}+xD+\left(\cot\theta+\frac{\partial}{\partial\theta}\right)z\\
&\quad -\frac{1}{p^+}\left(\cot(\theta)+\frac{\partial}{\partial\theta}\right)\frac{\partial}{\partial z}x^+
\end{aligned}
\tag{B.2.3}
$$

Now, rescaling each of the generators L as follows $L\to\mu L\frac{1}{\mu}$ where $\mu=2\pi p^+\sin\theta$, the algebra is obviously unchanged. To understand why this similarity transform is required,

note that our map can be written as

$$\begin{aligned}\Phi(X^+,p^+,X,Z,\theta) &= 2\pi p^+\sin\theta\ \eta(X^+,p^+\cos^2\frac{\theta}{2},X+Z\tan\frac{\theta}{2},p^+\sin^2\frac{\theta}{2},X-Z\cot\frac{\theta}{2})\\ &= \mu\ \eta(X^+,p^+\cos^2\frac{\theta}{2},X+Z\tan\frac{\theta}{2},p^+\sin^2\frac{\theta}{2},X-Z\cot\frac{\theta}{2}) \qquad \text{(B.2.4)}\end{aligned}$$

The rescaling is required since

$$\tilde{\eta}=L\eta \qquad \Rightarrow \qquad \mu\tilde{\eta}=\mu L\frac{1}{\mu}\mu\eta \qquad \Rightarrow \qquad \tilde{\Phi}=\mu L\frac{1}{\mu}\ \Phi \qquad \text{(B.2.5)}$$

so that if the generator acting on the bilocal η is L, then the generator acting on $\Phi=\mu\eta$ is $\mu L\frac{1}{\mu}$. After the rescaling the generators become

$$\begin{aligned}P^+ &= p^+\\ P^x &= \frac{\partial}{\partial x}\\ P^- &= -\frac{1}{2p^+}\left(\frac{\partial^2}{\partial x^2}+\frac{\partial^2}{\partial z^2}\right)\\ J^{+-} &= x^+P^- -\left(-\frac{\partial}{\partial p^+}\right)p^+\\ J^{+x} &= -p^+x+x^+\frac{\partial}{\partial x}\\ J^{-x} &= \left(-\frac{\partial}{\partial p^+}\right)\frac{\partial}{\partial x}-xP^-+\frac{1}{p^+}\left(\frac{\partial}{\partial\theta}\right)\frac{\partial}{\partial z}\\ D &= x^+P^-+x\frac{\partial}{\partial x}+z\frac{\partial}{\partial z}+p^+\left(-\frac{\partial}{\partial p^+}\right)\\ K^+ &= -\left(x^+\left(-\frac{\partial}{\partial p^+}\right)+\frac{1}{2}(x^2+z^2)\right)p^++x^+D\\ K^- &= -\left(x^+\left(-\frac{\partial}{\partial p^+}\right)+\frac{1}{2}(x^2+z^2)\right)P^-+\left(-\frac{\partial}{\partial p^+}\right)D\\ &\quad +\frac{1}{p^+}\left(x\frac{\partial}{\partial z}-z\frac{\partial}{\partial x}\right)\left(\frac{\partial}{\partial\theta}\right)+\frac{1}{p^+}\left(\frac{\partial}{\partial\theta}\right)^2\\ K^x &= -x^+\left(-\frac{\partial}{\partial p^+}\right)\frac{\partial}{\partial x}-\frac{1}{2}(x^2+z^2)\frac{\partial}{\partial x}+xD+\left(\frac{\partial}{\partial\theta}\right)z\\ &\quad -\frac{1}{p^+}\left(\frac{\partial}{\partial\theta}\right)\frac{\partial}{\partial z}x^+ \qquad \text{(B.2.6)}\end{aligned}$$

A comparison with the expressions in section 3.8 of [172] shows complete agreement, for all generators except for D, after identifying

$$\begin{aligned}&\partial^+ \longleftrightarrow p^+ \qquad && x^- \longleftrightarrow -\tfrac{\partial}{\partial p^+}\\ &M^{xz}\longleftrightarrow \tfrac{\partial}{\partial\theta} \qquad && M^{i-}\longleftrightarrow -\tfrac{1}{p^+}\tfrac{\partial}{\partial\theta}\tfrac{\partial}{\partial z}\end{aligned} \qquad \text{(B.2.7)}$$

along with $A = 0$. The first two relations are simple consequences of the Fourier transform. To understand the last two relations we need to interpret, for example, the operator M^{xz}. Recall that the special conformal generators generate a local scaling and Lorentz rotation. Consequently, it must be that M^{xz} is generating a rotation in the X, Z plane. It is clear from Figure 5 that the angle describing rotations in this plane is θ so that the above expression for M^{xz} is indeed correct. The difference between the expression for D in (B.2.6) and that in [172] is easily explained as follows: D in [172] acts on the field $\Phi(X^+, X^-, X, Z, \theta)$ which has dimension $\Delta = 1$. D in (B.2.6) acts on the field

$$\Phi(X^+, p^+, X, Z, \theta) = \int dX^- e^{ip^+X^-} \Phi(X^+, X^-, X, Z, \theta) \tag{B.2.8}$$

which has dimension $\Delta = 0$. The requirement that our change of coordinates implements the passage from the direct product representation (natural for the CFT) to the direct sum representation (natural for bulk AdS) determines the map (3.2.9) and (3.2.10).

C Other approaches

A work that is closely related to bilocal holography was given in [152]. The map proposed in [152] intertwines a given bulk SO(2,3) representation labeled by dimension Δ and spin J in the bulk with the SO(2,3) representation of the bilocal. Since intertwining maps are unique, this shows how the representation of SO(2,3) in the bulk and the bilocal representation in the boundary determine the map of [152]. In this sense it is similar to the bilocal holography map of [145] which maps the representation of the bilocal to all relevant bulk representations.

The map of [152] is written using the bulk to boundary propagator $G_{\Delta,J}(X, P; W, D_Q)$ written in embedding space both for the CFT and the AdS, as well as conformal three point functions $\langle O_{\frac{1}{2}}(P_1) O_{\frac{1}{2}}(P_2) O_{\tilde{\Delta},J}(P, Q)\rangle$. We refer the reader to the original paper for further explanation of the notation. To understand the map of [152] we use two known facts:

1. Section 5.1 of [203] proves

$$[L^{\text{bulk}}_{\Delta,J} \Phi_J](X, W) = \int dP\ G_{\Delta,J}(X, P; W, D_Q) [L^{\text{boundary}}_{\Delta,J} O_{\Delta,J}](P, Q) \tag{C.0.1}$$

   This says that the bulk-to-boundary map intertwines the bulk and boundary representations.

2. Formula (3.2) of [204] proves

$$\begin{aligned} & L^{\text{boundary}}_{\Delta,J} \left(\int dP_1 dP_2 \langle O_{\frac{1}{2}}(P_1) O_{\frac{1}{2}}(P_2) O_{\tilde{\Delta},J}(P, Q)\rangle \eta(P_1, P_2) \right) \\ & \int dP_1 dP_2 \langle O_{\frac{1}{2}}(P_1) O_{\frac{1}{2}}(P_2) [L^{\text{boundary}}_{\Delta,J} O_{\tilde{\Delta},J}](P, Q)\rangle \eta(P_1, P_2) \\ = & \int dP_1 dP_2 \langle O_{\frac{1}{2}}(P_1) O_{\frac{1}{2}}(P_2) O_{\tilde{\Delta},J}(P, Q)\rangle [L^{\text{bilocal}} \tilde{\eta}](P_1, P_2) \end{aligned} \tag{C.0.2}$$

   This says the three point function intertwines the representation Δ, J and the bilocal representation.

It is useful to write the map of [152] as ($\tilde{\eta}$ is the shadow of η)

$$\begin{aligned}\Phi_J(X,W) &= \frac{16\pi^d\Gamma^2(\frac{d}{2}-\frac{1}{2})}{\Gamma^2(\frac{1}{2})2N_{\Delta,J}\lambda_{\Delta,J}}\left(\frac{\Gamma(\frac{d-2}{2})}{4\pi^{\frac{d}{2}}}\right)^2\int_{P.S.}\frac{d\Delta}{2\pi i}\int\frac{dP}{J!\left(\frac{d}{2}-1\right)_J}\int dP_1dP_2 \\ &\times G_{\Delta,J}(X,P;W,D_Q)\langle O_{\frac{1}{2}}(P_1)O_{\frac{1}{2}}(P_2)O_{\tilde{\Delta},J}(P,Q)\rangle\tilde{\eta}(P_1,P_2) \qquad \text{(C.0.3)}\end{aligned}$$

The map of [152] is an intertwining operator, intertwining a Δ, J representation of the bulk SO(2,3) with the bilocal representation. This follows because the map of [152] is a composition of the map defined by the three point function with the map defined by the bulk-to-boundary map. The proof is immediate using the above two results

$$\begin{aligned}[L^{\text{bulk}}_{\Delta,J}\Phi_J](X,W) &= \frac{16\pi^d\Gamma^2(\frac{d}{2}-\frac{1}{2})}{\Gamma^2(\frac{1}{2})2N_{\Delta,J}\lambda_{\Delta,J}}\left(\frac{\Gamma(\frac{d-2}{2})}{4\pi^{\frac{d}{2}}}\right)^2\int_{P.S.}\frac{d\Delta}{2\pi i}\int\frac{dP}{J!\left(\frac{d}{2}-1\right)_J}\int dP_1dP_2 \\ &\times G_{\Delta,J}(X,P;W,D_Q)[L^{\text{boundary}}_{\Delta,J}\langle O_{\frac{1}{2}}(P_1)O_{\frac{1}{2}}(P_2)O_{\tilde{\Delta},J}(P,Q)\rangle]\tilde{\eta}(P_1,P_2) \\ &= \frac{16\pi^d\Gamma^2(\frac{d}{2}-\frac{1}{2})}{\Gamma^2(\frac{1}{2})2N_{\Delta,J}\lambda_{\Delta,J}}\left(\frac{\Gamma(\frac{d-2}{2})}{4\pi^{\frac{d}{2}}}\right)^2\int_{P.S.}\frac{d\Delta}{2\pi i}\int\frac{dP}{J!\left(\frac{d}{2}-1\right)_J}\int dP_1dP_2 \\ &\times G_{\Delta,J}(X,P;W,D_Q)\langle O_{\frac{1}{2}}(P_1)O_{\frac{1}{2}}(P_2)O_{\tilde{\Delta},J}(P,Q)\rangle[L^{\text{bilocal}}\tilde{\eta}](P_1,P_2) \qquad \text{(C.0.4)}\end{aligned}$$

References

[1] G. 't Hooft, "A Planar Diagram Theory for Strong Interactions," Nucl. Phys. B **72**, 461 (1974). doi:10.1016/0550-3213(74)90154-0

[2] J. M. Maldacena, "The Large N limit of superconformal field theories and supergravity," Int. J. Theor. Phys. **38**, 1113 (1999) [Adv. Theor. Math. Phys. **2**, 231 (1998)] doi:10.1023/A:1026654312961, 10.4310/ATMP.1998.v2.n2.a1 [hep-th/9711200].

[3] Z. J., Jean and Jentschura, Ulrich D, "Multi-instantons and exact results I: Conjectures, WKB expansions, and instanton interactions," Annals of Physics **1**, 313 (2004)

[4] D. Dorigoni, "An Introduction to Resurgence, Trans-Series and Alien Calculus," arXiv:1411.3585 [hep-th].

[5] Hooft. Gerard'T, "Dimensional reduction in quantum gravity,"(1993) [arXiv preprint gr-qc/9310026].

[6] Kemp. Garreth James T, "A non-perturbative theory of giant gravitons using AdS/CFT,"(2015) [University of the Witwatersrand, Faculty of Science, School of Physics].

[7] Bayona. Carlos Alfonso. Braga. Nelson RF, "Anti-de Sitter boundary in Poincaré coordinates,"(2007) [arXiv 0512182v3 Springer].

[8] Jones, Peter. Waldram, Daniel, "A review of the n= 4 super yang-mills/type iib ads/cft correspondence,"(2013) [URL http://www. imperial. ac. uk/media/imperial-college/researchcentres-and-groups/theoretical-physics/msc/dissertations/2013/Peter-Jones-Dissertation. pdf].

[9] Qualls, Joshua D, "Lectures on conformal field theory,"(2015) [arXiv preprint arXiv:1511.04074].

[10] E. Witten, "Anti-de Sitter space and holography," Adv. Theor. Math. Phys. **2**, 253 (1998) doi:10.4310/ATMP.1998.v2.n2.a2 [hep-th/9802150].

[11] Hubeny. Veronika. E, "The ads/cft correspondence,"(2015) [IOP Publishing].

[12] Y. Sekino and L. Susskind, "Fast Scramblers," JHEP **10**, 065 (2008) [arXiv:0808.2096 [hep-th]].

[13] Hayden. Patrick and Preskill. John, "Black holes as mirrors: quantum information in random subsystems," JHEP **09**, 120 (2007) [arXiv:0708.4025 [hep-th]].

[14] Page. Don N, "Expected entropy of a subsystem," **71**, 1291 (1993) [Phys. Rev. Lett].

[15] Ryu Shinsei and Takayanagi, Tadashi, "Holographic derivation of entanglement entropy from the anti–de sitter space/conformal field theory correspondence," **18**, 96 (2006) [Physical review letters, APS].

[16] Ryu Shinsei and Takayanagi, Tadashi, "Aspects of holographic entanglement entropy," **18**, 96 (2006) [Journal of High Energy Physics, IOP Publishing].

[17] Cotler, Jordan and Hayden, Patrick and Penington, Geoffrey and Salton, Grant and Swingle, Brian and Walter, Michael, "Entanglement wedge reconstruction via universal recovery channels," **3**, 9 (2019) [Physical Review X, APS].

[18] Chen, Chi-Fang and Penington, Geoffrey and Salton, Grant, "Entanglement wedge reconstruction using the Petz map," **1**, 114 (2020) [Journal of High Energy Physics, Springer].

[19] Almheiri A. and Dong, Xi and Harlow, Daniel, "Bulk locality and quantum error correction in AdS/CFT," **4**, 134 (2015) [Journal of High Energy Physics].

[20] S. S. Gubser, I. R. Klebanov and A. M. Polyakov, "Gauge theory correlators from non-critical string theory," Phys. Lett. B **428**, 105 (1998) doi:10.1016/S0370-2693(98)00377-3 [hep-th/9802109].

[21] D. E. Berenstein, J. M. Maldacena and H. S. Nastase, "Strings in flat space and pp waves from N=4 superYang-Mills," JHEP **0204**, 013 (2002) doi:10.1088/1126-6708/2002/04/013 [hep-th/0202021].

[22] M. T. Grisaru, R. C. Myers and O. Tafjord, "SUSY and goliath," JHEP **0008**, 040 (2000) doi:10.1088/1126-6708/2000/08/040 [hep-th/0008015].

[23] A. Hashimoto, S. Hirano and N. Itzhaki, "Large branes in AdS and their field theory dual," JHEP **0008**, 051 (2000) doi:10.1088/1126-6708/2000/08/051 [hep-th/0008016].

[24] V. Balasubramanian, M. Berkooz, A. Naqvi and M. J. Strassler, "Giant gravitons in conformal field theory," JHEP **0204**, 034 (2002) doi:10.1088/1126-6708/2002/04/034 [hep-th/0107119].

[25] S. Corley, A. Jevicki and S. Ramgoolam, "Exact correlators of giant gravitons from dual N=4 SYM theory," Adv. Theor. Math. Phys. **5**, 809 (2002) doi:10.4310/ATMP.2001.v5.n4.a6 [hep-th/0111222].

[26] H. Lin, O. Lunin and J. M. Maldacena, "Bubbling AdS space and 1/2 BPS geometries," JHEP **0410**, 025 (2004) doi:10.1088/1126-6708/2004/10/025 [hep-th/0409174].

[27] D. Berenstein, "A Toy model for the AdS / CFT correspondence," JHEP **0407**, 018 (2004) doi:10.1088/1126-6708/2004/07/018 [hep-th/0403110].

[28] V. Balasubramanian, J. de Boer, V. Jejjala and J. Simon, "The Library of Babel: On the origin of gravitational thermodynamics," JHEP **0512**, 006 (2005) doi:10.1088/1126-6708/2005/12/006 [hep-th/0508023].

[29] V. Balasubramanian, J. de Boer, S. El-Showk and I. Messamah, "Black Holes as Effective Geometries," Class. Quant. Grav. **25**, 214004 (2008) doi:10.1088/0264-9381/25/21/214004 [arXiv:0811.0263 [hep-th]].

[30] D. Garner, S. Ramgoolam and C. Wen, "Thresholds of large N factorization in CFT_4: exploring bulk spacetime in AdS_5," JHEP **1411**, 076 (2014) doi:10.1007/JHEP11(2014)076 [arXiv:1403.5281 [hep-th]].

[31] M. Baggio, J. de Boer and K. Papadodimas, "A non-renormalization theorem for chiral primary 3-point functions," JHEP **1207**, 137 (2012) doi:10.1007/JHEP07(2012)137 [arXiv:1203.1036 [hep-th]].

[32] A. Voros, "The return of the quartic oscillator: The complex WKB method," Annales de l'Institut Henri Poincare Section A, Physique Theorique, 39, 211-338 (1983).

[33] E. Delabaere and F. Pham, "Resurgent methods in semi-classical asymptotics," Annales de l'Institut Henri Poincare Section A, Physique Theorique, 71, 1-94 (1999).

[34] E. Delabaere, H. Dillinger and F. Pham, "Exact semi-classical expansions for one-dimensional quantum oscillators," J. Math Phys., 38 6126-6184 (1997).

[35] T. Kawai and Y. Takei, "Algebraic Analysis of Singular Perturbation Theory," Translation of Mathematical Monographs, 227, AMS, 2005.

[36] T. Aoki and M. Tanda, "Borel sums of Voros coefficients of hypergeometric differential equations with a large parameter," RIMS Kokyuroku, Kyoto University **1861** (2013) 17.

[37] Mika Tanda, "Alien derivatives of the WKB solutions of the Gauss hypergeometric differential equation with a large parameter," Opuscula Mathematica 35.5 (2015): 803-823.

[38] T. Aoki, T. Takahashi and M. Tanda, "The hypergeometric function and WKB Solutions," RIMS Kokyuroku Bessatsu **B57** (2016) 061-068.

[39] Aoki, Takashi, and Mika Tanda. "Parametric Stokes phenomena of the Gauss hypergeometric differential equation with a large parameter." Journal of the Mathematical Society of Japan 68.3 (2016): 1099-1132.

[40] Talk given by T. Koike in the RIMS workshop "Exact WKB analysis - Borel summability of WKB solutions", September 2010.

[41] S. Hirano and Y. Sato, "Giant graviton interactions and M2-branes ending on multiple M5-branes," JHEP **1805**, 065 (2018) doi:10.1007/JHEP05(2018)065 [arXiv:1803.04172 [hep-th]].

[42] M. M. Sheikh-Jabbari, "Tiny graviton matrix theory: DLCQ of IIB plane-wave string theory, a conjecture," JHEP **0409**, 017 (2004) doi:10.1088/1126-6708/2004/09/017 [hep-th/0406214].

[43] S. Corley and S. Ramgoolam, "Finite factorization equations and sum rules for BPS correlators in N=4 SYM theory," Nucl. Phys. B **641**, 131 (2002) doi:10.1016/S0550-3213(02)00573-4 [hep-th/0205221].

[44] R. Bhattacharyya, S. Collins and R. de Mello Koch, "Exact Multi-Matrix Correlators," JHEP **0803**, 044 (2008) doi:10.1088/1126-6708/2008/03/044 [arXiv:0801.2061 [hep-th]].

[45] R. de Mello Koch, E. Gandote and J. H. Huang, "Non-Perturbative String Theory from AdS/CFT," JHEP **02** (2019), 169 doi:10.1007/JHEP02(2019)169 [arXiv:1901.02591 [hep-th]].

[46] Y. Kimura and S. Ramgoolam, "Branes, anti-branes and brauer algebras in gauge-gravity duality," JHEP **0711**, 078 (2007) doi:10.1088/1126-6708/2007/11/078 [arXiv:0709.2158 [hep-th]].

[47] T. W. Brown, P. J. Heslop and S. Ramgoolam, "Diagonal multi-matrix correlators and BPS operators in N=4 SYM," JHEP **0802**, 030 (2008) doi:10.1088/1126-6708/2008/02/030 [arXiv:0711.0176 [hep-th]].

[48] T. W. Brown, P. J. Heslop and S. Ramgoolam, "Diagonal free field matrix correlators, global symmetries and giant gravitons," JHEP **0904**, 089 (2009) doi:10.1088/1126-6708/2009/04/089 [arXiv:0806.1911 [hep-th]].

[49] T. W. Brown, R. de Mello Koch, S. Ramgoolam and N. Toumbas, "Correlators, Probabilities and Topologies in N=4 SYM," JHEP **0703**, 072 (2007) doi:10.1088/1126-6708/2007/03/072 [hep-th/0611290].

[50] R. Bhattacharyya, R. de Mello Koch and M. Stephanou, "Exact Multi-Restricted Schur Polynomial Correlators," JHEP **0806**, 101 (2008) doi:10.1088/1126-6708/2008/06/101 [arXiv:0805.3025 [hep-th]].

[51] J. Ecalle, "Les Fonctions R'esurgentes", Pr'epub. Math. Universit'e Paris-Sud 81-05 (1981), 81-06 (1981), 85-05 (1985).

[52] M. Mariño, "Lectures on non-perturbative effects in large N gauge theories, matrix models and strings," Fortsch. Phys. **62**, 455 (2014) doi:10.1002/prop.201400005 [arXiv:1206.6272 [hep-th]].

[53] I. Aniceto, G. Basar and R. Schiappa, "A Primer on Resurgent trans-series and Their Asymptotics," arXiv:1802.10441 [hep-th].

[54] G. V. Dunne and M. Unsal, "WKB and Resurgence in the Mathieu Equation," pages 249-298, in "Resurgence, Physics and Numbers", F. Fauvet et al (Eds), Edizioni Della Normale (2017) [arXiv:1603.04924 [math-ph]].

[55] J. Zinn-Justin and U. D. Jentschura, "Multi-instantons and exact results I: Conjectures, WKB expansions, and instanton interactions," Annals Phys. **313**, 197 (2004) doi:10.1016/j.aop.2004.04.004 [quant-ph/0501136].

[56] J. Zinn-Justin and U. D. Jentschura, "Multi-instantons and exact results II: Specific cases, higher-order effects, and numerical calculations," Annals Phys. **313**, 269 (2004) doi:10.1016/j.aop.2004.04.003 [quant-ph/0501137].

[57] G. Alvarez. "Langer-Cherry derivation of the multi-instanton expansion for the symmetric double well," J. Math. Phys.,**45**, (2004) 3095-3108.

[58] G. Alvarez and C. Casares, "Exponentially small corrections in the asymptotic expansion of the eigenvalues of the cubic anharmonic oscillator," J. Phys. **A33**, 2000, 5171.

[59] G. Alvarez and C. Casares, "Uniform asymptotic and JWKB expansions for anharmonic oscillators," J. Phys. **A33**,(2000) 2499.

[60] G. V. Dunne and M. Unsal, "Uniform WKB, Multi-instantons, and Resurgent Trans-Series," Phys. Rev. D **89**, no. 10, 105009 (2014) doi:10.1103/PhysRevD.89.105009 [arXiv:1401.5202 [hep-th]].

[61] G. Basar, G. V. Dunne and M. Unsal, "Quantum Geometry of Resurgent Perturbative/Nonperturbative Relations," JHEP **1705**, 087 (2017) doi:10.1007/JHEP05(2017)087 [arXiv:1701.06572 [hep-th]].

[62] A. Banerjee, A. Chowdhury, S. Thakur and G. Yang, "On interpolating anomalous dimension of twist-two operators with general spins," arXiv:1812.07331 [hep-th].

[63] R. de Mello Koch, T. K. Dey, N. Ives and M. Stephanou, "Correlators Of Operators with a Large R-charge," JHEP **0908**, 083 (2009) doi:10.1088/1126-6708/2009/08/083 [arXiv:0905.2273 [hep-th]].

[64] R. de Mello Koch, C. Mathwin and H. J. R. van Zyl, "LLM Magnons," JHEP **1603**, 110 (2016) doi:10.1007/JHEP03(2016)110 [arXiv:1601.06914 [hep-th]].

[65] R. de Mello Koch, M. Kim and H. J. R. Zyl, "Integrable Subsectors from Holography," JHEP **1805**, 198 (2018) doi:10.1007/JHEP05(2018)198 [arXiv:1802.01367 [hep-th]].

[66] R. de Mello Koch, J. H. Huang and L. Tribelhorn, "Exciting LLM Geometries," JHEP **1807**, 146 (2018) doi:10.1007/JHEP07(2018)146 [arXiv:1806.06586 [hep-th]].

[67] M. Kim and H. J. R. van Zyl, "Semiclassical $SL(2)$ strings on LLM backgrounds," Phys. Lett. B **784**, 62 (2018) doi:10.1016/j.physletb.2018.07.031 [arXiv:1805.12460 [hep-th]].

[68] P. Dorey and R. Tateo, "Anharmonic oscillators, the thermodynamic Bethe ansatz, and nonlinear integral equations," J. Phys. A **32**, L419 (1999) doi:10.1088/0305-4470/32/38/102 [hep-th/9812211].

[69] K. Ito, M. Mariño and H. Shu, "TBA equations and resurgent Quantum Mechanics," arXiv:1811.04812 [hep-th].

[70] N. Beisert, C. Ahn, L. F. Alday, Z. Bajnok, J. M. Drummond, L. Freyhult, N. Gromov, R. A. Janik, V. Kazakov, T. Klose, G. P. Korchemsky, C. Kristjansen, M. Magro, T. McLoughlin, J. A. Minahan, R. I. Nepomechie, A. Rej, R. Roiban, S. Schafer-Nameki, C. Sieg, M. Staudacher, A. Torrielli, A. A. Tseytlin, P. Vieira, D. Volin and K. Zoubos, "Review of AdS/CFT Integrability: An Overview," Lett. Math. Phys. **99**, 3-32 (2012) [arXiv:1012.3982 [hep-th]].

[71] I. Bena, J. Polchinski and R. Roiban, "Hidden symmetries of the AdS(5) x S**5 superstring," Phys. Rev. D **69**, 046002 (2004) [arXiv:hep-th/0305116 [hep-th]].

[72] V. Kazakov, A. Marshakov, J. Minahan and K. Zarembo, "Classical/quantum integrability in AdS/CFT," JHEP **05**, 024 (2004) [arXiv:hep-th/0402207 [hep-th]].

[73] L. Vidmar and M. Rigol, "Generalized Gibbs ensemble in integrable lattice models," Journal of Statistical Mechanics: Theory and Experiment 2016, no. 6 (2016): 064007.

[74] S. H. Shenker and D. Stanford, "Black holes and the butterfly effect," JHEP **03**, 067 (2014) [arXiv:1306.0622 [hep-th]].

[75] O. Aharony, Y. E. Antebi, M. Berkooz and R. Fishman, "'Holey sheets': Pfaffians and subdeterminants as D-brane operators in large N gauge theories," JHEP **12**, 069 (2002) [arXiv:hep-th/0211152 [hep-th]].

[76] D. Berenstein, "Shape and holography: Studies of dual operators to giant gravitons," Nucl. Phys. B **675**, 179-204 (2003) [arXiv:hep-th/0306090 [hep-th]].

[77] V. Balasubramanian, D. Berenstein, B. Feng and M. x. Huang, "D-branes in Yang-Mills theory and emergent gauge symmetry," JHEP **03**, 006 (2005) [arXiv:hep-th/0411205 [hep-th]].

[78] Y. Kimura and S. Ramgoolam, "Enhanced symmetries of gauge theory and resolving the spectrum of local operators," Phys. Rev. D **78**, 126003 (2008) [arXiv:0807.3696 [hep-th]].

[79] W. Carlson, R. de Mello Koch and H. Lin, "Nonplanar Integrability," JHEP **03**, 105 (2011) [arXiv:1101.5404 [hep-th]].

[80] R. de Mello Koch, M. Dessein, D. Giataganas and C. Mathwin, "Giant Graviton Oscillators," JHEP **10**, 009 (2011) [arXiv:1108.2761 [hep-th]].

[81] R. de Mello Koch and S. Ramgoolam, "A double coset ansatz for integrability in AdS/CFT," JHEP **06**, 083 (2012) [arXiv:1204.2153 [hep-th]].

[82] S. de Carvalho, R. de Mello Koch and A. Larweh Mahu, "Anomalous dimensions from boson lattice models," Phys. Rev. D **97**, no.12, 126004 (2018) [arXiv:1801.02822 [hep-th]].

[83] R. de Mello Koch, J. H. Huang, M. Kim and H. J. Van Zyl, "Emergent Yang-Mills theory," [arXiv:2005.02731 [hep-th]].

[84] N. Lashkari, D. Stanford, M. Hastings, T. Osborne and P. Hayden, "Towards the Fast Scrambling Conjecture," JHEP **04**, 022 (2013) [arXiv:1111.6580 [hep-th]].

[85] G. Bentsen, Y. Gu and A. Lucas, "Fast scrambling on sparse graphs," Proc. Nat. Acad. Sci. **116**, no.14, 6689-6694 (2019) [arXiv:1805.08215 [cond-mat.str-el]].

[86] J. G. Hartmann, J. Murugan and J. P. Shock, "Chaos and Scrambling in Quantum Small Worlds," [arXiv:1901.04561 [hep-th]].

[87] A. Lucas, "Quantum many-body dynamics on the star graph," [arXiv:1903.01468 [cond-mat.str-el]].

[88] C. F. Chen and A. Lucas, "Operator growth bounds from graph theory," [arXiv:1905.03682 [math-ph]].

[89] A. M. García-García, Y. Jia, D. Rosa and J. J. M. Verbaarschot, "Sparse Sachdev-Ye-Kitaev model, quantum chaos and gravity duals," [arXiv:2007.13837 [hep-th]].

[90] S. Xu, L. Susskind, Y. Su and B. Swingle, "A Sparse Model of Quantum Holography," [arXiv:2008.02303 [cond-mat.str-el]].

[91] E. Lieb and D. Robinson, "The finite group velocity of quantum spin systems," Commun. Math. Phys. **28**, 251-257 (1972)

[92] V. Balasubramanian, J. de Boer, V. Jejjala and J. Simon, "Entropy of near-extremal black holes in AdS(5)," JHEP **05**, 067 (2008) [arXiv:0707.3601 [hep-th]].

[93] R. Fareghbal, C. N. Gowdigere, A. E. Mosaffa and M. M. Sheikh-Jabbari, "Nearing Extremal Intersecting Giants and New Decoupled Sectors in N = 4 SYM," JHEP **08**, 070 (2008) [arXiv:0801.4457 [hep-th]].

[94] M. Reed and B. Simon, "Methods of modern mathematical physics I: Functional Analysis," (San Diego: Academic Press),
M. Reed and B. Simon, "Methods of Modern Mathematical Physics. 2. Fourier Analysis, Self-adjointness," (San Diego: Academic Press).

[95] C. Gogolin, and J. Eisert, "Equilibration, thermalisation, and the emergence of statistical mechanics in closed quantum systems." Reports on Progress in Physics **79**(5) (2016): 056001.

[96] J. M. Magan, "Black holes as random particles: entanglement dynamics in infinite range and matrix models," JHEP **08**, 081 (2016) [arXiv:1601.04663 [hep-th]].

[97] N. Iizuka and J. Polchinski, "A Matrix Model for Black Hole Thermalization," JHEP **10**, 028 (2008) [arXiv:0801.3657 [hep-th]].

[98] N. Iizuka, T. Okuda and J. Polchinski, "Matrix Models for the Black Hole Information Paradox," JHEP **02**, 073 (2010) [arXiv:0808.0530 [hep-th]].

[99] https://en.wikipedia.org/wiki/Directed_graph.

[100] P. Jacquet and W.Szpankowski, "Markov types and minimax redundancy for Markov sources," IEEE Transactions on Information Theory **50**, no. 7 (2004): 1393-1402,
P. Jacquet, C. Knessl and W. Szpankowski, "Markov Types Again Revisited," (2009).

[101] Roman Frigg, "Typicality and the approach to equilibrium in Boltzmannian statistical mechanics," Philosophy of Science **76**, no. 5 (2009): 997-1008.

[102] A. Kitaev http://online.kitp.ucsb.edu/online/entangled15/kitaev2

[103] S. Sachdev and J. Ye, "Gapless spin fluid ground state in a random, quantum Heisenberg magnet," Phys. Rev. Lett. **70**, 3339 (1993) [arXiv:cond-mat/9212030 [cond-mat]].

[104] J. Maldacena and D. Stanford, "Remarks on the Sachdev-Ye-Kitaev model," Phys. Rev. D **94**, no.10, 106002 (2016) [arXiv:1604.07818 [hep-th]].

[105] D. A. Roberts, D. Stanford and L. Susskind, "Localized shocks," JHEP **03**, 051 (2015) [arXiv:1409.8180 [hep-th]].

[106] Y. D. Lensky and X. L. Qi, "Chaos and High Temperature Pure State Thermalization," JHEP **06**, 025 (2019) [arXiv:1805.03675 [cond-mat.stat-mech]].

[107] P. Hosur, X. L. Qi, D. A. Roberts and B. Yoshida, "Chaos in quantum channels," JHEP **02**, 004 (2016) [arXiv:1511.04021 [hep-th]].

[108] S. Sahu and B. Swingle, "Information scrambling at finite temperature in local quantum systems," [arXiv:2005.10814 [cond-mat.stat-mech]].

[109] M. Cramer, A. Serafini, and J. Eisert, "Locality of dynamics in general harmonic quantum systems," arXiv preprint arXiv:0803.0890.

[110] D. N. Page, "Information loss in black holes and/or conscious beings?," [arXiv:hep-th/9411193 [hep-th]].

[111] L.C. Venuti, "The recurrence time in quantum mechanics," arXiv preprint arXiv:1509.04352.

[112] L. Susskind, "Three Lectures on Complexity and Black Holes," [arXiv:1810.11563 [hep-th]].

[113] M. Cramer, C. M. Dawson, J. Eisert and T. J. Osborne, "Exact Relaxation in a Class of Nonequilibrium Quantum Lattice Systems," Phys. Rev. Lett. **100**, 030602 (2008) [arXiv:cond-mat/0703314 [cond-mat.stat-mech]].

[114] M. Cramer and J. Eisert, "A quantum central limit theorem for non-equilibrium systems: exact local relaxation of correlated states," New Journal of Physics **12**, no. 5 (2010): 055020.

[115] A.S. Holevo, M. Sohma, and O. Hirota, "Capacity of quantum Gaussian channels," Physical Review A 59.3 (1999): 1820.

[116] A. S. Holevo, "Probabilistic and statistical aspects of quantum theory," Vol. 1. Springer Science & Business Media, 2011.

[117] https://en.wikipedia.org/wiki/Kullback%E2%80%93Leibler_divergence

[118] https://en.wikipedia.org/wiki/Baker%E2%80%93Campbell%E2%80%93Hausdorff_formula

[119] P. Calabrese and J. L. Cardy, "Time-dependence of correlation functions following a quantum quench," Phys. Rev. Lett. **96**, 136801 (2006) [arXiv:cond-mat/0601225 [cond-mat]].

[120] L.J. Landau, "Bessel functions: monotonicity and bounds," Journal of the London Mathematical Society 61, no. 1 (2000): 197-215.

[121] D. Berenstein, "Large N BPS states and emergent quantum gravity," JHEP **01**, 125 (2006) [arXiv:hep-th/0507203 [hep-th]].

[122] R. de Mello Koch, "Geometries from Young Diagrams," JHEP **11**, 061 (2008) [arXiv:0806.0685 [hep-th]].

[123] R. de Mello Koch and J. Murugan, "Emergent Spacetime," [arXiv:0911.4817 [hep-th]].

[124] D. Berenstein, "Sketches of emergent geometry in the gauge/gravity duality," Fortsch. Phys. **62**, 776-785 (2014) [arXiv:1404.7052 [hep-th]].

[125] H. Lin and K. Zeng, "Detecting topology change via correlations and entanglement from gauge/gravity correspondence," J. Math. Phys. **59**, no.3, 032301 (2018) [arXiv:1705.10776 [hep-th]].

[126] D. Berenstein and A. Miller, "Code subspaces for LLM geometries," Class. Quant. Grav. **35**, no.6, 065003 (2018) [arXiv:1708.00035 [hep-th]].

[127] D. Berenstein, "Negative specific heat from non-planar interactions and small black holes in AdS/CFT," JHEP **10**, 001 (2019) [arXiv:1810.07267 [hep-th]].

[128] A. Almheiri, X. Dong and D. Harlow, "Bulk Locality and Quantum Error Correction in AdS/CFT," JHEP **04**, 163 (2015) doi:10.1007/JHEP04(2015)163 [arXiv:1411.7041 [hep-th]].

[129] F. Pastawski, B. Yoshida, D. Harlow and J. Preskill, "Holographic quantum error-correcting codes: Toy models for the bulk/boundary correspondence," JHEP **06**, 149 (2015) doi:10.1007/JHEP06(2015)149 [arXiv:1503.06237 [hep-th]].

[130] D. Harlow, "The Ryu–Takayanagi Formula from Quantum Error Correction," Commun. Math. Phys. **354**, no.3, 865-912 (2017) doi:10.1007/s00220-017-2904-z [arXiv:1607.03901 [hep-th]].

[131] A. Laddha, S. G. Prabhu, S. Raju and P. Shrivastava, "The Holographic Nature of Null Infinity," SciPost Phys. **10**, 041 (2021) doi:10.21468/SciPostPhys.10.2.041 [arXiv:2002.02448 [hep-th]].

[132] S. Banerjee, J. W. Bryan, K. Papadodimas and S. Raju, "A toy model of black hole complementarity," JHEP **05**, 004 (2016) doi:10.1007/JHEP05(2016)004 [arXiv:1603.02812 [hep-th]].

[133] G. Penington, "Entanglement Wedge Reconstruction and the Information Paradox," JHEP **09**, 002 (2020) doi:10.1007/JHEP09(2020)002 [arXiv:1905.08255 [hep-th]].

[134] A. Almheiri, N. Engelhardt, D. Marolf and H. Maxfield, "The entropy of bulk quantum fields and the entanglement wedge of an evaporating black hole," JHEP **12**, 063 (2019) doi:10.1007/JHEP12(2019)063 [arXiv:1905.08762 [hep-th]].

[135] A. Almheiri, R. Mahajan and J. Maldacena, "Islands outside the horizon," [arXiv:1910.11077 [hep-th]].

[136] G. Penington, S. H. Shenker, D. Stanford and Z. Yang, "Replica wormholes and the black hole interior," [arXiv:1911.11977 [hep-th]].

[137] A. Almheiri, T. Hartman, J. Maldacena, E. Shaghoulian and A. Tajdini, "Replica Wormholes and the Entropy of Hawking Radiation," JHEP **05**, 013 (2020) doi:10.1007/JHEP05(2020)013 [arXiv:1911.12333 [hep-th]].

[138] I. R. Klebanov and A. M. Polyakov, "AdS dual of the critical O(N) vector model," Phys. Lett. B **550**, 213-219 (2002) doi:10.1016/S0370-2693(02)02980-5 [arXiv:hep-th/0210114 [hep-th]].

[139] E. Sezgin and P. Sundell, "Massless higher spins and holography," Nucl. Phys. B **644**, 303-370 (2002) [erratum: Nucl. Phys. B **660**, 403-403 (2003)] doi:10.1016/S0550-3213(02)00739-3 [arXiv:hep-th/0205131 [hep-th]].

[140] M. A. Vasiliev, "Consistent equation for interacting gauge fields of all spins in (3+1)-dimensions," Phys. Lett. B **243**, 378-382 (1990) doi:10.1016/0370-2693(90)91400-6

[141] M. A. Vasiliev, "Nonlinear equations for symmetric massless higher spin fields in (A)dS(d)," Phys. Lett. B **567**, 139-151 (2003) doi:10.1016/S0370-2693(03)00872-4 [arXiv:hep-th/0304049 [hep-th]].

[142] V. E. Didenko and E. D. Skvortsov, "Elements of Vasiliev theory," [arXiv:1401.2975 [hep-th]].

[143] S. Giombi and X. Yin, "Higher Spin Gauge Theory and Holography: The Three-Point Functions," JHEP **09**, 115 (2010) doi:10.1007/JHEP09(2010)115 [arXiv:0912.3462 [hep-th]].

[144] S. R. Das and A. Jevicki, "Large N collective fields and holography," Phys. Rev. D **68**, 044011 (2003) doi:10.1103/PhysRevD.68.044011 [arXiv:hep-th/0304093 [hep-th]].

[145] R. de Mello Koch, A. Jevicki, K. Jin and J. P. Rodrigues, "AdS_4/CFT_3 Construction from Collective Fields," Phys. Rev. D **83**, 025006 (2011) doi:10.1103/PhysRevD.83.025006 [arXiv:1008.0633 [hep-th]].

[146] A. Jevicki, K. Jin and Q. Ye, "Collective Dipole Model of AdS/CFT and Higher Spin Gravity," J. Phys. A **44**, 465402 (2011) doi:10.1088/1751-8113/44/46/465402 [arXiv:1106.3983 [hep-th]].

[147] A. Jevicki, K. Jin and J. Yoon, "1/N and loop corrections in higher spin AdS_4/CFT_3 duality," Phys. Rev. D **89**, no.8, 085039 (2014) doi:10.1103/PhysRevD.89.085039 [arXiv:1401.3318 [hep-th]].

[148] R. de Mello Koch, A. Jevicki, J. P. Rodrigues and J. Yoon, "Holography as a Gauge Phenomenon in Higher Spin Duality," JHEP **01**, 055 (2015) doi:10.1007/JHEP01(2015)055 [arXiv:1408.1255 [hep-th]].

[149] R. de Mello Koch, A. Jevicki, J. P. Rodrigues and J. Yoon, "Canonical Formulation of $O(N)$ Vector/Higher Spin Correspondence," J. Phys. A **48**, no.10, 105403 (2015) doi:10.1088/1751-8113/48/10/105403 [arXiv:1408.4800 [hep-th]].

[150] R. de Mello Koch, A. Jevicki, K. Suzuki and J. Yoon, "AdS Maps and Diagrams of Bilocal Holography," JHEP **03**, 133 (2019) doi:10.1007/JHEP03(2019)133 [arXiv:1810.02332 [hep-th]].

[151] M. Flato and C. Fronsdal, "One Massless Particle Equals Two Dirac Singletons: Elementary Particles in a Curved Space. 6.," Lett. Math. Phys. **2**, 421-426 (1978) doi:10.1007/BF00400170

[152] O. Aharony, S. M. Chester and E. Y. Urbach, "A Derivation of AdS/CFT for Vector Models," [arXiv:2011.06328 [hep-th]].

[153] D. L. Jafferis, A. Lewkowycz, J. Maldacena and S. J. Suh, "Relative entropy equals bulk relative entropy," JHEP **06**, 004 (2016) doi:10.1007/JHEP06(2016)004 [arXiv:1512.06431 [hep-th]].

[154] X. Dong, D. Harlow and A. C. Wall, "Reconstruction of Bulk Operators within the Entanglement Wedge in Gauge-Gravity Duality," Phys. Rev. Lett. **117**, no.2, 021601 (2016) doi:10.1103/PhysRevLett.117.021601 [arXiv:1601.05416 [hep-th]].

[155] J. Cotler, P. Hayden, G. Penington, G. Salton, B. Swingle and M. Walter, "Entanglement Wedge Reconstruction via Universal Recovery Channels," Phys. Rev. X **9**, no.3, 031011 (2019) doi:10.1103/PhysRevX.9.031011 [arXiv:1704.05839 [hep-th]].

[156] C. F. Chen, G. Penington and G. Salton, "Entanglement Wedge Reconstruction using the Petz Map," JHEP **01**, 168 (2020) doi:10.1007/JHEP01(2020)168 [arXiv:1902.02844 [hep-th]].

[157] K. Papadodimas and S. Raju, "State-Dependent Bulk-Boundary Maps and Black Hole Complementarity," Phys. Rev. D **89**, no.8, 086010 (2014) doi:10.1103/PhysRevD.89.086010 [arXiv:1310.6335 [hep-th]].

[158] K. Papadodimas and S. Raju, "An Infalling Observer in AdS/CFT," JHEP **10**, 212 (2013) doi:10.1007/JHEP10(2013)212 [arXiv:1211.6767 [hep-th]].

[159] M. Freedman and M. Headrick, "Bit threads and holographic entanglement," Commun. Math. Phys. **352**, no.1, 407-438 (2017) doi:10.1007/s00220-016-2796-3 [arXiv:1604.00354 [hep-th]].

[160] M. Headrick and V. E. Hubeny, "Riemannian and Lorentzian flow-cut theorems," Class. Quant. Grav. **35**, no.10, 10 (2018) doi:10.1088/1361-6382/aab83c [arXiv:1710.09516 [hep-th]].

[161] S. X. Cui, P. Hayden, T. He, M. Headrick, B. Stoica and M. Walter, "Bit Threads and Holographic Monogamy," Commun. Math. Phys. **376**, no.1, 609-648 (2019) doi:10.1007/s00220-019-03510-8 [arXiv:1808.05234 [hep-th]].

[162] A. Jevicki and A. van Tonder, "Finite [Q oscillator] representation of 2-D string theory," Mod. Phys. Lett. A **11**, 1397-1410 (1996) doi:10.1142/S0217732396001405 [arXiv:hep-th/9601058 [hep-th]].

[163] A. Jevicki and S. Ramgoolam, "Noncommutative gravity from the AdS / CFT correspondence," JHEP **04**, 032 (1999) doi:10.1088/1126-6708/1999/04/032 [arXiv:hep-th/9902059 [hep-th]].

[164] A. Jevicki and B. Sakita, "The Quantum Collective Field Method and Its Application to the Planar Limit," Nucl. Phys. B **165**, 511 (1980) doi:10.1016/0550-3213(80)90046-2

[165] A. Jevicki and B. Sakita, "Collective Field Approach to the Large N Limit: Euclidean Field Theories," Nucl. Phys. B **185**, 89-100 (1981) doi:10.1016/0550-3213(81)90365-5

[166] A. Jevicki and J. P. Rodrigues, "Master Variables and Spectrum Equations in Large N Theories," Nucl. Phys. B **230**, 317-335 (1984) doi:10.1016/0550-3213(84)90216-5

[167] R. de Mello Koch and J. P. Rodrigues, Phys. Rev. D **54**, 7794-7814 (1996) doi:10.1103/PhysRevD.54.7794 [arXiv:hep-th/9605079 [hep-th]].

[168] T. Banks, M. R. Douglas, G. T. Horowitz and E. J. Martinec, "AdS dynamics from conformal field theory," [arXiv:hep-th/9808016 [hep-th]].

[169] I. Bena, "On the construction of local fields in the bulk of AdS(5) and other spaces," Phys. Rev. D **62**, 066007 (2000) doi:10.1103/PhysRevD.62.066007 [arXiv:hep-th/9905186 [hep-th]].

[170] A. Hamilton, D. N. Kabat, G. Lifschytz and D. A. Lowe, "Holographic representation of local bulk operators," Phys. Rev. D **74**, 066009 (2006) doi:10.1103/PhysRevD.74.066009 [arXiv:hep-th/0606141 [hep-th]].

[171] D. Harlow and D. Stanford, "Operator Dictionaries and Wave Functions in AdS/CFT and dS/CFT," [arXiv:1104.2621 [hep-th]].

[172] R. R. Metsaev, "Light cone form of field dynamics in Anti-de Sitter space-time and AdS / CFT correspondence," Nucl. Phys. B **563**, 295-348 (1999) doi:10.1016/S0550-3213(99)00554-4 [arXiv:hep-th/9906217 [hep-th]].

[173] T. Faulkner and A. Lewkowycz, "Bulk locality from modular flow," JHEP **07**, 151 (2017) doi:10.1007/JHEP07(2017)151 [arXiv:1704.05464 [hep-th]].

[174] V. E. Hubeny, M. Rangamani and T. Takayanagi, "A Covariant holographic entanglement entropy proposal," JHEP **07**, 062 (2007) doi:10.1088/1126-6708/2007/07/062 [arXiv:0705.0016 [hep-th]].

[175] S. Ryu and T. Takayanagi, "Holographic derivation of entanglement entropy from AdS/CFT," Phys. Rev. Lett. **96**, 181602 (2006) doi:10.1103/PhysRevLett.96.181602 [arXiv:hep-th/0603001 [hep-th]].

[176] S. Ryu and T. Takayanagi, "Aspects of Holographic Entanglement Entropy," JHEP **08**, 045 (2006) doi:10.1088/1126-6708/2006/08/045 [arXiv:hep-th/0605073 [hep-th]].

[177] B. Czech, J. L. Karczmarek, F. Nogueira and M. Van Raamsdonk, "The Gravity Dual of a Density Matrix," Class. Quant. Grav. **29**, 155009 (2012) doi:10.1088/0264-9381/29/15/155009 [arXiv:1204.1330 [hep-th]].

[178] M. Headrick, V. E. Hubeny, A. Lawrence and M. Rangamani, "Causality \& holographic entanglement entropy," JHEP **12**, 162 (2014) doi:10.1007/JHEP12(2014)162 [arXiv:1408.6300 [hep-th]].

[179] A. C. Wall, "Maximin Surfaces, and the Strong Subadditivity of the Covariant Holographic Entanglement Entropy," Class. Quant. Grav. **31**, no.22, 225007 (2014) doi:10.1088/0264-9381/31/22/225007 [arXiv:1211.3494 [hep-th]].

[180] P. Hayden and G. Penington, "Learning the Alpha-bits of Black Holes," JHEP **12**, 007 (2019) doi:10.1007/JHEP12(2019)007 [arXiv:1807.06041 [hep-th]].

[181] C. A. Agón, J. De Boer and J. F. Pedraza, "Geometric Aspects of Holographic Bit Threads," JHEP **05**, 075 (2019) doi:10.1007/JHEP05(2019)075 [arXiv:1811.08879 [hep-th]].

[182] A. Almheiri, D. Marolf, J. Polchinski and J. Sully, "Black Holes: Complementarity or Firewalls?," JHEP **02**, 062 (2013) doi:10.1007/JHEP02(2013)062 [arXiv:1207.3123 [hep-th]].

[183] A. Almheiri, D. Marolf, J. Polchinski, D. Stanford and J. Sully, "An Apologia for Firewalls," JHEP **09**, 018 (2013) doi:10.1007/JHEP09(2013)018 [arXiv:1304.6483 [hep-th]].

[184] D. Marolf and J. Polchinski, "Gauge/Gravity Duality and the Black Hole Interior," Phys. Rev. Lett. **111**, 171301 (2013) doi:10.1103/PhysRevLett.111.171301 [arXiv:1307.4706 [hep-th]].

[185] S. D. Mathur, "The Information paradox: A Pedagogical introduction," Class. Quant. Grav. **26**, 224001 (2009) doi:10.1088/0264-9381/26/22/224001 [arXiv:0909.1038 [hep-th]].

[186] S. D. Mathur, "The Fuzzball proposal for black holes: An Elementary review," Fortsch. Phys. **53**, 793-827 (2005) doi:10.1002/prop.200410203 [arXiv:hep-th/0502050 [hep-th]].

[187] K. Skenderis and M. Taylor, "The fuzzball proposal for black holes," Phys. Rept. **467**, 117-171 (2008) doi:10.1016/j.physrep.2008.08.001 [arXiv:0804.0552 [hep-th]].

[188] S. D. Mathur and D. Turton, "Comments on black holes I: The possibility of complementarity," JHEP **01**, 034 (2014) doi:10.1007/JHEP01(2014)034 [arXiv:1208.2005 [hep-th]].

[189] S. G. Avery, B. D. Chowdhury and A. Puhm, "Unitarity and fuzzball complementarity: 'Alice fuzzes but may not even know it!'," JHEP **09**, 012 (2013) doi:10.1007/JHEP09(2013)012 [arXiv:1210.6996 [hep-th]].

[190] M. Mulokwe and J. P. Rodrigues, "Large N bilocals at the infrared fixed point of the three dimensional O(N) invariant vector theory with a quartic interaction," JHEP **11**, 047 (2018) doi:10.1007/JHEP11(2018)047 [arXiv:1808.00042 [hep-th]].

[191] N. Beisert, "The complete one loop dilatation operator of N=4 superYang-Mills theory," Nucl. Phys. B **676**, 3-42 (2004) [arXiv:hep-th/0307015 [hep-th]].

[192] D. Berenstein, "Giant gravitons: a collective coordinate approach," Phys. Rev. D **87**, no. 12, 126009 (2013) [arXiv:1301.3519 [hep-th]].

[193] D. Berenstein and E. Dzienkowski, "Open spin chains for giant gravitons and relativity," JHEP **1308**, 047 (2013) [arXiv:1305.2394 [hep-th]].

[194] D. Berenstein and E. Dzienkowski, "Giant gravitons and the emergence of geometric limits in beta-deformations of $\mathcal{N} = 4$ SYM," JHEP **1501**, 126 (2015) [arXiv:1408.3620 [hep-th]].

[195] D. Berenstein, "On the central charge extension of the $\mathcal{N} = 4$ SYM spin chain," JHEP **1505**, 129 (2015) [arXiv:1411.5921 [hep-th]].

[196] R. de Mello Koch, N. H. Tahiridimbisoa and C. Mathwin, "Anomalous Dimensions of Heavy Operators from Magnon Energies," JHEP **1603**, 156 (2016) [arXiv:1506.05224 [hep-th]].

[197] J. McGreevy, L. Susskind and N. Toumbas, "Invasion of the giant gravitons from Anti-de Sitter space," JHEP **0006**, 008 (2000) doi:10.1088/1126-6708/2000/06/008 [hep-th/0003075].

[198] N. Beisert, "The su(2|3) dynamic spin chain," Nucl. Phys. B **682**, 487 (2004) [hep-th/0310252].

[199] B. Eden, C. Jarczak and E. Sokatchev, "A Three-loop test of the dilatation operator in N = 4 SYM," Nucl. Phys. B **712**, 157-195 (2005) [arXiv:hep-th/0409009 [hep-th]].

[200] R. de Mello Koch and S. Ramgoolam, "Strings from Feynman Graph counting : without large N," Phys. Rev. D **85**, 026007 (2012) [arXiv:1110.4858 [hep-th]].

[201] S. de Carvalho, R. de Mello Koch and M. Kim, "Central Charges for the Double Coset," JHEP **05**, 007 (2020) [arXiv:2001.10181 [hep-th]].

[202] R. de Mello Koch, P. Diaz and N. Nokwara, "Restricted Schur Polynomials for Fermions and integrability in the su(2—3) sector," JHEP **03**, 173 (2013) [arXiv:1212.5935 [hep-th]].

[203] N. Aizawa and V. K. Dobrev, "Intertwining Operator Realization of anti de Sitter Holography," Rept. Math. Phys. **75**, 179 (2015) doi:10.1016/S0034-4877(15)30002-1 [arXiv:1406.2129 [hep-th]].

[204] V. K. Dobrev, G. Mack, I. T. Todorov, V. B. Petkova and S. G. Petrova, "On the Clebsch-Gordan Expansion for the Lorentz Group in n Dimensions," Rept. Math. Phys. **9**, 219-246 (1976) doi:10.1016/0034-4877(76)90057-4

[205] D. E. Berenstein and L. F. Urrutia, "The Relation between the Mandelstam and the Cayley-Hamilton identities," J. Math. Phys. **35**, 1922-1930 (1994) [arXiv:hep-th/9305156 [hep-th]].

[206] Bekensteint. Jacob D, "Black Holes and Entr0py,"(1973) [PHYS. REV. D7].